Characterization of small molecule inhibitors of the NLRP3 inflammasome

Dissertation

zur

Erlangung des Doktorgrades (Dr. rer. nat.)

der

Mathematisch-Naturwissenschaftlichen Fakultät

der

Rheinischen Friedrich-Wilhelms-Universität Bonn

vorgelegt von

Brian Monks

aus

Hamilton, Bermuda (United Kingdom)

Bonn, September 2020

Angefertigt mit Genehmigung der Mathematisch-Naturwissenschaftlichen Fakultät der
Rheinischen Friedrich-Wilhelms-Universität Bonn

1. Gutachter: Prof. Dr. Eicke Latz

2. Gutachter: Prof. Dr. rer. nat. Michael Pankratz

Tag der Promotion: 26.03.2021
Erscheinungsjahr: 2021

Table of Contents

1 Summary

To respond quickly to infection, the innate immune system contains many germline encoded pattern recognition receptors (PRRs) that recognize a myriad of danger signals released by pathogens and damaged tissues. NLRP3 (nucleotide-binding oligomerization domain, leucine rich repeat and pyrin domain containing 3) is a cytosolic PRR that responds to a broad range of activators, including bacterial pore-forming toxins, extracellular ATP and monosodium urate crystals. Activation of NLRP3 leads to the recruitment of ASC (apoptosis-associated speck like protein containing a caspase recruitment domain) forming a large oligomeric protein platform called the inflammasome. The inflammasome recruits procaspase-1, which is then activated by autocleavage. Active caspase-1 cleaves several know targets, including the interleukin-1 family cytokines, leading to their release as mature active cytokines. Gasdermin D (GSDMD) is also cleaved by active caspase-1, leading to a type of cell death termed pyroptosis.

Gain-of function mutations, leading to hyperactive NLRP3 were found to be the cause of a spectrum of systemic autoinflammatory diseases termed cryopyrin associated periodic syndrome (CAPS). NLRP3 activation has also been shown to be a key factor in the severity of chronic diseases involving aggregate or crystalline substances, such as gout, atherosclerosis, and Alzheimer's disease.

Several factors have been shown to be important for activation of NLRP3, such as reactive oxygen species (ROS) and potassium efflux, but the exact mechanism that mediates the response of NLRP3 to its diverse triggers is poorly understood. A further complication is the requirement in macrophages for an initial step, termed priming, in order to be NLRP3 competent. In this step, NLRP3 protein level is increased by the induction of transcription, and then is post translationally modified in several ways, such as deubiquitination and dephosphorylation for full function. Separating inhibition of priming verses inhibition of NLRP3 activation can be difficult.

To study direct small molecule inhibition of NLRP3, a mouse NLRP3 Knockout cell line was used that constitutively expresses NLRP3, removing the need for priming, and also expresses fluorescently tagged ASC to allow detection of inflammasome formation. This cell line was used to screen two commercially available small molecule libraries for the ability to inhibit NLRP3 activation.

In order to identify the domain of NLRP3 targeted by inhibitors, several chimeric receptors were constructed which contained the pyrin domain of NLRP3 or AIM2. Upon activation, these receptors interact with ASC through the pyrin domain, allowing them to induce the condensation of ASC into a single speck within the cell.

In this study, I could show that several NLRP3 inhibitory compounds resulting from these screens, and several previously identified NLRP3 inhibitors, were able to inhibit the ability of

chimeric receptors containing the pyrin domain of NLRP3, but not the pyrin domain of AIM2, to initiate ASC speck formation.

1 Zusammenfassung

Um schnell auf eine Infektion reagieren zu können, enthält das angeborene Immunsystem viele keimbahnkodierte Mustererkennungsrezeptoren (PRRs). Diese PPRs erkennen eine Vielzahl von Gefahrensignale, die von Krankheitserregern und geschädigten Geweben freigesetzt werden. Das Protein NLRP3 (Nucleotid-bindende Oligomerisierungsdomäne, die Leucin-reiche Wiederholungen in der Aminosäuresequenz besitzt und eine Pyrin-Domäne enthält) ist ein zytosolischer PRR, das auf eine breite Palette von Aktivatoren reagiert, einschließlich bakterieller porenbildender Toxine, extrazelluläres ATP- und Mononatriumuratkristalle. Die Aktivierung von NLRP3 führt zur Rekrutierung von ASC (Apoptose-assoziiertes aggregierendes Protein, das eine Caspase-Rekrutierungsdomäne enthält), welches eine große oligermerische Proteinplattform bildet, die als Inflammasom bezeichnet wird. Das Inflammasom rekrutiert Procaspase-1, die dann durch Autospaltung aktiviert wird. Aktive Caspase-1 spaltet mehrere bekannte Proteine, einschließlich der Zytokine der Interleukin-1-Familie, was zu ihrer Freisetzung als ausgebildete aktive Zytokine führt. Gasdermin D (GSDMD) wird ebenfalls durch aktive Caspase-1 gespalten, was zu einer Art Zelltod führt, der als Pyroptose bezeichnet wird.
Es wurde festgestellt, dass Mutationen mit Funktionsgewinn, die zu hyperaktivem NLRP3 führen, die Ursache für ein Spektrum systemischer autoinflammatorischer Erkrankungen sind, die als Kryopyrin-assoziiertes periodisches Syndrom (CAPS) bezeichnet werden. Es wurde auch gezeigt, dass die NLRP3-Aktivierung ein Schlüsselfaktor für die Schwere chronischer Erkrankungen ist, an denen aggregierte oder kristalline Substanzen eine Rolle spielen wie in Gicht, Atherosklerose und Alzheimer.
Es wurde weiterhin gezeigt, dass verschiedene Faktoren für die Aktivierung von NLRP3 wichtig sind, wie z. B. reaktive Sauerstoffspezies (ROS) und Kaliumausfluss, aber der genaue Mechanismus, wie NLRP3 auf seine verschiedenen Auslöser reagiert, ist kaum bekannt.

Eine weitere Komplikation ist die Erfordernis eines ersten Schritts bei Makrophagen, der als „Priming“ bezeichnet wird. Dieses „Priming“ ist erforderlich, um NLRP3 überhaupt aktivieren zu können. In diesem Schritt wird der NLRP3-Proteinspiegel durch Induktion der Transkription erhöht und dann auf verschiedene Weise posttranslational modifiziert, beispielsweise durch Deubiquitinierung und Dephosphorylierung um eine vollständige Funktionalität herbeizuführen. Es ist schwierig, die Faktoren die das „Priming“ hemmen von denen , die eine Hemmung der NLRP3-Aktivierung verursachen auseinanderzuhalten.
Um die direkte Hemmung von NLRP3 durch kleine Moleküle zu untersuchen, wurde eine NLRP3-Knockout-Zelllinie der Maus verwendet, die NLRP3 ständig exprimiert, um somit unabhängig von der zuvor beschriebenen Notwendigkeit des „Primings“ zu sein. Gleichzeitig

exprimiert diese Zelllinie auch fluoreszenzmarkiertes ASC, um den Nachweis der Bildung von Inflammasomen zu ermöglichen. Diese Zelllinie wurde verwendet, um zwei kommerziell erhältliche Bibliotheken von kleinen Molekülen auf ihre Fähigkeit hin zu untersuchen, die NLRP3-Aktivierung zu hemmen.
Um die Domäne von NLRP3 zu identifizieren, auf die diese Inhibitoren abzielen, wurden mehrere chimäre Rezeptoren konstruiert, die die Pyrindomäne von NLRP3 oder AIM2 enthalten. Bei der Aktivierung interagieren diese Rezeptoren über die Pyrindomäne mit ASC, wodurch sie die Kondensation von ASC zu einem einzelnen Aggregat innerhalb der Zelle induzieren.
In dieser Studie konnte ich zeigen, dass mit mehreren NLRP3-inhibitorischen Verbindungen, die aus diesen Screenings resultieren, aber auch mit mehreren zuvor identifizierten NLRP3-Inhibitoren bei chimären Rezeptoren, die die Pyrindomäne von NLRP3, jedoch nicht die Pyrindomäne von AIM2 enthalten, die Fähigkeit eine ASC Aggregation zu verursachen, verhindert werden konnte.

2 Introduction

2.1 The Immune System

In order to protect an organism from pathogens, immune systems have evolved to recognize foreign from self, and to initiate protective response against the attacking pathogens. The immune system is divided into two general categories, innate or acquired.
Innate immune systems consist of germ-line encoded receptors which sense pathogens directly by sensing PAMPs (Pathogen-Associated Molecular Patterns) [1], or indirectly by sensing damage to the host by sensing DAMPs (Damage-Associated Molecular Patterns or Danger-Associated Molecular Patterns)[2]. PAMPs consist of expressed molecular structures that are conserved in pathogenic organisms, but are not expressed by the host. DAMPs include self molecules that have been modified by the infection process, or as a consequence of infection, now exist in compartments they would normally be excluded from.
Acquired immune systems, also known as adaptive immune systems, consist of germ-line encoded genes which have been modified to detect a specific pathogen after an initial infection [3]. These systems can both help clear the current infection, and help to quickly protect an organism from subsequent infections by the same or similar pathogens. The pathogen specific targets include protein epitopes, polysaccharides, or specific RNA or DNA sequences. Acquired immune systems were originally discovered in vertebrate animals, and were thought to be present only in vertebrates. The acquired immune system consists of specialized cells, T and B cells, which rearrange germ-line encoded receptors and are clonally selected to result in cells expressing receptors highly specific for the pathogen [4]. Some of these cells can survive for years and can initiate a rapid specific immune response to future reinfection by a pathogen. More recently, other forms of acquired immune systems have been discovered in other organisms. For instance, many bacteria and archea species have the CRISPR acquired immune system [5]. In this system, short DNA sequences from invading bacteriophages are inserted into clusters of repeat sequences in the bacterial genome [6-8]. These sequences are expressed as RNA, which guides a nuclease, Cas9, to bind to and cut invading bacteriophage DNA which contains the same sequence [9].

2.1.1 The Innate Immune System

The innate immune system is the first line of defense against invading organisms. It is critical for a rapid initial response to infection, and is also required for the proper function of the acquired immune system, which takes several days to develop[10].
Innate immune cells, such as macrophages and dendritic cells, express a finite set of cell surface and intracellular receptors called PRRs (Pattern Recognition Receptor) that respond

to foreign PAMPs or sense DAMPs. Once activated, most PRRs initiate a cascade of activated kinases that trigger the translocation of transcription factors into the nucleus leading to the synthesis of proinflammatory molecules. The activated cell upregulates additional sensing receptors, and is enhanced for the phagocytosis and clearing of pathogens. Soluble cytokines and chemokines, are produced and released, signaling distant cells that there is an infection, both activating them to increase competence at clearing the pathogen and guiding them towards the area of the body where the pathogen was detected.

2.1.2 Pattern Recognition Receptors PRRs

There are both membrane-bound and cytosolic PRRs. The family of Toll-Like Receptors (TLRs) is a major class of membrane-bound PRRs. These receptors were named TLRs due to their homology to the *Drosophila melanogaster* Toll gene, which has a role in both dorsoventral pattern development and in anti-fungal responses [11]. The TLR family shown to be important as PRRs in mammals when it was discovered that a mutation in the TLR4 gene was responsible for the inability of C3H/HeJ mice to respond to Gram-negative bacterial Lipopolysaccharide (LPS) [12]. There are ten human TLR receptors which have been shown to respond to distinct PAMPs from a wide range of pathogens, including bacteria, viruses and fungi [13]. The known TLR ligands range from bacterial products, such as LPS, lipoproteins, and flagellin, to Nucleic acids, such as unmethylated CpG DNA from both bacteria and DNA viruses, and both single and double-stranded RNA from viruses [14]. TLRs consist of a ligand sensing leucine-rich repeat (LRR) domain, a transmembrane domain, and a cytoplasmic signaling Toll/Interleukin-1 Receptor (TIR) domain. TLRs exist as a monomer or a preformed dimer, depending on the specific TLR involved[15]. Upon ligand binding to the LRR domains, the TLR dimer undergoes a conformational change that brings the TIR domains closer together, enabling them to interact with several adaptor molecules. Which adaptors are engaged depends on which TLR dimer is activated [16]. These adaptors then initiate a kinase activation cascade resulting in the activation of several transcription factors, including NF-κB, which upregulates the production of a large number of proinflammatory molecules. TLRs are an important part of the innate immune system in both vertebrates and invertebrates, with some species of invertebrates having genomes containing hundreds of TLRs[17].
NLRs are a family of cytosolic PRRs which contain both Nucleotide-binding Oligomerization Domain (NOD) and LRR domains. The LRR domain is thought to be the ligand binding domain in these receptors, as it is with TLRs. The NOD domain, also know as Nucleotide-Binding Domain (NBD) or NAIP, CIITA, HET-E and TP1 (NACHT) domain, mediates ATP dependent self-oligomerization. Several of these NLRs, such as NOD1 and NOD2, lead to

the activation of transcription factors such as NF-κB and the production of pro-inflammatory molecules as TLRs do. Others, such as NLRP3 lead to the formation of an inflammasome.

2.1.3 Inflammasomes

Inflammasomes are cytosolic large molecular complexes that recruit procaspase-1 via binding to its CARD domain, resulting in its autocleavage to and maturation to being an active enzyme. Active caspase-1 cleaves proIL-1β, and proIL-18, resulting in the release of the mature forms of these cytokines. IL-1β is a powerful proinflammatory mediator that, upon binding to its receptor, induces the transcription of genes which lead to fever, and which facilitate the infiltration of immune cells through epithelial layers to allow access to infected or damaged tissue. IL-18 is needed for the production of interferon gamma (IFN-γ), and can mediate adaptive immune responses[18]. Caspase-1 also cleaves Gasdermin D (GSDMD), releasing the N-terminal domain from inhibition by the C-terminal domain. The N-terminal domain of GSDMD binds to lipid membranes and oligomerizes to form pores, which allow the release of mature IL-1β and cause the cell to swell and lyse. This caspase-1 dependent form of proinflammatory cell death is termed pyroptosis[19].

Inflammasome forming PRRs which contain a CARD domain are able to directly interact with caspase-1 upon activation. Those containing a PYD domain only, require the adaptor ASC to bind to caspase-1. Upon activation and self-oligomerization, the PYD domain of these receptors binds to the PYD domain of ASC, incorporating it into the inflammasome. The CARD domain of ASC then interacts with the CARD domain of caspase-1 resulting in its autocleavage and an active inflammasome.

Three PRRs that initiate active Inflammasomes through ASC speck formation were used in this study, NLRP3 as the target receptor for inhibition, and NLRP1 and AIM2 as controls for inhibitor specificity. Human NLRP1 was the first NLR shown to be able to form an inflammasome [20]. In rodents, there are 3 NLRP1 paralogs of the human NLRP1 gene, NLRP1A-C. It has been shown that strain specific variants of NLRP1B are activated through proteolytic cleavage by Anthrax Lethal Toxin (LT) [21]. NLRP1B contains a CARD domain, instead of a PYD domain, yet it is still capable of forming an ASC speck upon cleavage by LT, even though ASC is not required for IL-1β processing [22] .

AIM2 contains two domains, an N-terminal PYD domain and a C-terminal Hematopoietic Interferon-Inducible Nuclear protein (HIN) domain. AIM2 is a cytosolic receptor that binds to double-stranded DNA (dsDNA), in a sequence independent manner, via its HIN domain [23,24]. The binding of AIM2 to dsDNA results in the recruitment of ASC via the PYD domain of

AIM2, the formation of an ASC speck, and the recruitment of caspase-1 to generate an active inflammasome [25,26].

2.1.4 NLRP3

NLRP3 is the most extensively studied inflammasome PRR. It consists of three domains, an N-terminal PYD domain, a central NACHT domain, and a C-terminal LRR domain. The LRR is thought to fold back and interact with the NACHT domain, keeping it in an inactive state. This interaction is thought to be disrupted upon activation, allowing the NACHT domain of multiple NLRP3 molecules to oligomerize, causing the PYD domain to interact with the PYD domain of ASC, initiating the formation of an inflammasome [27].

In macrophages, NLRP3 is activated in two steps. First, a priming stimulus is required which activates the transcription factor NF-κB. This can be the result of PAMP activation of receptors such as TLRs, or NOD1 and NOD2; or as a result of stimulation by proinflammatory cytokines, such as TNFα. The activation of NF-κB increases the expression of NLRP3 to a level high enough for function, and also initiates the expression of pro-IL-1β [28]. Priming also initiates several forms of posttranslational modification of NLRP3 to modulate function [29]. For instance, phosphorylation or ubiquitination of amino acids in NLRP3 can either enhance or inhibit its function. The expression level of NLRP3 is critical for function. If NLRP3 is expressed at a high enough level, then priming and posttranslational modifications are no longer required for function. If NLRP3 is expressed at a high enough level, then it becomes constitutively active and forms an inflammasome without the need for any additional signals.

Secondly, NLRP3 is then activated by a diverse number of triggers, such as ATP, bacterial pore forming toxins, Crystals and aggregate proteins [30]. While several factors have been shown to be important for NLRP3 activation, potassium efflux [31], reactive oxygen species [32], and protease activity [33], for example. There has been no proposed mechanism of activation that adequately explains how the diverse agonists for NLRP3 cause activation.

NLRP3 has been shown to be important in immune response to a variety of pathogens, including bacterial infections such as Staphylococcus aureus and Listeria monocytogenes [34]; viral infections such as West Nile Virus [35] and Influenza A Virus [36]; and parasitic infections such as *Neospora Caninum* [37] and *Toxoplasma gondii* [38].

2.1.5 NLRP3 Inflammasome Associated Diseases

Gain of function mutations in NLRP3 were identified in 2001 as the cause of a rare hereditary spectrum of inflammatory diseases termed cryopyrin-associated periodic syndromes (CAPS) [39]. CAPS encompasses three phenotypes: familial cold autoinflammatory syndrome (FCAS), Muckle-Wells syndrome (MWS), and neonatal-onset multisystem inflammatory disease (NOMID), which is also called chronic infantile neurologic cutaneous articular (CINCA). Symptoms range from rashes, cold induced fever, and in severe forms of the syndrome, neurologic inflammation, deafness and chronic meningitis [40].

Activation of the NLRP3 inflammasome by crystals or aggregate proteins has also been identified as being involved in many sterile inflammatory diseases. Monosodium urate (MSU) crystal induced gout has been shown to be mediated by NLRP3 [41]. Saturated fatty acids and pancreatic islet amyloid protein have been shown to activate the NLRP3 inflammasome leading to loss of β-cells in type 2 diabetes [42,43]. Cholesterol crystal deposition in atherosclerosis has also been shown to activate NLRP3 [44].

Amyloid-β plaques found in Alzheimer's disease have been shown to activate NLRP3 in microglial cells, and mice lacking NLRP3 or ASC showed less special reference memory loss than control mice [45 46].

2.1.6 Inhibition of the NLRP3 Inflammasome as Therapy

Currently, several NLRP3 associated diseases are treated by blocking the activity of the mature IL-1β released through inflammasome activation. Both the IL-1β trap Rilonacept and the monoclonal IL-1β neutralizing antibody Canakinumab, have been licensed as a treatment for CAPS patients. Canakinumab was shown to lower systemic inflammation and decreased cardiovascular events in the CANTOS trial involving cardiovascular disease patients [47].

Targeting NLRP3 directly would be a more specific therapy than blocking down stream IL-1β effects. Several mouse models of NLRP3 inflammasome based pathologies have been shown to be improved by the administration of small molecule NLRP3 inhibitors. Many reported inhibitors of NLRP3 have been used in mouse models of disease, but few of them are know to be specific for inhibiting NLRP3 only [48]. CRID3, also known as MCC950 and CP-456,773, is a specific NLRP3 inhibitor that has recently been shown to directly target the NACHT domain of NLRP3 [49-51]. The oral administration of CRID3 has been shown to be effective in lowering inflammation in mouse models of dermal and pulmonary inflammation [52]. CRID3 has also been shown to effective in several models of neurological pathologies. It reduced dopaminergic degeneration in a mouse model of Parkinson's disease [53], and improved cognitive function and amyloid-β clearance in a mouse model of Alzheimer's

disease [54]. While CRID3 blocks pathologies cause by the activation of NLRP3, it does not efficiently inhibit gain of function CAPS mutations in mouse models [51].
While there are model NLRP3 inhibitory compounds used in animal models, no NLRP3 inhibitors are currently approved for the treatment of diseases in humans.

2.2 Objectives of this study

The activation of NLRP3 leads to the release of mature IL-1β, a powerful proinflammatory cytokine, and pyroptotic cell death. Chronic activation of NLRP3 leads to, or exacerbates, many sterile inflammatory diseases, including gout, atherosclerosis, diabetes and Alzheimer's disease. The mechanism by which NLRP3 is activated is poorly understood, impeding the development of targeted drug therapies to reduce NLRP3 mediated inflammation. Current small molecule inhibitors of NLRP3 have been found by blindly screening for NLRP3 inhibitory activity, and many have poor NLRP3 target specificity. The mechanism of action of these inhibitors on NLRP3 is also poorly understood.
The first aim of this work was to identify and confirm new inhibitors of NLRP3 to be used for further studies To accomplish this aim, a cell line expressing constitutive NLRP3 and fluorescently tagged ASC was used to screen for inhibitors of NLRP3 induce inflammasome formation using high throughput confocal microscopy. The second aim of this work was to functionally separate the PYD domain of NLRP3 and test NLRP3 inhibitors for the ability to inhibit the NLRP3 PYD. In order to achieve this aim, chimeric receptors were made in which the CARD domains of NOD2 were replaced with the PYD domain of either NLRP3 or AIM2. The PYD of these receptors interact with ASC upon activation, and can be monitored for inhibition by confocal microscopy. Mutations were made in the NLRP3 PYD domain of this chimeric receptor to identify residues required for inhibitor function. The third aim of this study was to investigate CRID3 a highly specific inhibitor of NLRP3, and test the reported gene targets of CRID3. Gene silencing using siRNA mediated knockdown of potential CRID3 targets was used to study both their involvement in NLRP3 activation, and as targets for CRID3 activity.

3 Materials and Methods

3.1 Materials

3.1.1 Devices

Product	Supplier
-150 ^{O}C Freezer	Sanyo Biomedical
-20 ^{O}C Freezer	Siemens
-80 ^{O}C Freezer	Thermo Scientific
+4 ^{O}C Refrigerator	Siemens
Centrifuge 5810R	Eppendorf
DNA gel electrophoresis system PerfectBlue	Peqlab
Electronic E4 XLS+ multichannel pipets	Mettler-Toledo
Freezing containers	True North
Gel imaging system VersaDoc	Biorad
Heatblock Thermomixer	Eppendorf
Microcentrifuge 5424	Eppendorf
Microscope Leica DMI3000B	Leica
Microscope Leica DMIL LED	Leica
Microscope Zeiss Observer.Z1	Carl Zeiss Jena GmbH
NanoDrop 2000 Spectrophotometer	Thermo Scientific
NN-E245W microwave oven	Panasonic
Pipettes (0.1 µl – 1 ml)	Mettler-Toledo
Pipetting device pipet boy acu	Integra Biosciences
Power Supply EV202	Siemens
QuanStudio 6 Flex Real-Time PCR System	Thermo Scientific
Sonorex Super Ultrasonic Bath	Bandelin
SpectraMax i3 Microplate Reader	Molecular Devices
Tali Image-based Cytometer	Thermo Scientific
Thermocycler T3000	Analytica Jena
Thermocycler Tadvanced (96 well)	Biometra
Tissue Culture Hood	Thermo Scientific
Tissue Culture Incubator	Sanyo Biomedical
UV table for DNA imaging UVstar	Biometra

3.1.2 Consumables

Product	Supplier
0.22 µM ,0.45 µM Syringe Filters	Merck Millipore
1.5 ml, 2 ml Microcentrifuge Tubes	Eppendorf
14 ml Snap-Cap Centrifuge Tubes	VWR
15 ml, 50 ml Centrifuge Tubes	Greiner bio-one
384-well Microscopy Black Plate	Greiner bio-one
384-well qPCR plate	Applied Biosystems

5 ml, 10 ml, 25 ml Serological Pipettes	Greiner bio-one
96-well Microscopy Black Plate	Greiner bio-one
Cell scrapers	Sarstedt
Cell Strainer (70 μM)	VWR
Maxi-Sorp 96-well ELISA Plates	Nunc
Needles	Braun Melsungen
Opti-Seal optical disposable adhesive	Bioplastics
Pipette Tips 0.2 μl - 1ml	Rainin
Scapel	Feather
Syringe Needles	Braun Meslungen
Syringes	BD Biosciences
Tissue Culture Flasks	Greiner bio-one
Tissue Culture Plates	Greiner bio-one

3.1.3 Chemicals and Kits

Product	**Supplier**
10x PBS (2 g Potassium Chloride, 2 g Potassium Dihydrogen phosphate, 80 g Sodium chloride, 11.5 g di-Sodium hydrogen phosphate anhydrous Per 1 L)	Pan Biotech
16% Formaldehyde, methanol-free	Sigma-Aldrich
Agarose	Biozym
Ampicillin	Sigma-Aldrich
Bicinchoninic acid (BCA) assay	Thermo Scientific
Blasticidin	Invivogen
Bovine serum albumin (BSA)	Roth
CloneJet Blunt PCR Cloning Kit	Thermo Scientific
DNase I	Invitrogen
dNTP mix (10 mM)	Thermo Scientific
ELISA substrate solution BD Opteia	BD Biosciences
Ethidium bromide	Sigma Aldrich
Ethylenediaminetetraacetic acid (EDTA, 0.5 M, pH 8.0)	Life Technologies
Fast Digest Restriction Enzymes	Fermentas
Glycerol	Merck
Isopropanol	Roth
LB Agar (Lennox L agar, 10 g Peptone 140, 5 g Yeast Extract, 5 g NaCl, 12 g Agar per 1 L)	Life Technologies
LB Medium (Luria/Miller, 10 g Tryptone, 10 g Yeast Extract, 10 g NaCl per 1 L)	Roth
Maxima Sybr Green/ROX 2x master mix	Thermo Scientific
Mouse IL-1b ELISA	R&D Systems
Mouse TNFa ELISA	R&D Systems

NaCl	Roth
PeqGreen	PeqLab
PfuUltra II Hotstart PCR Master Mix	Agilent
PureLink Quick Gel Extraction Kit	Life Technologies
PureLink Quick Plasmid Maxiprep Kit	Life Technologies
PureLink Quick Plasmid Miniprep Kit	Life Technologies
Random Hexamers	Thermo Scientific
RNAse Inhibitor	Thermo Scientific
RNeasy mini kit	Qiagen
Sodium dodecyl sulfate (SDS)	Sigma Aldrich
Superscript III reverse transcriptase	Thermo Scientific
T4 DNA Ligase, HC	Fermentas
Tris Acetate EDTA (TAE) pH 8,5 (50x, 2M Tris, 1M acetic acid, 50mM EDTA)	Roth
Tris HCl pH 7.4	Roth
Tris HCl pH 8.0	Roth
Tween 20	Roth
β-mercaptoethanol	Sigma Aldrich

3.1.4 Cell Culture Reagents

Product	**Supplier**
0.05% trypsin/EDTA	Life Technologies
Adenosine 5'-triphosphate (ATP) disodium salt	Sigma-Aldrich
B/B homodimerizer	Clontech
Dimethylsulfoxide (DMSO)	Sigma-Aldrich
DRAQ5	eBioscience
Dulbecco's Modified Eagle Medium (DMEM), high glucose, with glutamine	Life Technologies
Dulbecco's Phosphate Buffered Saline (DPBS)	Life Technologies
Fetal Bovine Serum (FBS)	Life Technologies
GeneJuice	Merck Millipore
HEPES 1M	Sigma-Aldrich
Hygromycin B	PAA
Lethal Factor (LF) from *B. anthracis*	List Biologicals
Leu-Leu-OMe	Chem-Impex
Lipofectamine2000	Life Sciences
Lipofectamine RNAiMAX	Life Sciences
Nigericin	Life Technologies
OPTIMEM	Life Technologies
Penicillin/Streptomycin 100x	Life Technologies
Poly-L-lysine solution (0.01% m/v)	Sigma-Aldrich
Poly(dA:dT)	Sigma-Aldrich
Protective Antigen (PA) from *B. anthracis*	List Biologicals

Puromycin	Life Technologies
StemPro Accutase	Life Technologies
Trypsin-EDTA (0.05%)	Life Technologies
Ultrapure Lipopolysaccharide (LPS) from E. coli 0111:B4	Invivogen
Viability measurement Cell Titer Blue (CTB)	Promega

3.1.5 NLRP3 Inhibitors

Product	**Supplier**
5Z-7-Oxozeanol	Tocris
7-Dehydrogedunin	Sigma-Aldrich
Arglabin	Sigma-Aldrich
BAY-11-7082	Sigma-Aldrich
CH 55	Tocris Bioscience
CRID3	Pfizer
Ebselen	Sigma-Aldrich
NSC632839	Tocris Bioscience
Parthenolide	Sigma-Aldrich
Pifithrin-μ	Tocris Bioscience

3.1.6 siRNAs

Silencer Select siRNA from Thermo-Fisher

Target Gene	**Identifier**
Negative control #1	4390847
Negative control #2	4390844
CLIC1 1	s100126
CLIC1 2	s100127
CLIC1 3	s100128
GSTO1 1	s67153
GSTO1 2	s67154
GSTO1 3	s201431
NLRP3 2	s103711

3.1.7 QPCR Primers

Target gene	**Primer sequence**
CLIC1- forward	CTGAGTCCAACACCTCGGGA
CLI1- reverse	ACCTTCAGGGCTTTCAGGAGTC
GSTO1- forward	GCGTTGGAGAACGAATTCAA
GSTO1- reverse	GAGCTCCAATGCTTCCAGTC

HPRT- forward	TGAAGTACTCATTATAGTCAAGGGCA
HPRT- reverse	CTGGTGAAAAGGACCTCTCG
NLRP3 - forward	TGGGGTTGGTGAATTCCGGC
NLRP3 - reverse	AGCCTGAGTCCTGTGTCTCCA

3.1.8 Plasmids

I designed and created the parental chimeric NOD2 constructs. Rainer Stahl designed and created the chimeric hNLRP3 PYD-AIM2 construct and all cysteine to alanine constructs.

ID	Insert	Vector
56	VSV-G	pOG44
57	MMLV Gag-Pol	pCMV
106	Polylinker	pUC18
716	hNLRP3 PYD-NOD2-TagGFP2	pRP
1131	hASC-TagBFP	pRBH
1044	hAIM2-TagGFP2	pRP
1045	hNLRP3 PYD-hAIM2-TagGFP2	pRP
1154	hAIM2 PYD-NOD2-TagGFP2	pRH
1296	(C8A) hNLRP3 PYD-NOD2-TagGFP2	pRP
1478	(C38A) hNLRP3 PYD-NOD2-TagGFP2	pRP
1479	(C108A) hNLRP3 PYD-NOD2-TagGFP2	pRP
1480	(C130A) hNLRP3 PYD-NOD2-TagGFP2	pRP
1481	(C8A, C38A) hNLRP3 PYD-NOD2-TagGFP2	pRP
1482	(C108A, C130A) hNLRP3 PYD-NOD2-TagGFP2	pRP
1484	(C8A, C38A, C108A, C130A) hNLRP3 PYD-NOD2-TagGFP2	pRP

3.1.9 Unmodified Cell Lines

Bacteria	**Source**
E. Coli DH5-α	Life Technologies

Mammalian	**Source**
BALB/c iMacs	Andrea Stutz
HEK-293T	ATCC
19.5 Reporter	Andrea Stutz / Gabor Horvath

3.1.10 Generated Cell Lines

I created and characterized all generated cell lines used in this study.

Generated line	Parental line	Insert
D6	HEK-293T	hASC-TagBFP
D6-716-5	D6	hNLRP3 PYD-NOD2
D6-1044-1-C5	D6	hAIM2-TagGFP
D6-1045-10-E3	D6	hNLRP3 PYD-hAIM2-TagGFP
D6-1154-1-A4	D6	hAIM2 PYD-NOD2
D6-1296-10	D6	(C8A) hNLRP3 PYD-NOD2
D6-1478-10	D6	(C38A) hNLRP3 PYD-NOD2
D6-1479-10	D6	(C108A) hNLRP3 PYD-NOD2
D6-1480-10	D6	(C130A h)NLRP3 PYD-NOD2
D6-1481-10	D6	(C8A, C38A) hNLRP3 PYD-NOD2
D6-1482-10	D6	(C108A, C130A) hNLRP3 PYD-NOD2
D6-1484-10	D6	(C8A, C38A, C108A, C130A) hNLRP3 PYD-NOD2

3.2 Cell culture and generation of cell lines

3.2.1 Passaging cell lines

Cells were cultured adherently in complete DMEM (DMEM supplemented with 10% FBS, 100U/ml penicillin and 100 μg/ml streptomycin), in a humidified 37^{O}C incubator at 5% CO_2. Cells were passaged every other day by removing the media, gently washing with DPBS, and detaching with Trypsin-EDTA. Cells were split into a new flask at a 1:10-1:20 dilution for immortalized mouse macrophages and 1:5-1:6 for HEK293T cells.

3.2.2 Freezing and thawing cell lines

Cells were harvested by removing the medium, gently washing with DPBS, and detaching with Trypsin-EDTA. Cells were counted and approximately 5 x 10^6 cells were aliquoted in 1 ml of 60% complete DMEM, 30% FBS, and 10% DMSO per cryo-vial. Using a cell freezing container, cells were placed in a -80 ^{O}C freezer and after 24 hours were transferred to a -150 ^{O}C freezer for long term storage. To thaw cells, the cryo-vial was rapidly heated until partially thawed using a 37 ^{O}C water bath. Cells were quickly transferred to a 50 ml centrifuge tube containing 10 ml complete DMEM and were pelleted by centrifugation at 340g for 5 minutes. Cells were resuspended in 12 ml complete DMEM and transferred to a T75 flask for culturing.

3.2.3 Counting Cell Number

Cells number was determined using the Tali Imaged-based cytometer, set to the Quick Count program, and averaging 20 images.

3.2.4 Generation of Packaged Retroviral Vector Supernatants

For each construct, 3 ml of media containing 5 x 10^5 HEK293T cells was plated in one well of a 6 well dish and incubated overnight. The medium was replaced with 1ml of fresh media. For transfection, a solution of 100 μl Optimem containing 8 μl Genejuice, and a solution of 10 μl Optimem containing a mixture of 100 ng VSV-G expression plasmid, 1 μg gag-pol expression plasmid and 2 μg of the retroviral construct to be packaged, were made and incubated for 5 minutes at room temperature. Both solutions were combined and incubated for an additional 20 minutes. All 110 μl was added to the cells and after overnight incubation, the media was replaced with 1 ml of DMEM containing 30% FBS and incubated overnight. The virus containing medium was removed and filtered through a 0.2 μM syringe filter.

3.2.5 Retroviral Transduction of Cell Lines

For each retroviral transduction, 1 x 10^5 cells were plated in 0.5 ml complete DMEM per well in a 24 well dish. After overnight incubation, cells were transferred to an S2 laboratory and filtered viral supernatant was added. The cells were incubated over night, then the medium was replaced with 0.5 ml fresh medium and incubated overnight. Cells were transferred 6 well dishes containing 2 ml medium containing selective antibiotic. After 3 days, the cells were passaged twice more before being transferred to an S1 laboratory.

3.2.6 Limiting Dilution Cloning of Cell Lines

Cells were grown to be 80-90% confluent in a T75 flask. The media was collected and filtered through an 0.2 μM syringe filter. Cells were collected, counted, and diluted to a concentration of 10 cells per ml in fresh medium containing 25% used media (conditioned media). 100 μl per well was added to four 96 well tissue culture dishes and incubated until distinct colonies had grown, which took a minimum of 6 days. Wells containing only one colony were transferred to a single 96 well tissue culture dish. The plate was split for 2 to 3 passages with each well split to approximately equalize the cell number. Two identical 96 well tissue culture plates were made, and one plate was assayed for function. Functional

clones were grown to 6 well tissue culture dishes, counted and re-assayed for function. The clone judged to have the best signal to noise ratio was chosen for further testing.

3.2.7 Transient Transfection of HEK293T Cells

10 μl Optimem containing the cDNA expression plasmid, brought to 100ng total plasmid DNA with plasmid #106 was added to the edge of each assay well inf a 96 well black optical plate. To the opposite edge of each assay well was added 10 μl Optimem containing 0.2 μl Lipofectamine 2000. After incubation at room temperature for 5 minutes, the separate solutions were mixed by gently tapping, and the plate was incubated at room temperature for 15 minutes. 1.8 x 10^4 cells in 100 μl of complete DMEM was added to each well and the plate was incubated in a humidified 37^{O}C incubator at 5% CO_2 for approximately 40 hours. 40 μl was removed from each well. 20 μl complete DMEM containing inhibitor was added to each well and the plate was incubated for 1 hour. 20 μl complete DMEM containing activator was added to each well and the plate was incubated for the time appropriate for the activator used. The cells were fixed by removing 80 μl from each well and adding 10 μl of 6x DRAQ5/ FA solution. Plates were stored at 4^{O}C, in the dark, until imaged.

3.2.8 siRNA transfection

Cells were harvested using Accutase, and diluted in complete DMEM to 2.4 x 10^5 cells per ml. 300 μl Optimem containing 3.6 μl siRNA (50 μM), and 300 μl Optimem containing 15 μl Lipofectamine RNAi Max were separately incubated at room temperature for 5 minutes, mixed in a 6 well dish, then incubated at room temperature for 5 minutes. 3 ml of Cells were added to each well and incubate overnight in a humidified 37^{O}C incubator at 5% CO_2. The media was replaced with fresh complete DMEM and incubated for a total transfection time of 40 hours. Cells were harvested using Accutase, pooled if multiple wells were identically transfected, and plated at 8 x 10^4 cells/well in a 96-well tissue culture plate. After 1.5 hours the medium was replaced with 100 μl media containing 200 ng/ml LPS and the cells were incubated for 2 hours in a humidified 37^{O}C incubator at 5% CO_2.

3.3 ASC Speck Imaging and Analysis

3.3.1 Stimulation of Macrophage Lines for imaging

Cells were harvested using Trypsin-EDTA, and 8 x 10^4 cells were plated in each well of a 96 well black clear bottom plate, in 80 μl complete DMEM. After overnight incubation in a humidified incubator at 5% CO_2, 20 μl of complete DMEM, with or without a 5x concentration of inhibitor, was added to each well and the plate was incubated again for 1 hour.
For nigericin stimulation, 20 μl of complete DMEM, containing 6x the final concentration of 10 μM nigericin, was added to each well and the plate was incubated again for 1.5 hours.
For poly (dA:dT) stimulation, 20 μl of Optimem containing 200ng poly (dA:dT) and 0.2 μl Lipofectamine 2000 was added to each well. The plate was centrifuged at 350g for 5 minutes, and then incubated again for 2 hours.
The cells were fixed by removing 80 μl from each well and adding 10 μl of 6x DRAQ5/ FA solution. Plates were stored at 4^{O}C, in the dark, until imaged.

3.3.2 Stimulation of HEK-293T Lines for imaging

Cells were harvested using Trypsin-EDTA, and 3 x 10^4 cells were plated in each well of a poly-L-Lysine coated 96 well black clear bottom plate, in 80 μl complete DMEM. After overnight incubation in a humidified 37^{O}C incubator at 5% CO_2, 20 μl of complete DMEM, with or without a 5x concentration of inhibitor, was added to each well and the plate was incubated again for 1 hour.
For L-18 MDP stimulation, 20 μl of complete DMEM, containing 6x the final concentration of 10 nM L18-MDP, was added to each well and the plate was incubated again for 2 hours.
For dsDNA stimulation, 20 μl of Optimem containing either poly (dA:dT) or Plasmid DNA, and 0.2 or 0.5 μl Lipofectamine 2000 was added to each well. The plate was centrifuged at 350g for 5 minutes, and then incubated again for 2 hours.
The cells were fixed by removing 80 μl from each well and adding 10 μl of 6x DRAQ5/ FA solution. Plates were stored at 4^{O}C, in the dark, until imaged.

3.4 Biochemical Assays

3.4.1 ELISA

Macrophage lines were stimulated in 96 well dishes. After incubation, plates were centrifuged at 350g for 5 minutes. 70-100μl supernatant was transferred to a new 96 well dish and stored

at either 4^{O}C or -20^{O}C until being assayed. ELISAs were performed according to the manufacturers recommended protocol, with the exception that all volumes were reduced by half. The resulting TMB substrate color change was measured at 450 nm and 570 nm using a Spectramax i3 plate reader. Standard curves and sample concentrations were calculated by the Spectramax i3 plate reader, using SoftMax Pro software.

3.5 Molecular Biology

3.5.1 Restriction Digestion

3-5 μg plasmid DNA, or a purified 50 μl PCR reaction, was digested in a final volume of 50 μl using 2 μl of each restriction enzyme, under the buffer conditions suggested by the manufacturer, for 1.5 h at 37^{O}C. Digested DNA bands were separated using an agarose gel of an appropriate percentage for the DNA band sizes (1-1.5% agarose). Agarose gels were made using 1x TAE buffer with either 1:50,000 ethidium bromide or 1:20,000 PeqGreen to allow the visualization of DNA bands using a UV table. Gels were run at 10V/cm until the DNA bands were clearly separated and the desired DNA bands were excised from the gel and purified using the PureLink Quick Gel Extraction Kit according to the manufacturers instructions.

3.5.2 Subcloning PCR

To transfer a DNA region from one plasmid to another, primers were designed to create wanted restriction sites flanking the desired region to be transferred, and were manufactured by Metabion. A 50 μl reaction containing 10 ng of the template DNA, 0.5 μM primers, and 25 μl PfuUltra II Hotstart PCR Master Mix was subjected to the following PCR program:

1x cycle: 95^{O}C 60 s
30x cycle: 95^{O}C 30 s, 60^{O}C 30 s, 72^{O}C 60 s per kb
1x cycle: 72^{O}C 8 min

PCR reactions were purified using the PureLink Quick Gel Extraction Kit according to the manufacturers instructions. Each PCR reaction was digested with restriction enzymes and the desired product was isolated and purified following the restriction digestion protocol.

3.5.3 Site Directed Mutagenesis

To add useful cloning restriction sites, remove start or stop codons, or create point mutations within approximately 30 bp of the ends of the PCR product, the PCR primers used for the subcloning PCR were designed to introduce these modifications into the PCR product. For more internal modifications, either overlap extension PCR, or the QuikChange site-directed mutagenesis protocol was used.

3.5.3.1 Overlap Extension PCR

For overlap extension PCR, two sets of PCR primers were designed to create two PCR products. The 5' primer of the N-terminal product contains a restriction site for cloning, and the 3' primer matches the target sequence except for the designed mutation. The 5' primer of the C-terminal product matches the sequence and designed mutation in the N-terminal product's 3' primer, creating the identical overlap between the two products. The 3' primer of the C-terminal product contains a restriction site for cloning. Each PCR product reaction was performed and purified using the subcloning PCR protocol. A new PCR reaction is created using an equimolar amount of both products as template and used the far 5' primer and 3' primers for amplification. The resulting full length product was digested and purified for cloning using the restriction digestion protocol.

3.5.3.2 QuikChange Site-Directed Mutagenesis

Primers of approximately 30-35 bp were designed to contain the wanted mutations in the center of the primers, with both the 5' and 3' primers being designed to the same plasmid sequence. PCR was used to copy the entire plasmid from each primer. A 50 μl reaction containing 10 ng of the template DNA, 0.25 μM primers, and 25 μl PfuUltra II Hotstart PCR Master Mix was subjected to 20 cycles of amplification using the subcloning PCR protocol. 1 μl of The restriction enzyme Dpn I was added to degrade any methylated template plasmid DNA, and the PCR reaction was incubated for 1 h at 37^{O}C. Part of the reaction was transformed into DH-5α using the standard protocol. Clone modification was verified by DNA sequencing. The insert from a clone with the introduced mutations was isolated by restriction digest and reinserted back into the parental background plasmid to remove any PCR introduced mutations in other regions of the plasmid.

3.5.4 Ligation

1.5 μl of Purified vector and insert(s) were combined with 0.5 μl ligase and 2 μl 5x ligase buffer in 10 μl final volume, and incubated at 22^{O}C for 1.5 h. Ligations were either used directly, or after storage at -20^{O}C for transformation into E. Coli.

3.5.5 Transformation

An aliquot of chemically competent *E. coli* K-12 strain DH-5α was thawed on ice. 0.5 μl of a ligation reaction was added to 10 μl of competent cells on ice, and was incubated for 30 min with occasional gentle tapping to mix. The cells were heat shocked at 42^{O}C for 45 s, then returned to ice for 2 min. 90 μl of LB medium was added and the tube was incubated at 37^{O}C for 1 h. The transformation mixture was spread evenly on an LB agar plate containing selective antibiotic, 100 μg/ml ampicillin in most cases. The plate was incubated at 37^{O}C overnight, and individual colonies were selected for growth and DNA preparation.

3.5.6 *E. coli* Glycerol Stock

For long term storage, *E. Coli* clones containing plasmids of interest were grown in 5 ml of LB medium containing the appropriate antibiotic, at 37^{O}C overnight with vigorous shaking for aeration. 600μl of freshly grown bacteria was added to 400μl 50% glycerol in a 1.5 ml snap cap tube. The tube was briefly mixed by vortexing, then stored at -80^{O}C.

3.5.7 Plasmid DNA Preparation

Isolated colonies were transferred from LB agar plates into 5 ml LB medium containing the appropriate antibiotic, normally 100 μg/ml ampicillin, and shaken overnight at 37^{O}C with vigorous shaking. Purified plasmid DNA was isolated from 2 ml of bacterial suspension using the PureLink Quick Plasmid Miniprep Kit, according to the manufacturer's protocol. Glycerol stocks were made of clones that were verified by restriction digest and sequencing. The larger plasmid DNA preparations used for experimentation, and to create cell lines, were made by adding 5 μl of a glycerol stock to 100 ml LB medium containing the appropriate antibiotic, and incubating overnight at 37^{O}C with gentle shaking for aeration. Plasmid DNA was isolated and purified using the PureLink Quick Plasmid Maxiprep Kit, according to the manufacturer's protocol. The identity of each large-scale plasmid preparation was confirmed by sequencing.

3.5.8 Plasmid DNA Sequencing

The cloned sequences in final plasmid constructs were confirmed using Sanger sequencing, by GATC Biotech. DNA Alignments and sequence comparisons were done using the Geneious DNA analysis software.

3.5.9 RNA extraction

Cells from 5 identical wells of siRNA transfected BALB/c immortalized macrophages plated in a 96 well dish were harvested and pooled. Cells were lysed in 350μl RLT buffer containing 1% β-mercaptoethanol, with brief vortexing. Lysates were stored at -80^{O}C until RNA was extracted using the RNeasy minikit according to the manufacturers protocol. DNase I digestion was performed on the RNA binding columns for 15 min at RT. RNA was eluted in RNase free water and quantified by measuring absorbance at 260 nm on the SpectraMax I3 plate reader. RNA was kept on ice while thawed, and stored frozen at -80^{O}C.

3.5.10 First-Strand cDNA synthesis

For each sample, 1 μg RNA was adjusted to 12.9μl with RNAse free water. 1μl of oligo-dT(18) primer was added and the mixture was incubated at 65^{O}C for 5 min, then transferred to ice. 4 μl 5x reaction buffer, 1 μl 100 mM DTT, 1 μl 10 mM dNTPs, and 0.1 μl Superscript III reverse transcriptase was added, and the reaction was incubated at 50^{O}C for 50 min. The reaction was terminated by incubation at 85^{O}C for 5 min. For each sample, an identical reaction, substituting RNase free water for the Superscript III reverse transcriptase, was done to control for genomic DNA contamination. cDNA samples were stored at -20^{O}C.

3.5.11 QPCR

For quantitative real time PCR, in each well of a 384-well qPCR plate, 2 μl of cDNA, diluted 1:200 in water, was mixed with 8 μl master mix containing 1 μl each of 2μM forward and reverse primers, 1μl RNAse free water and 5 μl 2x Maxima Sybr Green/ROX master mix. 40 cycles of amplification were performed with the following protocol using a QuantStudio 6 Real-Time PCR System.

1x cycle: 95^{O}C 10 min
40x cycle: 95^{O}C 15 s, 60^{O}C 1 min

After the PCR program was finished, a melt-curve analysis was performed from a range of 60^{O}C to 95^{O}C with 0.05 ^{O}C/s. Gene expression was normalized to the constitutive control gene *HPRT*.

4 Results

4.1 Screen of Small Molecule Compound Libraries for NLRP3 Inhibitory Activity

In order to screen compounds as small molecular inhibitors of NLRP3 mediated inflammasome activation, a reporter cell line was used that can monitor inflammasome activation by fluorescent confocal microscopy. An immortalized macrophage line derived from the NLRP3 knock out mouse, and reconstituted with mouse NLRP3, was used as the parental cell line. Human ASC-mCerulean was added by retroviral transduction, and a final cell line was selected after cloning by limiting dilution, and selection for low background and high response to inflammasome activators, as described in [55]. The clone chosen for screening was designated as the 19.5 reporter cell line.

Since the 19.5 reporter line constitutively expresses NLRP3 and ASC-mCerulean, it does not require priming for ASC speck formation in response to inflammasome activators. This allows screening for compounds that inhibit the ability of NLRP3 to interact with ASC to form a speck, instead of inhibitors of upstream priming or caspase-1 mediated downstream pathways.

A fully automated screening protocol was developed with Drs. Denner and Fava at the German center for neurodegenerative diseases (DZNE). The bacterial pore forming toxin, nigericin, and the lysosomal destabilizing agent Leu-Leu-OMe, were used as two types of NLRP3 activators.

Two commercially available libraries of pharmacologically active compounds, Lopac 1280 and Tocriscreen libraries, which have a combined total of approximately 2500 compounds, were screened at 3 doses (0.1μM, 1 μM, 10 μM) for their ability to inhibit nigericin and Leu-Leu-OMe induced ASC speck formation.

400 compounds, which showed at least some ability to inhibit or enhance either nigericin or Leu-Leu-OMe induced ASC speck formation, were rescreened in a larger dose range. 139 compounds showed some ability to inhibit nigericin and or Leu-Leu-OMe .

A final screen of these 139 compounds was performed with the addition of two non-NLRP3 mediated inflammasome activators, poly(dA-dT) for the AIM2 inflammasome, and Lethal toxin for the NLRP1B inflammasome, to confirm which inhibitory compounds were NLRP3 specific.

6 compounds were selected for further study as NLRP3 inhibitors (Figure 1). Two of these compounds, BAY 11-7082 and parthenolide, had been previously identified as NLRP3 inhibitors [56], and parthenolide was used as a positive control in the screen. Four of these compounds, CH55, ebselen, NSC632830, and pifithrin-μ, had not been published as NLRP3 inhibitors.

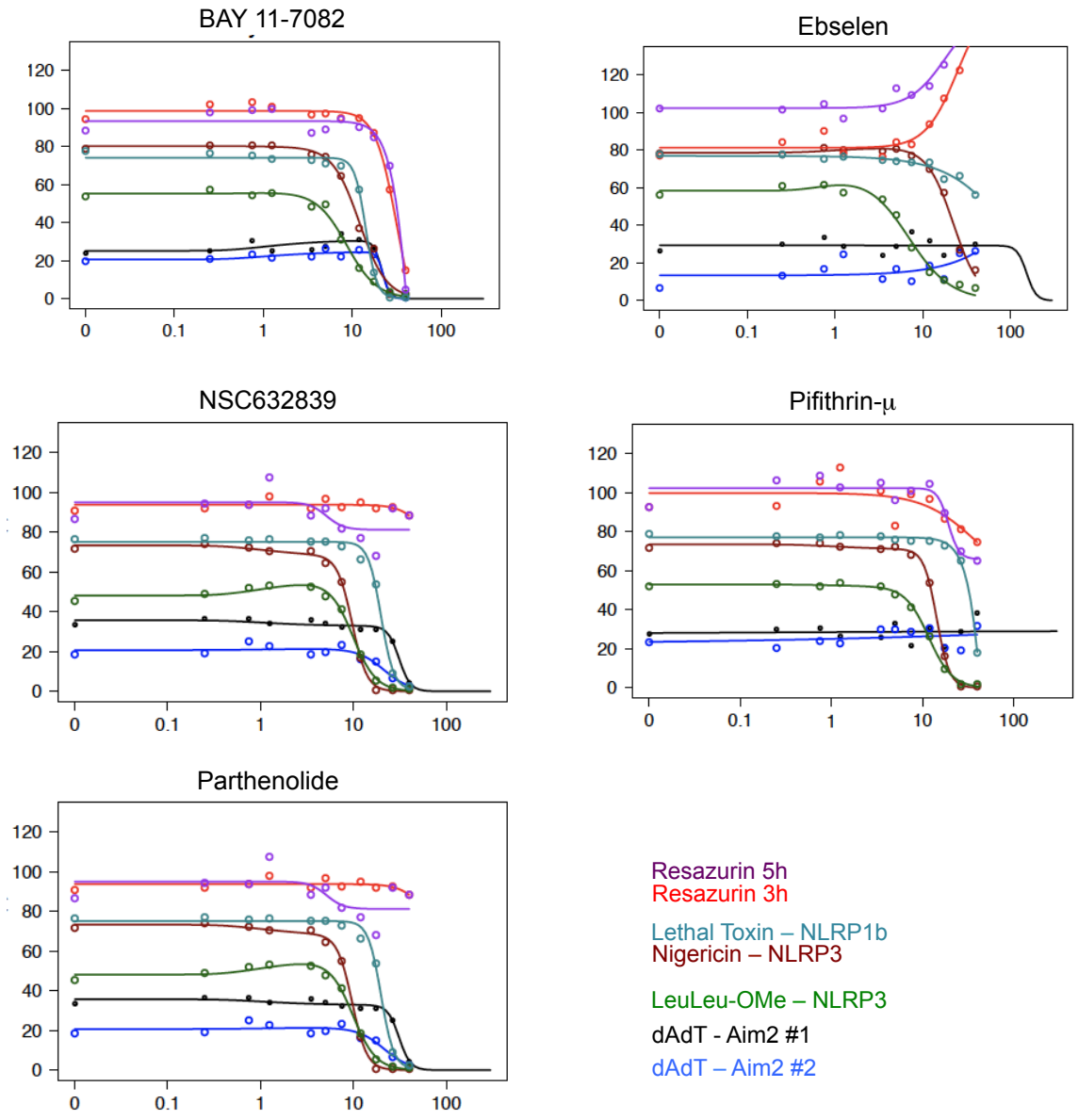

Figure 1: Compounds from library screen chosen for study as NLRP3 inhibitors
Immortalized mouse macrophage 19.5 reporter cells, were incubated with a titration of compound for 1 h. They were then stimulated with 10 μM nigericin for 1.5 h, 1 μg/ml lethal toxin, for 2 h, 0.5mM Leu-Leu-OMe for 2h, or 200 ng poly(dA-dT) for 4 h. Cells were fixed and the nuclei were stained using DRAQ5, Cells were imaged by confocal microscopy. Resazurin was used to monitor cell viablity after incubation for the time specified with compound. Graphs were created by Philip Denner.

4.2 Investigation of the PYD of NLRP3 as a Target of Small Molecule Inhibitors

NLRP3 has three functional domains which are possible targets of inhibitors, the pyrin domain, the Nacht domain, and the LRR domain. The pyrin domain is contained within the second exon of the NLRP3 gene, and is followed by a small exon linking it to the NACHT domain containing forth exon. The exon structure of AIM2 also has the pyrin domain encoded by a single exon, and a short exon linking it to the Hin domain. All pyrin domain containing constructs also include the short linker, unless specifically mentioned. In order to test for inhibition of the pyrin domain, three approaches using chimeric reporters were attempted.

The first system to induce NLRP3 pyrin mediated ASC specking involved combining the pyrin domain of NLRP3 with the Clontech's iDimerize system, which uses a modification of the rapamycin induced dimerization domain of FKBP12. In this case, the pyrin domains of NLRP3, and AIM2, were fused to the homodimerization DMRB domain and are fluorescently tagged with TagGFP2. This system is the most artificial system, but it also the simplest, relying on only on the forced dimerization of the pyrin domain.

The second system is the creation of a chimeric receptor, with the pyrin domain of NLRP3 replacing the pyrin domain of AIM2.

The third system involved the use of another NLR receptor, NOD2, which has a known ligand. NOD2 is an intracellular receptor, structurally similar to NLRP3, which contains a NACHT domain and a LRR domain. It differs from NLRP3 by containing two tandem CARD domains at it's N-terminus, instead of the single pyrin domain of NLRP3 [57,58]. Upon binding MDP to the LRR domain, the CARD domains of NOD2 interact with RIP2, leading to the activation of the NF-κB signaling pathway [59-61]. It was previously shown that replacing the two CARD domains of NOD2 with the CARD domain of NLRC4 resulted in an MDP inducible receptor able to interact with ASC [62,63] Similar chimeric receptors were made by replacing the two CARD domains of NOD2 with the pyrin domains of either AIM2 or NLRP3. These chimeric versions of NOD2, if functional as the published NLRC4 version, would be able to mediate pyrin induced ASC specking after MDP activation.

4.2.1 Small molecule induced Dimerization of the NLRP3 PYD to Induce ASC Specking

In the first system, chimeric receptors were made in which the pyrin domains of AIM2 and NLRP3 were fused to the iDimerize homodimerization domain. When stability expressed in

HEK293 cells containing ASC-Cerulean, dimerization of the pyrin domains can be induced by the addition of the cell permeable B/B homodimerizer. This forced dimerization of the pyrin domain is sufficient to initiate the nucleation of the Cerulean tagged ASC into a large speck-like aggregate. In order to test if single dimers were sufficient to induce ASC specking, as apposed to a larger lattice of pyrin domains, three variations of each pyrin domain chimeras were created. One, two, or three tandem dimerization domains were fused to the pyrin domains of NLRP3 or AIM2, and each was expressed in HEK/ASC-Cerulean cells by retroviral transfection. The design and construction of the expression vectors for these chimeric receptors, and the bulk transection into Flp-in HEK-293 expressing ASC-Cerulean, was done by Gabor Horvath. I created individual clones of each of these cell lines by dilution cloning, and tried to isolate clones that visibly specked ASC-Cerulean upon treatment with B/B homodimerizer. Acceptable clones were only isolated for the NLRP3 pyrin/ single DMRB, and the AIM2 pyrin / double DMRB, due to the large background of constitutively specking cells in the bulk population of each cell line. Several NLRP3 inhibitors were tested for the ability to inhibit dimerization induced specking, and both Parthenolide and 5-Z7-Oxozeanol were able to dose dependently inhibit The NLRP3 pyrin domain containing construct at does which did not inhibit the AIM2 pyrin domain containing construct (Figure 2).

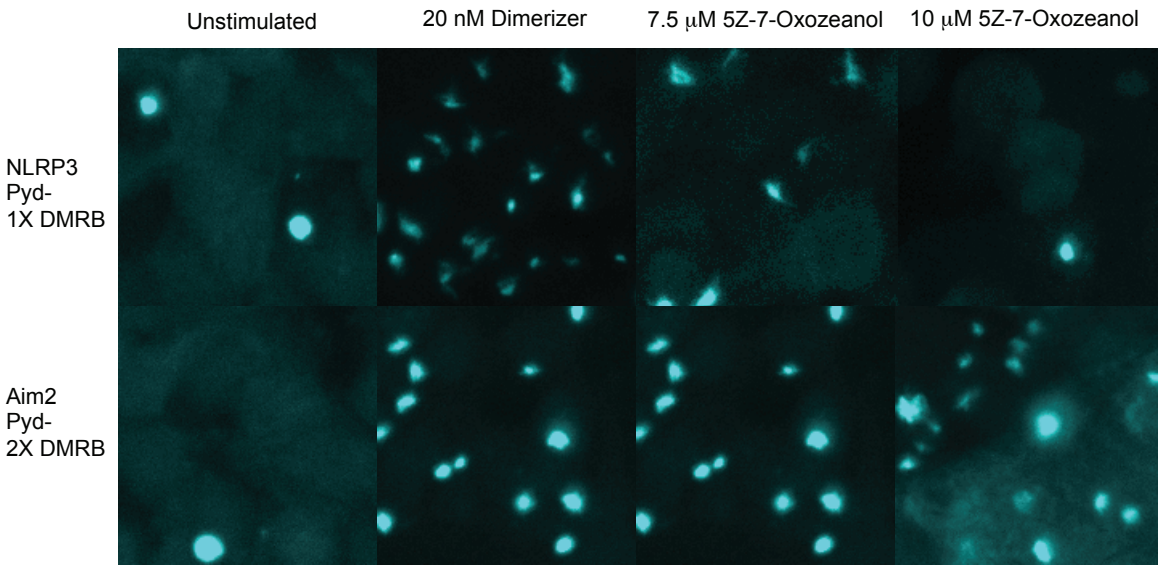

Figure 2: AIM2pyd and NLRP3pyd mediated ASC speck formation in HEK-293T cells
Flp-in TRex HEK cells expressing ASC-mCerulean and either NLRP3pyd-DMR or AIM2pyd-DMR2 were incubated in complete media containing a titration of 5Z-7-Oxozeanol for 1 h. Cells were then stimulated with 20 nM B/B Dimerizer for 2 h. Cells were fixed and ASC-mCerulean was imaged by using a Zeiss fluorecent microscope.

In order to create a properly matched set of clones for inhibitor screening, single DMRB-TagGFP2 constructs containing the non-tagged extended pyrin domain of either NLRP3 or AIM2 were created. These were transferred by retroviral transduction in an HEK293T line expressing ASC-TagBFP, which forms more distinct ASC specks than the large irregular ASC specks formed in the Flp-in HEK/ASC-mCerulean cell line. Unfortunately, no cell lines expressing the AIM2pyd construct were isolated with an acceptable signal to noise ratio. Due to the inability to create a matching AIM2pyd control line, the dimerizer induced pyrin domain mediated ASC specking system was not further explored.

4.2.2 Substituting the PYD of AIM2 with the PYD of NLRP3

Chimeric receptors swapping the pyrin domains of NLRP3 and AIM2 were retrovirally transfected into the HEK-293T/ASC-TagBFP cell line (D6 cells) and cloned by limiting dilution. For the AIM2pyd-NLRP3 construct, only constitutively active clones were isolated. Functional cell line clones of the AIM2 control and the NLRP3pyd-AIM2 chimera were isolated which initiate ASC specking in response to poly(dA-dT), a synthetic double-stranded DNA (dsDNA) ligand of AIM2.

I had previously observed in mouse iMacs, that if the plated cells were centrifuged briefly after the addition of the dsDNA transfection mixture, both the amount of IL-1β released was increased, and the time required for it to be released was reduced. To optimize percent ASC specking in the AIM2 based HEK lines in response to dsDNA, titrations of two AIM2 ligands, poly(dA-dT) and plasmid #106, were compared. Plasmid #106 is the E. Coli expression plasmid pUC18 with a modified polylinker. This plasmid lacks any mammalian expression elements. Transfection conditions were optimized by titrating the amount of DNA verses the amount of Lipofectamine2000 transfection reagent. Percent ASC specking induced by the AIM2 and NLRP3pyd-AIM2 receptors is summarized (Figure 3).

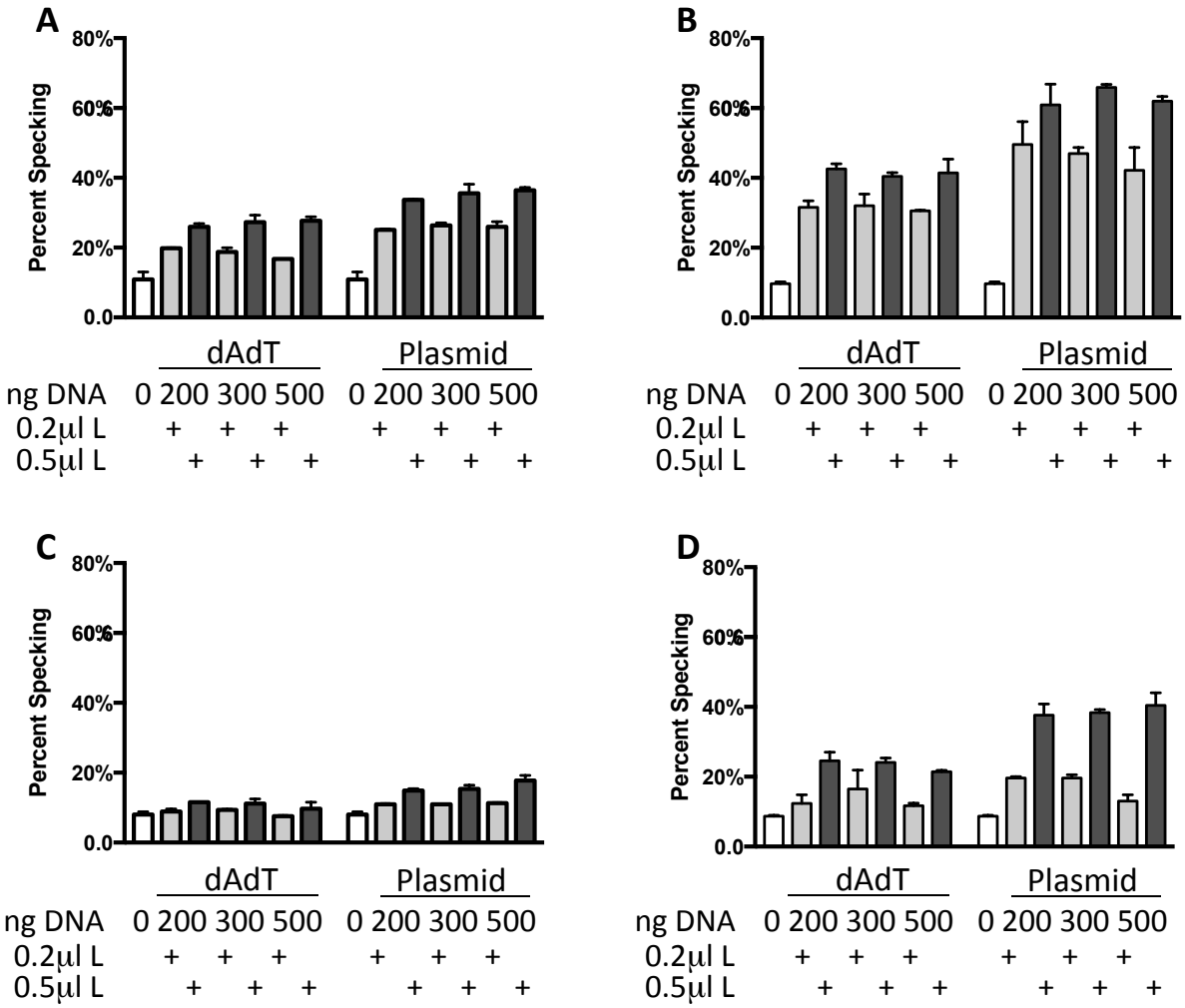

Figure 3 : Optimization of percent specking in activated of AIM2 and Chimeric AIM2-NLRP3pyd receptors.
(A-B) HEK cells expressing ASC-TagBFP and AIM2 were stimulated with a titration of poly(dA-dT) (dAdT) or plasmid DNA with 2 concentrations of Lipfectamine2000. Cells were either directly incubated (A) or centrifuged at 350g for 5 min (B). **(C-D)** Cells expressing ASC-TagBFP and chimeric AIM2-NLRP3pyd were treated identically to cells in (A-B). After 2 h cells were fixed and the nuclei were stained using DRAQ5. Cells were imaged by confocal microscopy. Results are of one experiment done in triplicate.

For both AIM2 based constructs, plasmid #106 DNA was a better activator than poly(dA-dT). Briefly centrifuging the DNA transfection mixture before incubation also significantly increased percent specking. Based on this data, a mixture of 200 ng of plasmid #106 and 0.5 μl Lipofectamine2000, with centrifugation, was used to activate AIM2 based receptors in HEK/ASC-TagBFP cells. An example of the ASC specking induced under these conditions is shown (Figure 4).

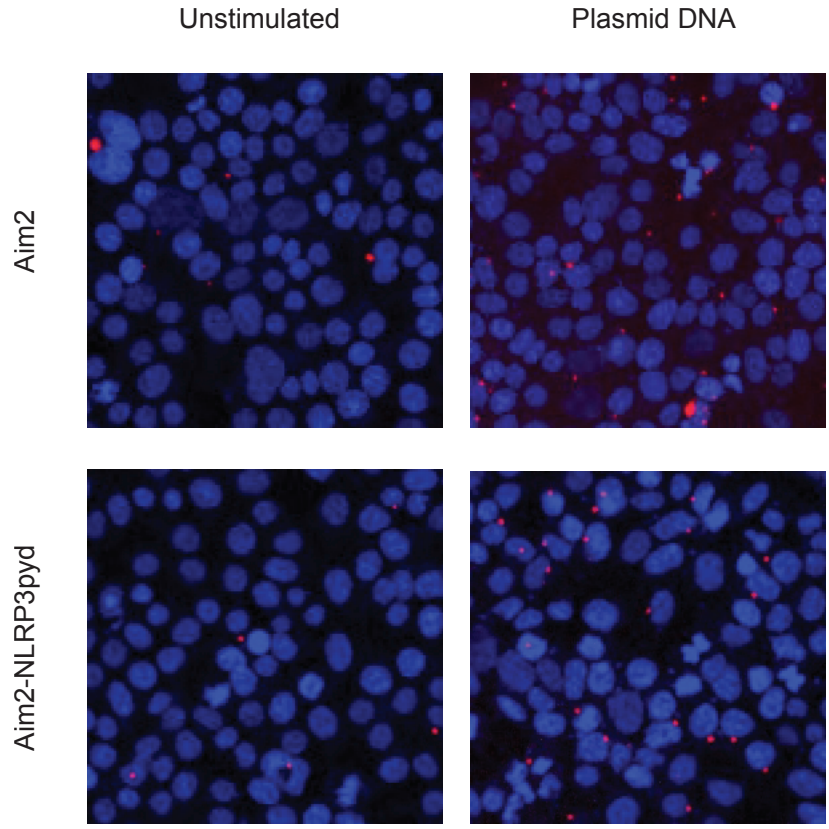

Figure 4: AIM2 and Chimeric AIM2-NLRP3pyd receptors mediate ASC speck formation in HEK-293T cells in response to plasmid DNA
HEK cells expressing ASC-TagBFP and either AIM2 or AIM2-NLRP3pyd were then stimulated with 200 ng plasmid DNA for 2 h. Cells were fixed and the nuclei were stained using DRAQ5. Cells were imaged by confocal microscopy. Representative images were chosen, with Nuclei being shown in blue and ASC specks being shown in red.

4.2.3 Replacing the CARDs of NOD2 with the AIM2 or NLRP3 PYD Results in ASC Specking in Response to L18-MDP

The NLRP3 PYD-NOD2 Chimera was tested by transient transfection into D6 (HEK/ASC-TagBFP) cells. This chimeric receptor was able to induce ASC speck formation in response to L18-MDP. Stable cell lines were created by retroviral transfection into D6 (HEK/ASC-TagBFP) cells with both the NLRP3 PYD and AIM2 PYD containing NOD2 chimeric constructs. Stable lines were selected for both constructs using puromycin. Clonal selection by limiting dilution was required to isolate an acceptable functioning cell line for the AIM2 PYD domain containing NOD2. The bulk population of the NLRP3 PYD-NOD2 expressing D6 cells was functional and did not require isolating individual clones. Examples of ASC speck induction in these cell lines are shown (Figure 5).

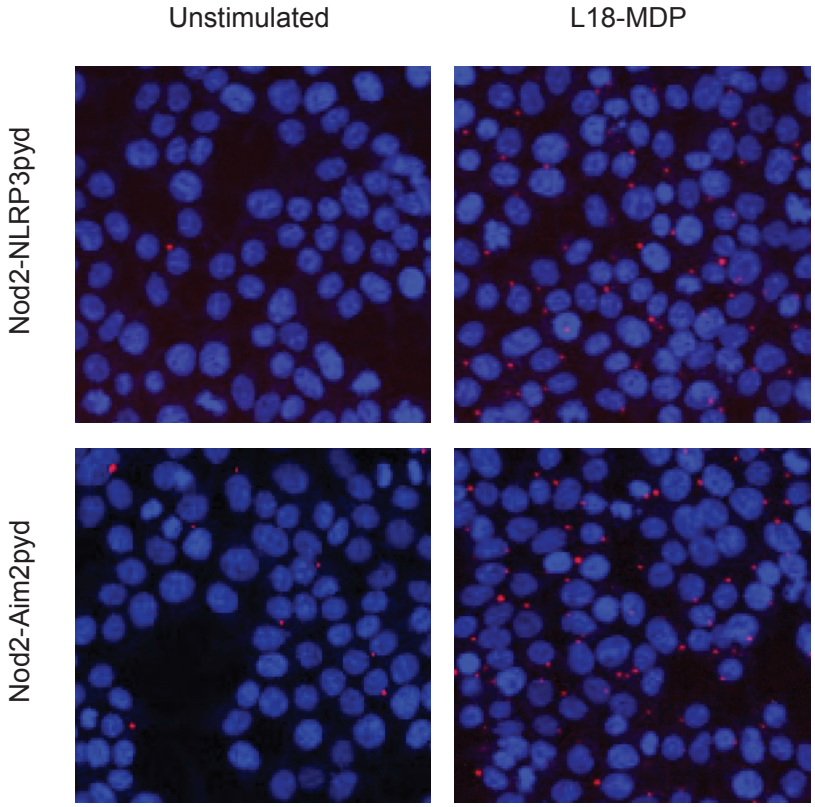

Figure 5 : Chimeric NOD2-NLRP3pyd and NOD2-AIM2pyd receptors mediate ASC speck formation in response to L18-MDP
HEK cells expressing ASC-TagBFP and either AIM2 or AIM2-NLRP3pyd were then stimulated with 10 nM L18-MDP for 2 h. Cells were fixed and the nuclei were stained using DRAQ5. Cells were imaged by confocal microscopy. Representative images were chosen, with Nuclei being shown in blue and ASC specks being shown in red.

4.2.4 Small Molecule Inhibitors of the PYD of NLRP3

All small compound inhibitors used, including the eight compounds examined in this section are shown in (Figure 6). Four compounds were identified from the inhibitor screen: CH55, ebselen, NSC632830, and pifithrin-μ. Four compounds had been previously published as NLRP3 inhibitors: 5-Z7-oxozeanol, arglabin, BAY 11-7082, and parthenolide. The compounds were tested to confirm their ability to inhibit NLRP3 induced specking in the 19.5 reporter cell line when compared to AIM2 induced specking (Figure 7).
All compounds were confirmed to inhibit NLRP3 mediated ASC speck formation with greater potency than AIM2 mediated ASC speck formation. All of the eight compounds were chosen to be further explored.

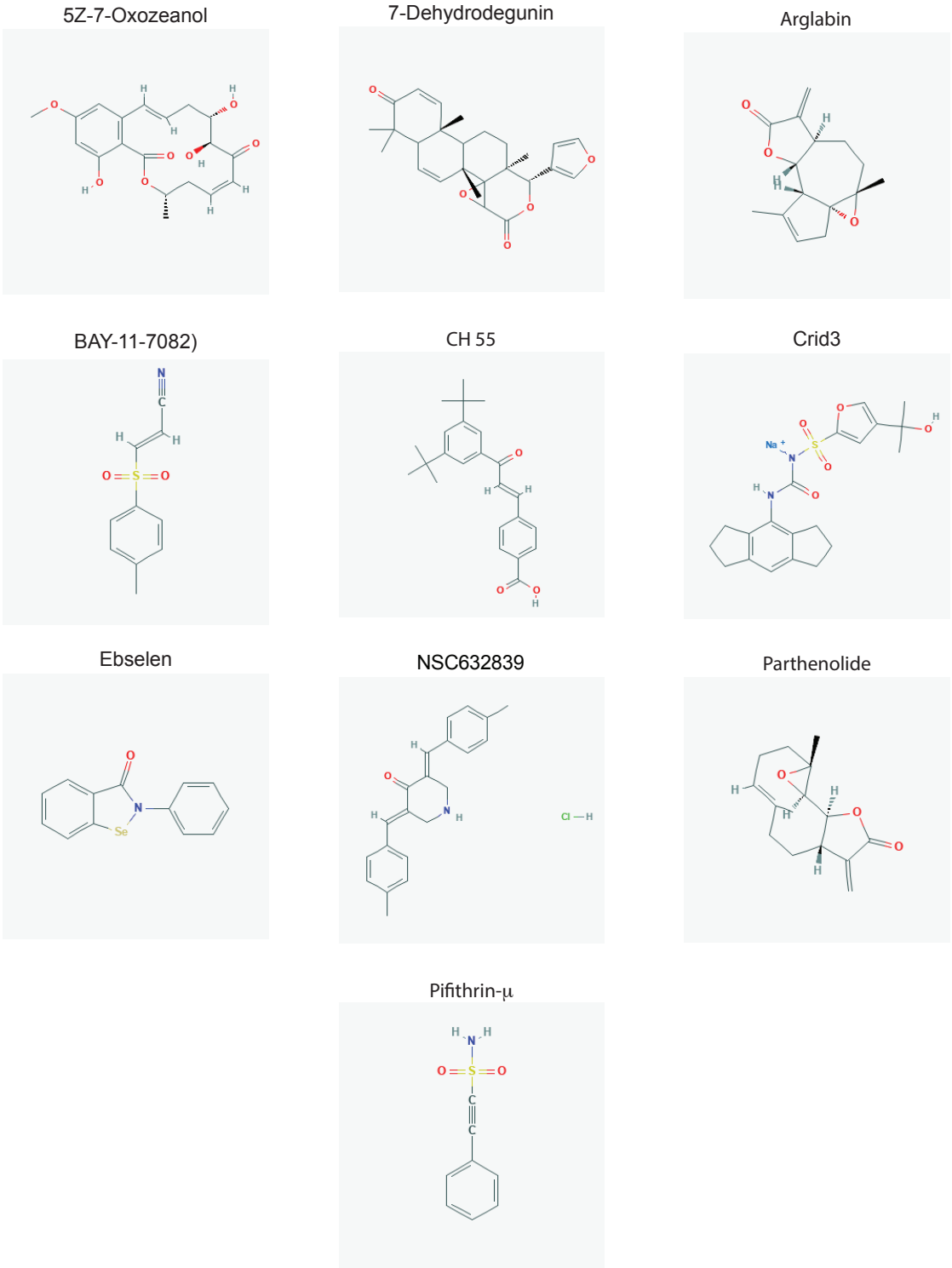

Figure 6 : Structure of small molecule compound investigated.
Structures are from pubchem.

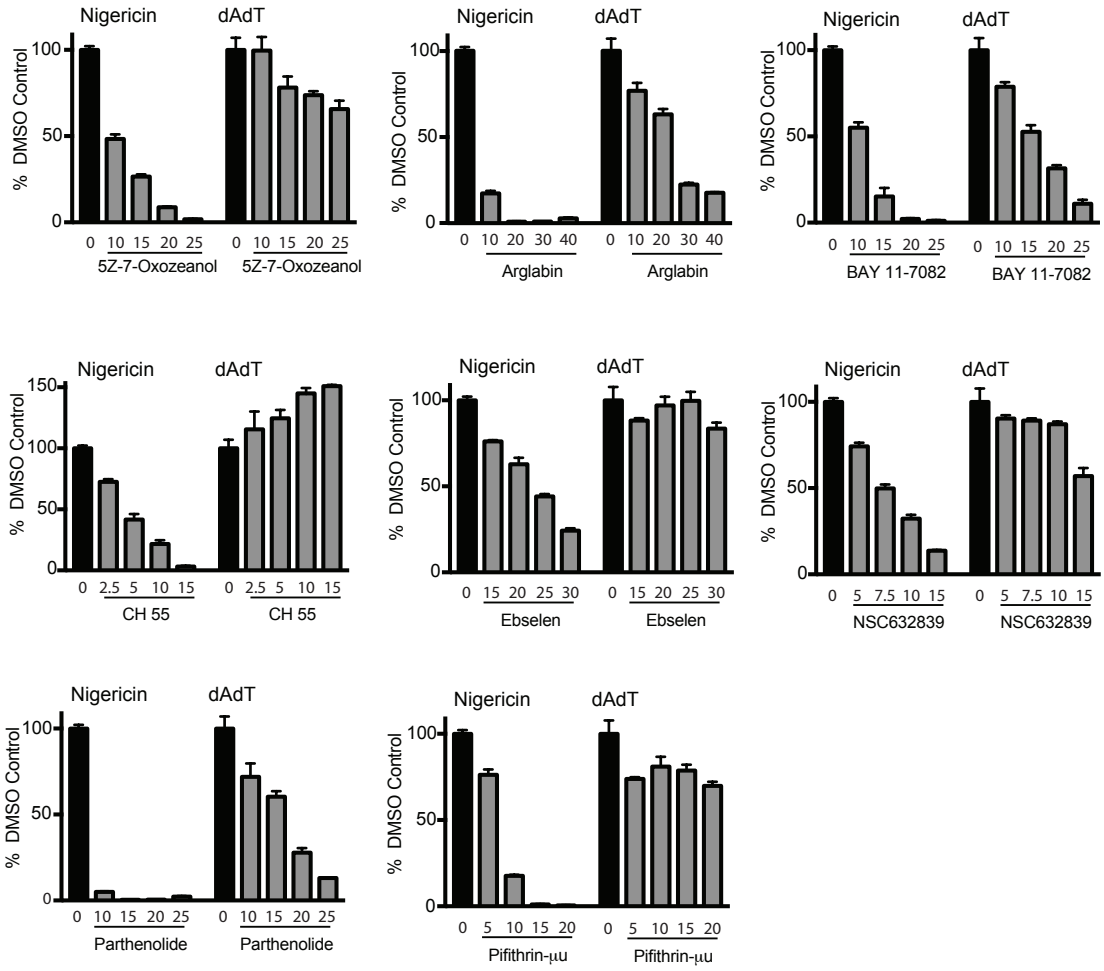

Figure 7 : Small molecule compounds which preferentially inhibit NLRP3 compared to AIM2 mediated specking.
Immortalized mouse macrophage 19.5 reporter cells, were incubated with a titration of compound for 1 h. They were then stimulated with 10 μM nigericin for 1.5 h or 200 ng poly(dA-dT) for 2 h. Cells were fixed and the nuclei were stained using DRAQ5, Cells were imaged by confocal microscopy.

The NOD2 chimeric reporters had a lower constitutive background and a higher induced percent specking when compared to the AIM2 based cell lines. Due to this increased dynamic range, the eight compounds were then tested on the NLRP3 PYD-NOD2 and AIM2 PYD-NOD2 reporter lines for their ability to inhibit specking (Figure 8). Of the eight compounds, four showed a dose dependent inhibition of the NLRP3 containing construct over the AIM2 PYD containing construct (Figure 8 A), and four did not (Figure 8 B).

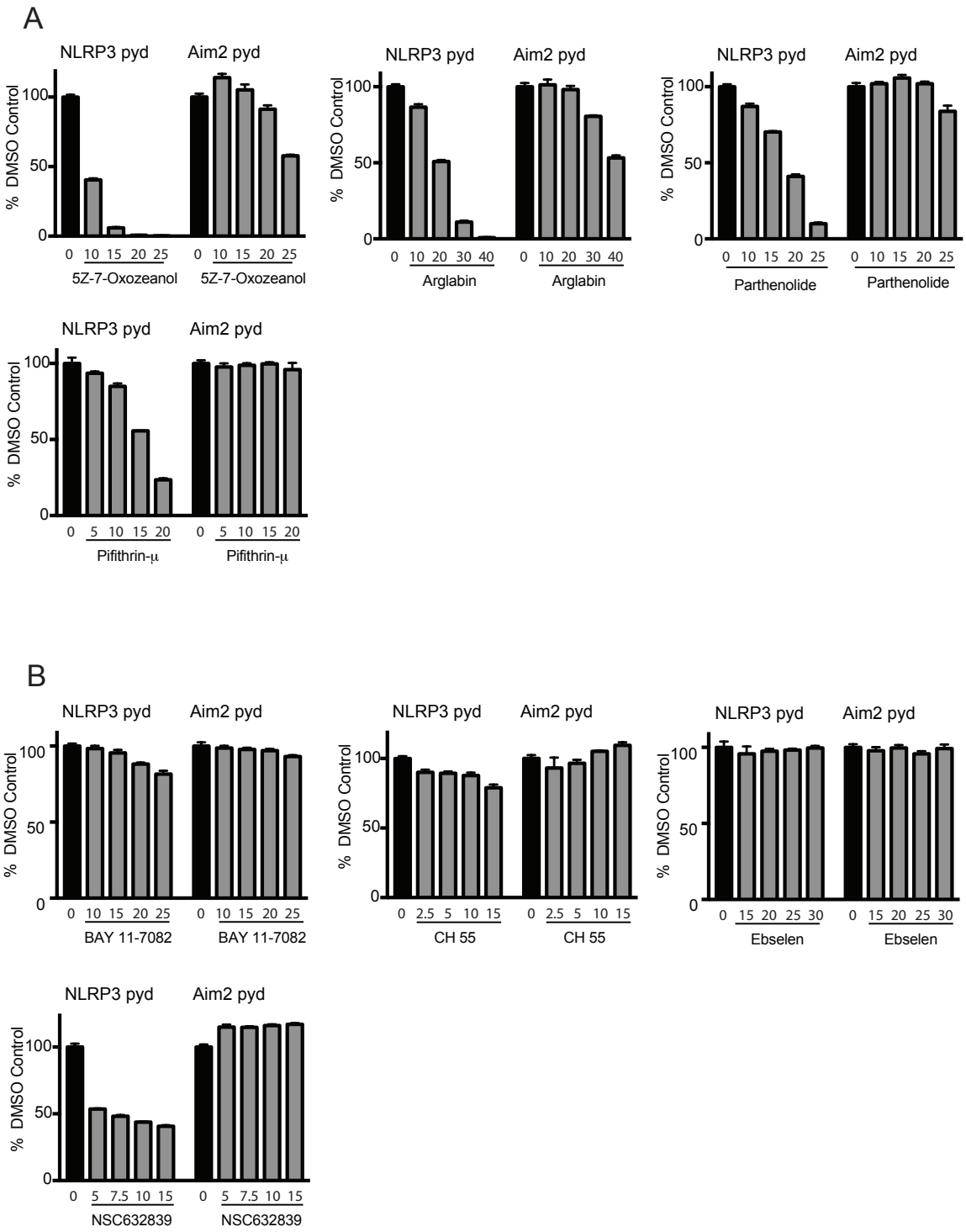

Figure 8 : 4 small molecules which preferentially inhibit NLRP3 pyd compared to AIM2 pyd mediated specking.
HEK-293T cells expressing Asc-TagBFP and either NOD2-NLRP3pyd or NOD2-AIM2pyd were incubated with a titration of compound for 1 h. They were then stimulated with 10 nM L18-MDP for 2 h. Four compounds tested showed dose dependent inhibition of NOD2-NLRP3pyd compared to NOD2-AIM2pyd **(A)** Four compounds did not **(B)**. Cells were fixed and the nuclei were stained using DRAQ5. Cells were imaged by confocal microscopy.

4.3 Investigation of Cysteines in the NLRP3 PYD as Possible Targets of Inhibitory Compounds.

Out of the 4 compounds which showed NLRP3 PYD specific inhibition, 3 of them are known to be cysteine binding compounds. The region from NLRP3 used in the NOD2 chimeric receptor contains four cysteines, the region of AIM2 in the chimeric receptor contains no cysteines.

It has been reported that two of the cysteines, C8 and C108, formed a disulfide bond when this region was subjected to X-ray crystallography [64]. The authors of this paper speculated that this disulfide bond could be important in the function of NLRP3, perhaps explaining the role of ROS in NLRP3 activation. They presented no data to confirm this hypothesis, and this finding does not seem to have been further explored.

4.3.1 Effect of Complete Cysteine to Alanine Substitution in the NLRP3 PYD on the Effectiveness of Inhibitory Compounds.

An NLRP3 PYD-NOD2 chimeric construct was made where the four cysteines within the NLRP3 PYD were substituted with alanine. A clonal HEK based D6 reporter line was made using this construct, and it was capable of inducing speck formation when activated by L18-MDP. This construct shows that none of these cysteines is critical for PYD/ASC interaction. The four NLRP3 PYD specific inhibitors were tested on this cell line and compared to the cell line containing parental construct (Figure 9).

When compared to the wild type NLRP3 PYD reporter, only one compound, pifithrin-μ, showed a reduced ability to inhibit the cysteine substituted construct. Interestingly, this compound is not known to be a cysteine reactive compound. For further study of the affect of pifithrin-μ on cysteine substituted receptors, a single dose of 25 μM is used (Figure 10).

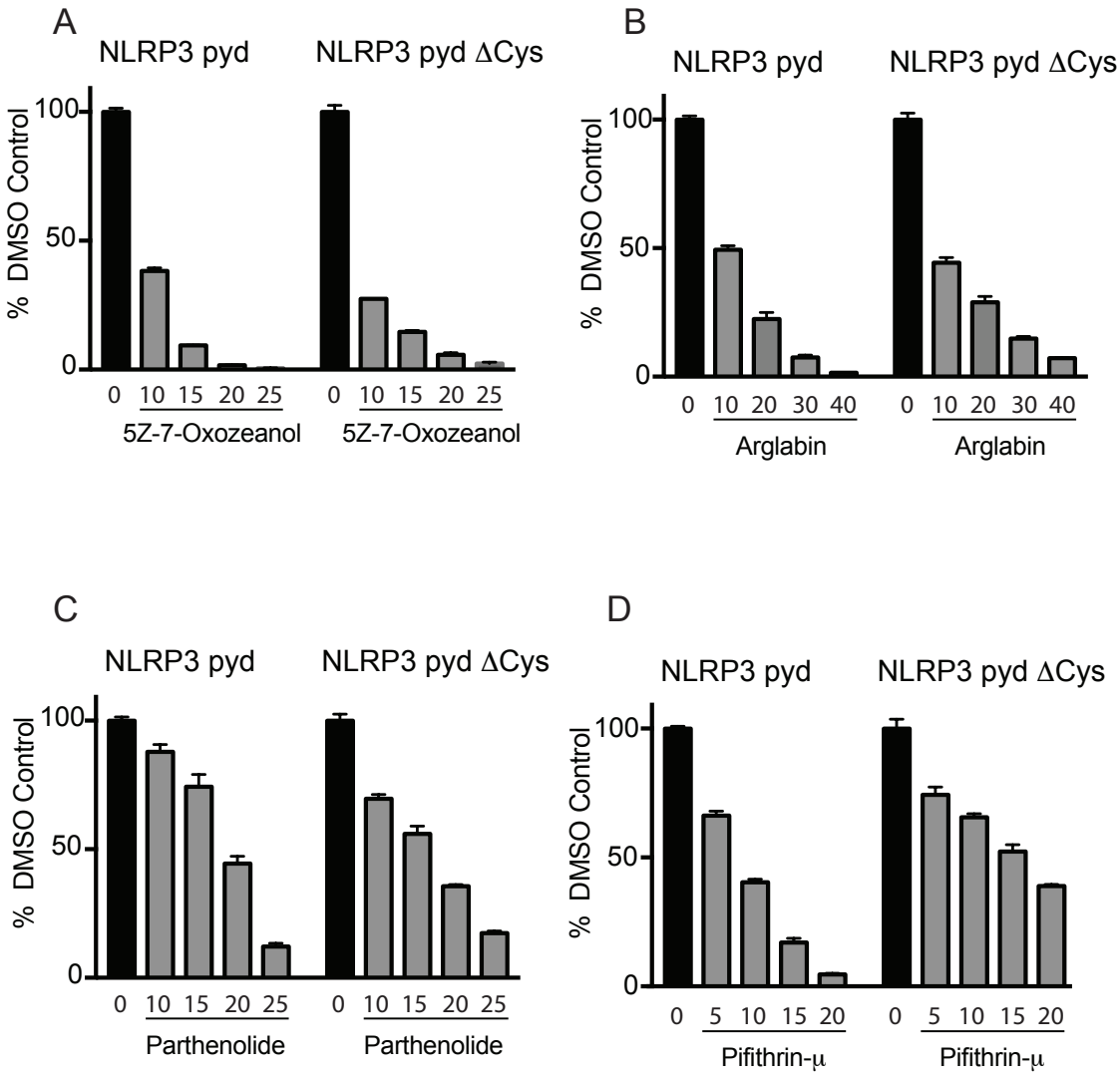

Figure 9 : Inhibition of the chimeric NOD2-NLRP3pyd receptor with all NLRP3 domain cysteines substituted to alanine.
(A-D) HEK cells expressing ASC-TagBFP and either NOD2-NLRP3pyd or NOD2-NLRP3pyd (C8A + C38A + C108A + C130A) were incubated with a titration of compound for 1 h. (A) 5Z-7-Oxozeanol, (B) arglabin, (C) parthenolide, (D) pifithrin-μ. Cells were then stimulated with 10 nM L18-MDP for 2 h. and fixed, with the nuclei being stained using DRAQ5. Cells were imaged by confocal microscopy

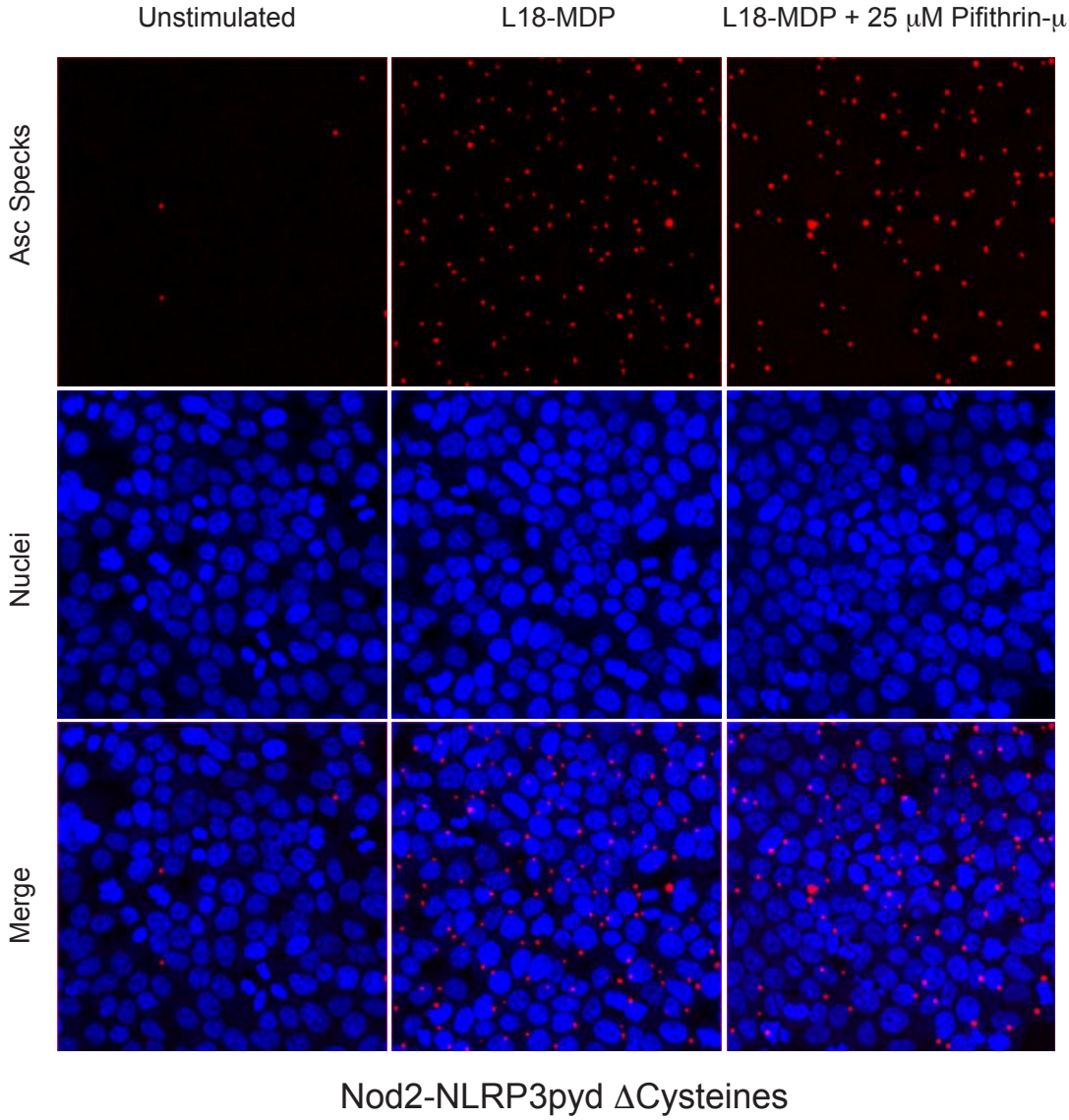

Figure 10 : Chimeric NOD2-NLRP3pyd receptor with all NLRP3 domain cysteines substituted to alanine is not inhibited by pifithrin-μ
HEK-293T cells expressing ASC-TagBFP and NOD2-NLRP3pyd (C8A + C38A * C108A + C130A) were incubated in complete media or 25 μM pifithrin-μ for 1 h and were then stimulated with 10 nM L18-MDP for 2 h. Cells were fixed and the nuclei were stained using DRAQ5, then cells were imaged by confocal microscopy. Representative images were chosen, with Nuclei being shown in blue and Asc specks being shown in red.

4.3.2 Effect of Regional Cysteine to Alanine substitutions in the NLRP3 PYD on Inhibition by Pifithrin-μ.

Three regional cysteine to alanine substitution receptors were created and tested for inhibition by pifithrin-μ. The pyrin domain CtoA (C8A and C38A) construct was unable to be inhibited by pifithrin-μ (Figure 11). The linker domain (C108A and C130A) construct was inhibited normally by pifithrin-μ (Figure 12). The disulfide bond cysteines (C8A and C108A) were also mutated together, and this construct was unable to be inhibited by pifithrin-μ (Figure 13).

The alanine substituted cysteine shared by the constructs that were not inhibited by pifithrin-μ is cysteine 8. The disulfide bond does not seem to be important for function, or the target of pifithrin-μ. If the disulfide bond was the target, then all constructs containing C108A would also be resistant to pifithrin-μ inhibition, and the (C108A and C130A) construct was not resistant.

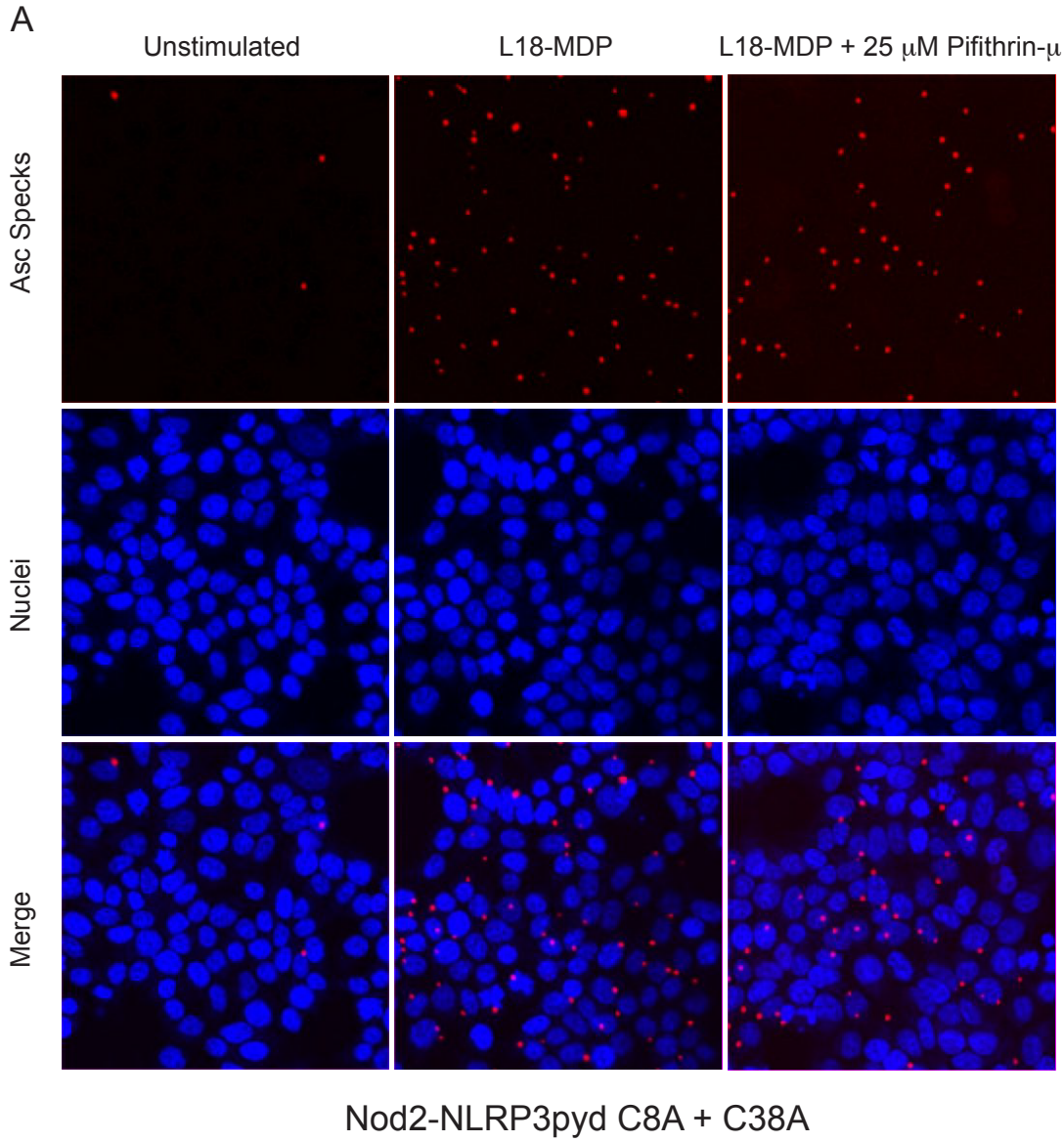

Figure 11 : Chimeric NOD2-NLRP3pyd receptor with both pyrin domain cysteines substituted to alanine is not inhibited by pifithrin-μ
HEK-293T cells expressing ASC-TagBFP and NOD2-NLRP3pyd (C8A + C38A) were incubated in complete media or 25 μM pifithrin-μ for 1 h and were then stimulated with 10 nM L18-MDP for 2 h. Cells were fixed and the nuclei were stained using DRAQ5, then cells were imaged by confocal microscopy. Representative images were chosen, with Nuclei being shown in blue and Asc specks being shown in red.

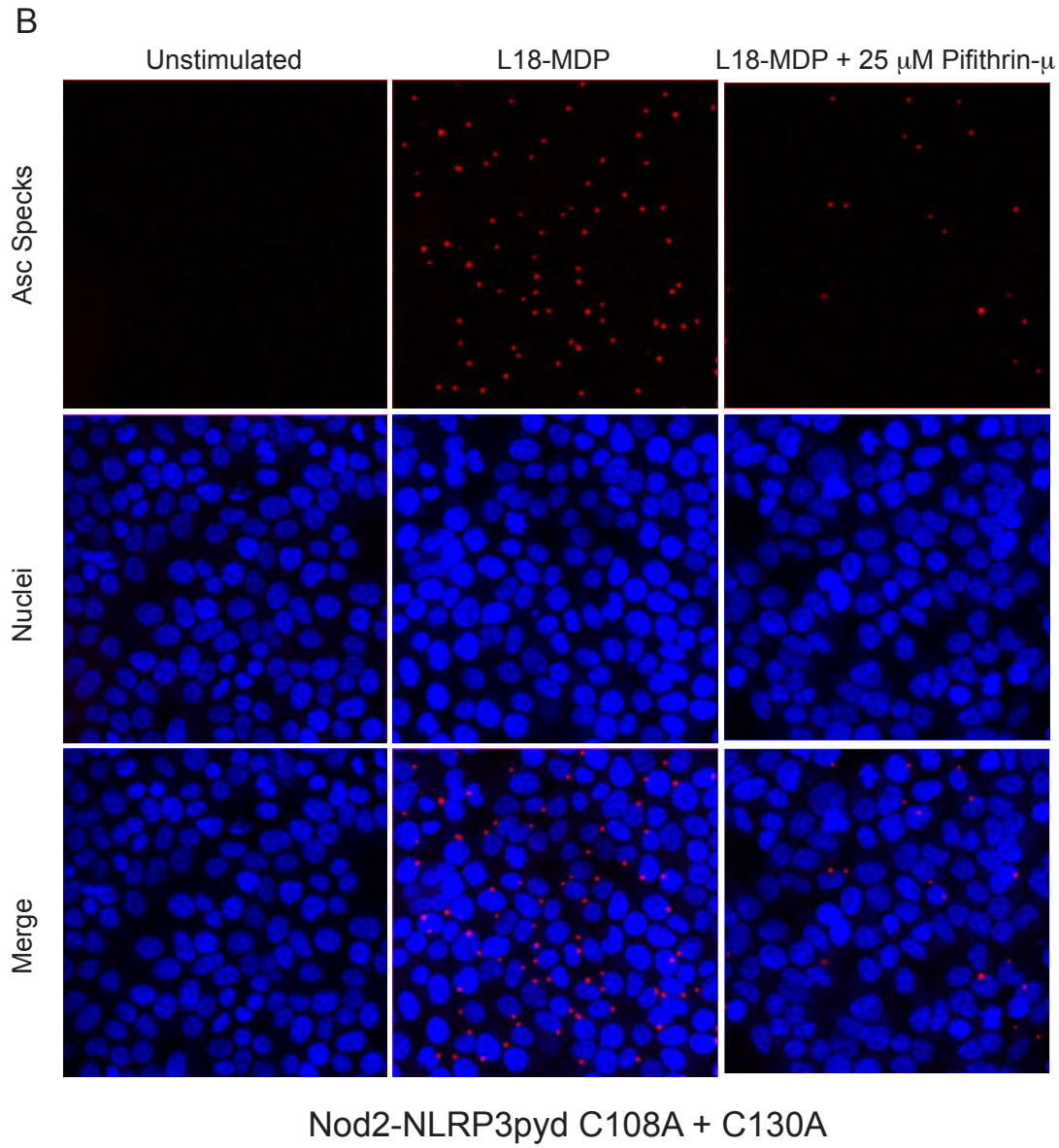

Figure 12: Chimeric NOD2-NLRP3pyd receptor with both linker domain cysteines substituted to alanine is inhibited by pifithrin-μ
HEK-293T cells expressing ASC-TagBFP and NOD2-NLRP3pyd (C108A + C130A) were incubated in complete media or 25 μM pifithrin-μ for 1 h and were then stimulated with 10 nM L18-MDP for 2 h. Cells were fixed and the nuclei were stained using DRAQ5, then cells were imaged by confocal microscopy. Representative images were chosen, with Nuclei being shown in blue and Asc specks being shown in red.

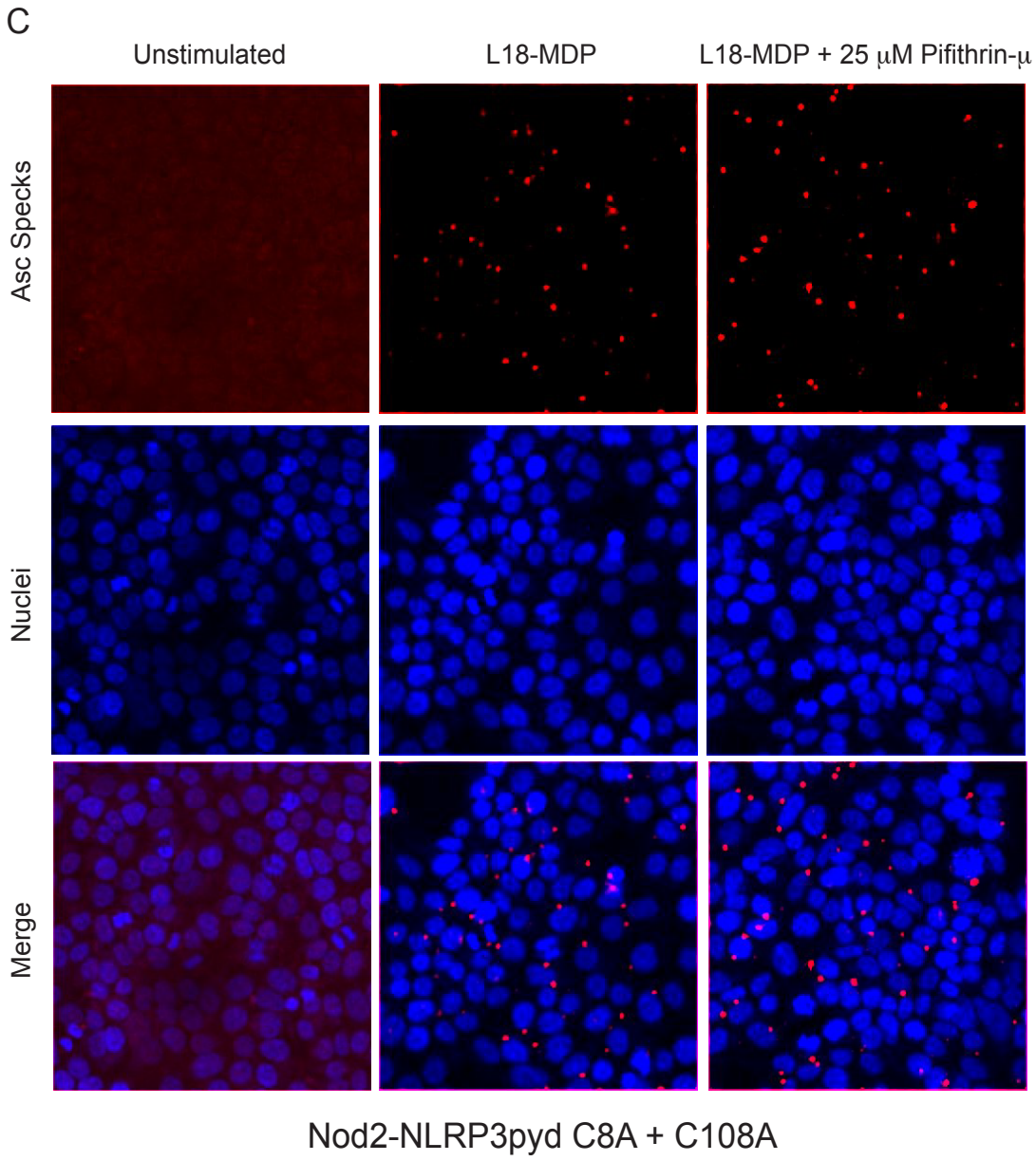

Figure 13 : Chimeric NOD2-NLRP3pyd receptor with both disulfide bond cysteines substituted to alanine is not inhibited by pifithrin-μ
HEK-293T cells expressing ASC-TagBFP and NOD2-NLRP3pyd (C8A + C108A) were incubated in complete media or 25 μM pifithrin-μ for 1 h and were then stimulated with 10 nM L18-MDP for 2 h. Cells were fixed and the nuclei were stained using DRAQ5, then cells were imaged by confocal microscopy. Representative images were chosen, with Nuclei being shown in blue and Asc specks being shown in red.

4.3.3 Effect of Individual Cysteine to Alanine Substitution in the NLRP3 PYD on Inhibition by Pifithrin-μ.

To confirm that cysteine 8 is the target of pifithrin-μ, the four cysteines in the NLRP3 region of the NLRP3 PYD-NOD2 construct were individually mutated to alanine. Clonal reporter lines containing these receptors were isolated and confirmed to be functional. When pifithrin-μ was tested on these lines, only the C8A line was unable to be inhibited (Figure 14). The constructs containing C38A (Figure 15), C108A (Figure 16) or C130A (Figure 17) were all inhibited by pifithrin-μ. The four independent reporter cell lines containing constructs with C8A all fail to be inhibited by pifithrin-μ, demonstrating that C8 in NLRP3 is the target for inhibition.

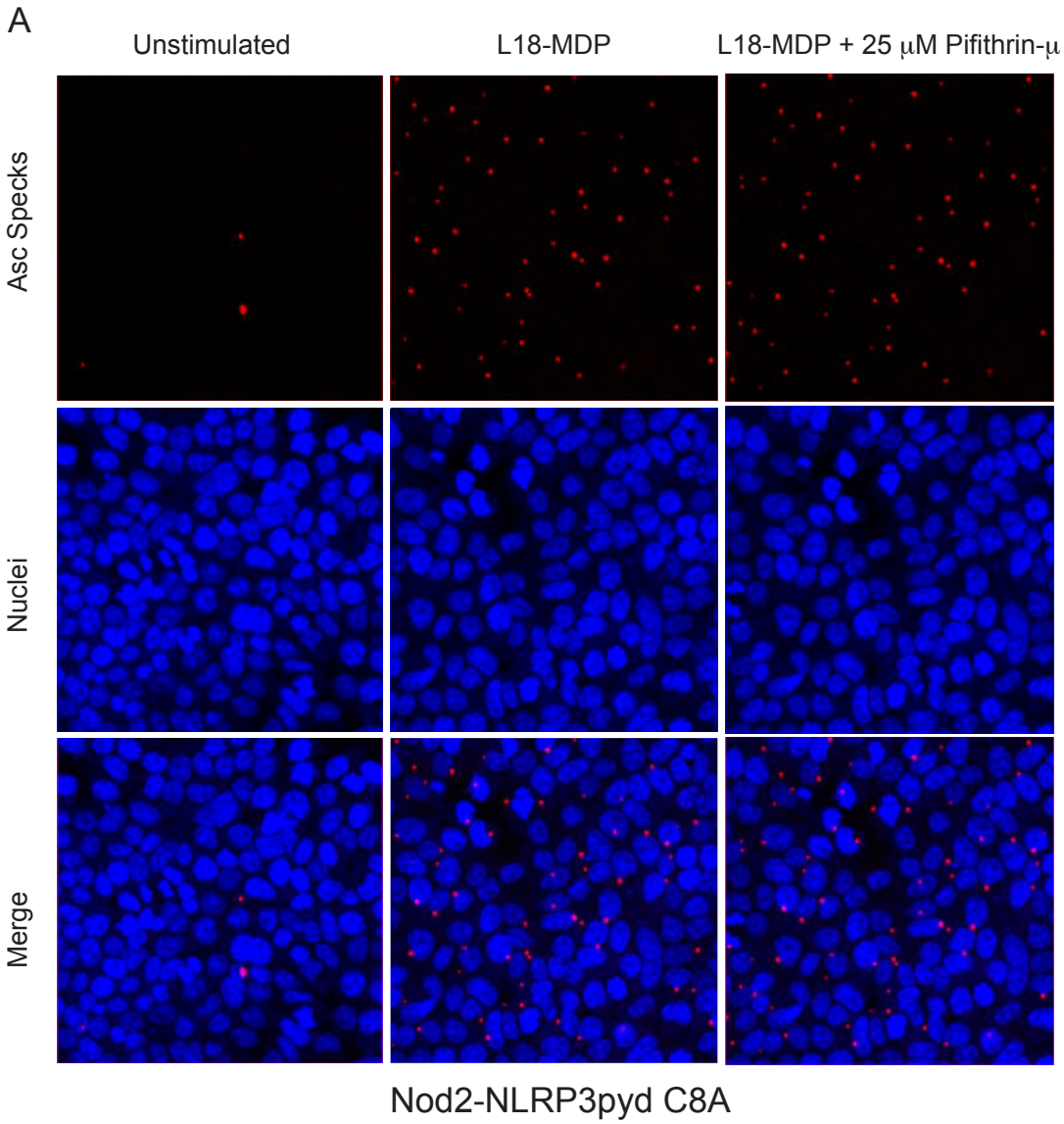

Figure 14 : Chimeric NOD2-NLRP3pyd receptor with cysteine 8 substituted to alanine is not inhibited by pifithrin-μ
HEK-293T cells expressing ASC-TagBFP and NOD2-NLRP3pyd (C8A) were incubated in complete media or 25 μM pifithrin-μ for 1 h and were then stimulated with 10 nM L18-MDP for 2 h. Cells were fixed and the nuclei were stained using DRAQ5, then cells were imaged by confocal microscopy. Representative images were chosen, with Nuclei being shown in blue and Asc specks being shown in red.

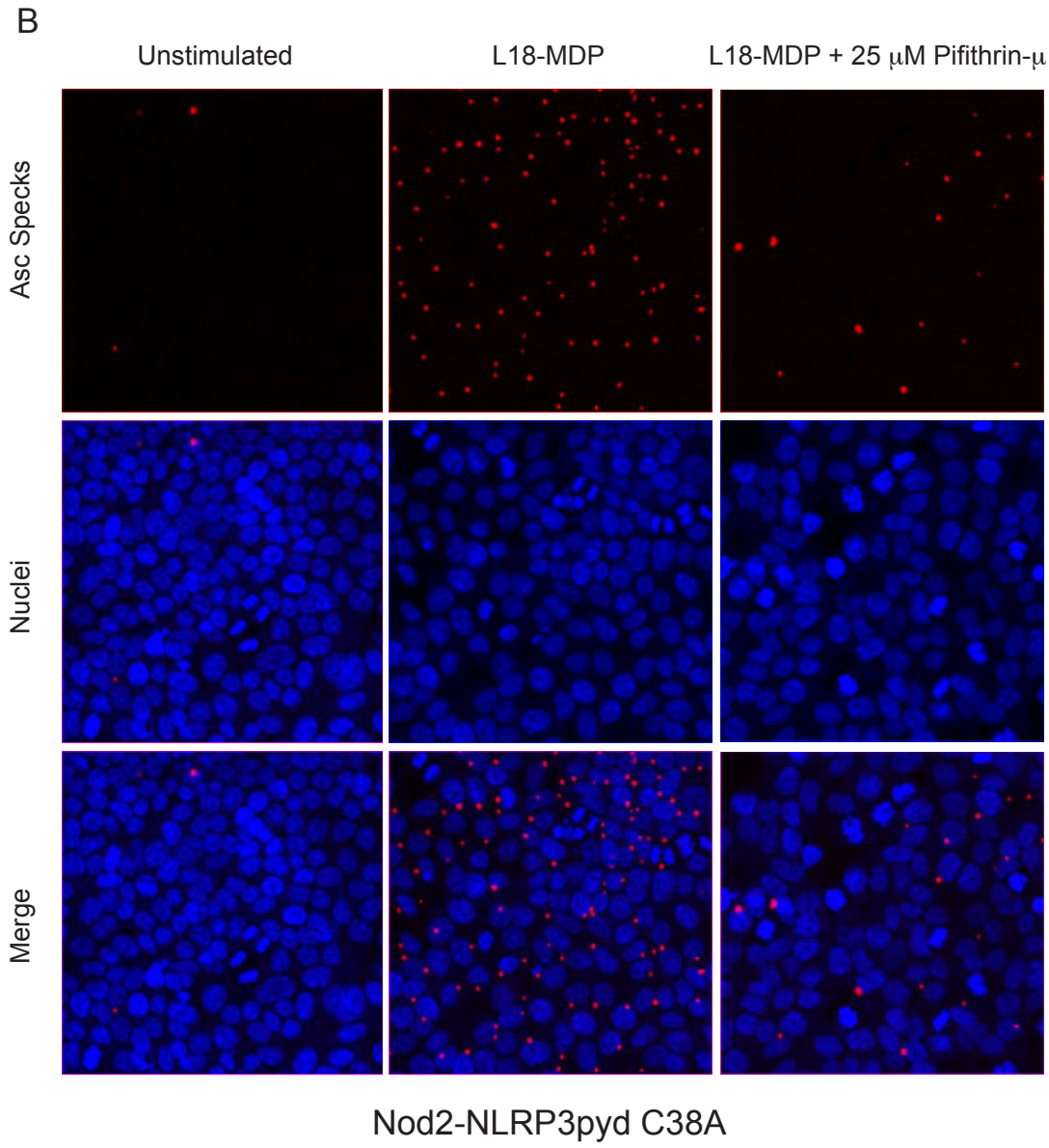

Figure 15: Chimeric NOD2-NLRP3pyd receptor with cysteine 38 substituted to alanine is inhibited by pifithrin-μ
HEK-293T cells expressing ASC-TagBFP and NOD2-NLRP3pyd (C38A) were incubated in complete media or 25 μM pifithrin-μ for 1 h and were then stimulated with 10 nM L18-MDP for 2 h. Cells were fixed and the nuclei were stained using DRAQ5, then cells were imaged by confocal microscopy. Representative images were chosen, with Nuclei being shown in blue and Asc specks being shown in red.

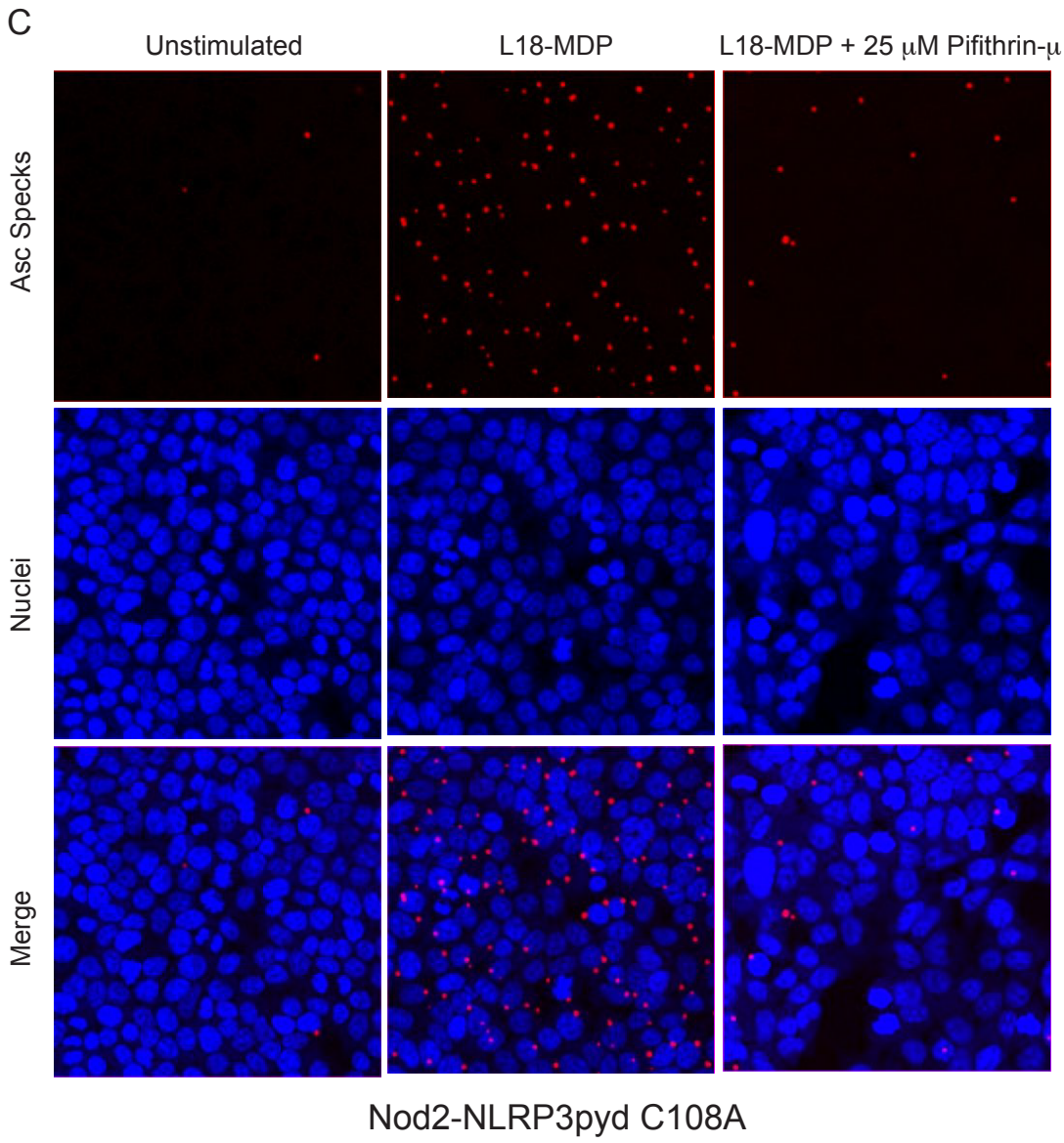

Figure 16: Chimeric NOD2-NLRP3pyd receptor with cysteine 108 substituted to alanine is inhibited by pifithrin-μ
HEK-293T cells expressing ASC-TagBFP and NOD2-NLRP3pyd (C108A) were incubated in complete media or 25 μM pifithrin-μ for 1 h and were then stimulated with 10 nM L18-MDP for 2 h. Cells were fixed and the nuclei were stained using DRAQ5, then cells were imaged by confocal microscopy. Representative images were chosen, with Nuclei being shown in blue and ASC specks being shown in red.

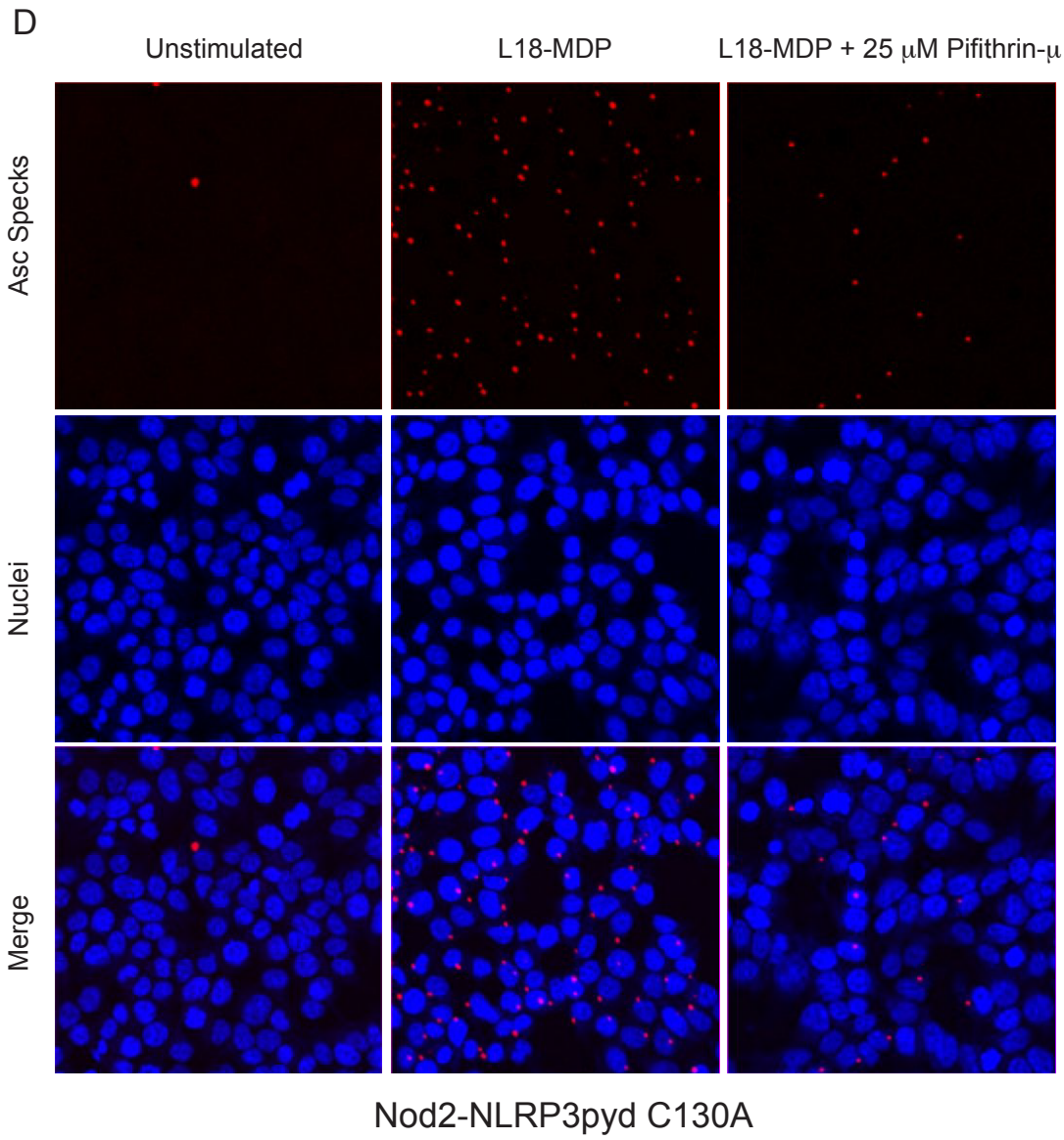

Figure 17: Chimeric NOD2-NLRP3pyd receptor with cysteine 130 substituted to alanine is inhibited by pifithrin-μ
HEK-293T cells expressing ASC-TagBFP and NOD2-NLRP3pyd (C130A) were incubated in complete media or 25 μM pifithrin-μ for 1 h and were then stimulated with 10 nM L18-MDP for 2 h. Cells were fixed and the nuclei were stained using DRAQ5, then cells were imaged by confocal microscopy. Representative images were chosen, with Nuclei being shown in blue and ASC specks being shown in red.

4.3.4 Investigation of CRID3

Perregaux et al. assayed a library of small molecule inhibitors of ion flux in cells and discovered that glyburide, a sulfonylurea compound which blocks ATP-sensitive K+ channels, was able to block ATP mediated IL-1β release in human monocytes. A panel of structurally related compounds were synthesized and two CRID (Cytokine Release Inhibitory Drugs) were identified and examined [65]. In a later paper, CRID3 was developed, and by use of C14-labeled, epoxide containing CRID2, cysteine 32 of GSTO-1 was identified as the major binding target in human THP-1 cells. Clic1, a structurally related protein with a similarly placed cysteine, was also identified as a possible target of CRID compounds [66]. Since these papers were published, NLRP3 has been shown to be the receptor mediating IL-1b release from ATP activation [34]

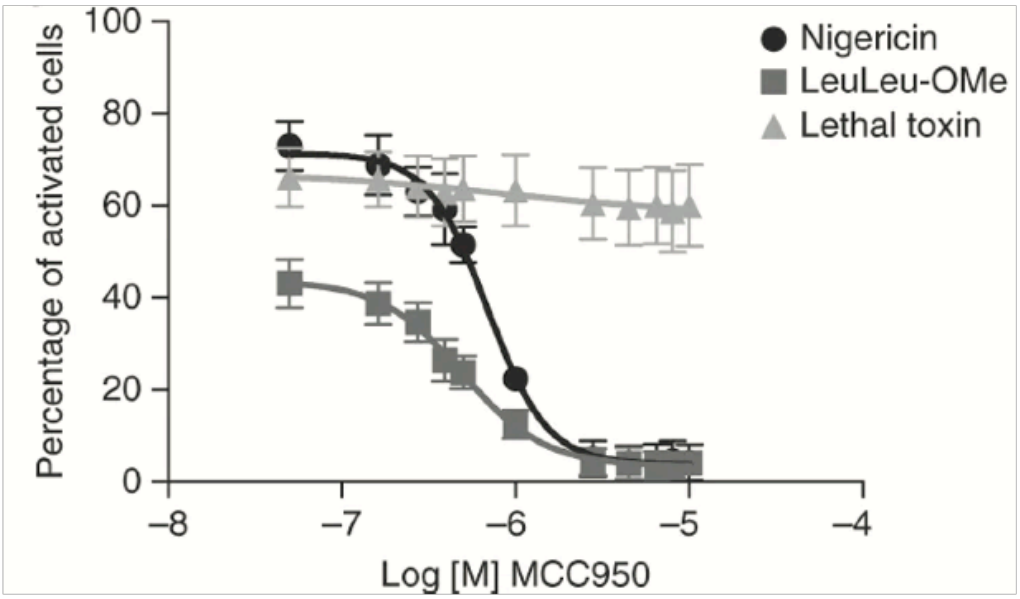

Figure 18 : CRID3 inhibits NLRP3 mediated Asc speck formation
Immortalized mouse macrophage 19.5 reporter cells, were incubated with a titration of CRID3 (0.05-10 μM) for 1 h. They were then stimulated with 10μM nigericin, 2 mM Leu-Leu-OMe, or 1 μg/ml lethal toxin, for 2 h. Cells were fixed and the nuclei were stained using DRAQ5, then cells were imaged by confocal microscopy. Figure was published in Coll et al. 2015

To test the specificity of CRID3 as a general NLRP3 inhibitor, 19.5 inflammasome reporter cells were activated with either of the NLRP3 activators nigericin and Leu-Leu-OMe, or the NLRP1B activator Lethal Toxin, along with a dose titration of CRID3. Cells were fixed, with DRAQ5 to stain the nuclei, then both nuclei and ASC specks were counted, and the percent of activated cells was determined. CRID3 showed an dose dependent inhibition of both of the NLRP3 activators, nigericin and Leu-Leu-OMe, while showing no inhibition of the NLRP1B mediated ASC specking (Figure 19) [67].

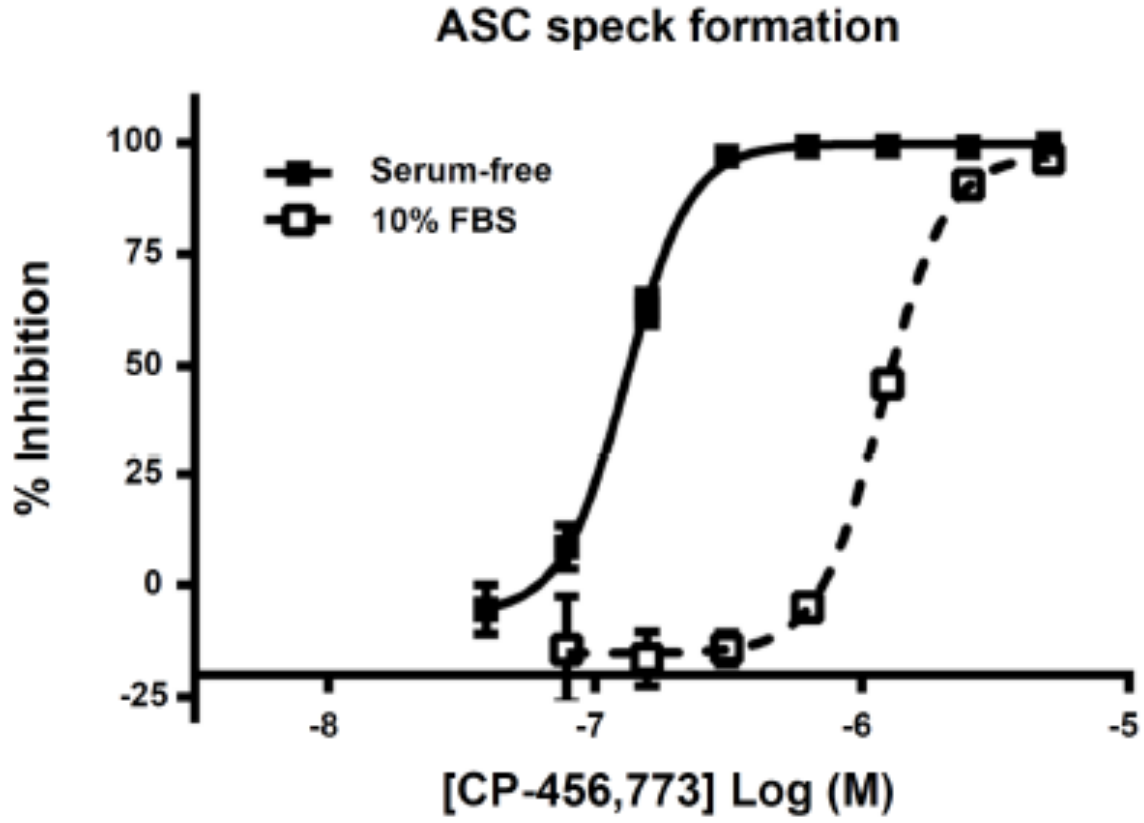

Figure 19 : Effect of serum proteins on CRID3 inhibition of ASC speck formation
Immortalized mouse macrophage 19.5 reporter cells, either in the presence of 10% FBS or serum free, were incubated with a titration of CRID3 for 30 min. They were then stimulated with 10μM nigericin for 1.5 h. . Cells were fixed and the nuclei were stained using DRAQ5, and were were imaged by confocal microscopy. Figure was published in Primiano et al. 2016

To assay the impact of plasma protein binding on the efficacy of CRID3, 19.5 cells were activated with nigericin, verses a dose titration of CRID3. This was performed either in the presence of 10% FBS, or in the absence of serum. CRID3 showed an approximately 90% reduction in activity in the presence of serum, going from an IC_{50} of 130nM to 1190 nM in the presence of 10% FBS.

CRID3 (also know as CP-456,733 or MCC950) has since been shown to be a specific inhibitor of the NLRP3 Inflammasome, and does not affect NLRP1, NLRC4, AIM2 [67], or Pyrin [68]. CRID3 has also been shown to be orally available and to have efficacy in a wide range of animal models shown to be dependent on NLRP3 activity for pathology. Examples include Asthma [69] [70], Dermal and pulmonary inflammation [52], traumatic brain injury [71], and Alzheimer's disease [54].

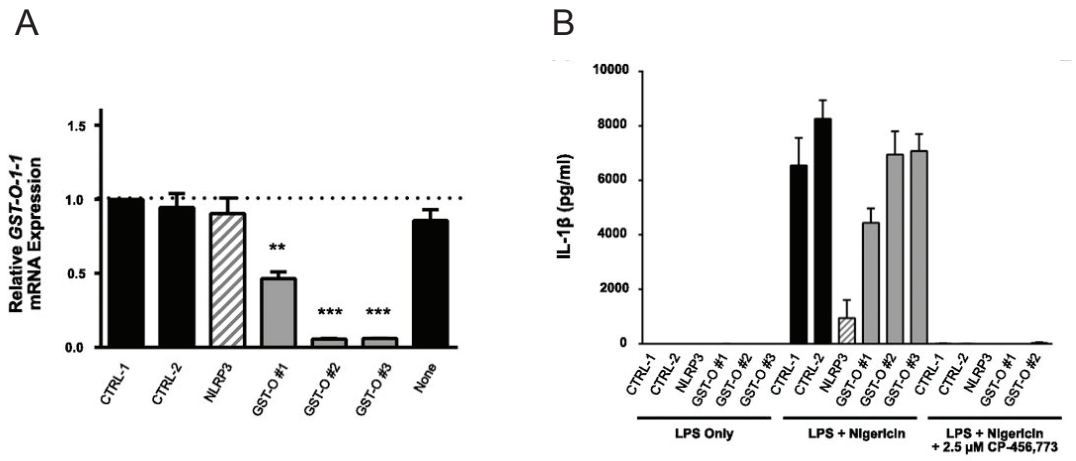

Figure 20 : *GST Omega 1-1* mRNA knockdown does not affect NLRP3 inflammasome-dependent IL-1β release or the ability of CRID3 to inhibit IL-1β release.
(**A**) Effect of *GST Omega 1-1* or *NLRP3* siRNA-mediated knockdown on *GST Omega 1-1* mRNA determined by quantitative PCR and relative to CTRL-1 normalized to 1. Graphs of mean ± SEM (*n* = 3–4 experiments). ***p* < 0.01, ****p* < 0.0001 compared with CTRL-1.
(**B**) Effect of *NLRP3* or *GST Omega 1-1* siRNA-mediated knockdown on IL-1β in supernatants from immortalized mouse macrophage BALB/c cells stimulated with 200 ng/ml LPS for 2 h followed by 1 h treatment with or without 2.5 μM CRID3 (CP-456,773) and then stimulated for 1.5 h with 10 μM nigericin. Figure published in Primiano et al. 2016.

To examine the possibility that either GSTO-1 or CLIC1 is the functional target of CRID3, BALB/c immortalized macrophages were transfected with siRNA. Cells were primed with LPS, then activated with nigericin or ATP, alone or with CRID3. TNFα was measured and showed that GSTO-1 siRNA knock down had little affect on priming. IL-1β was measured and showed that only NLRP3 specific siRNA inhibited NLRP3 activity. GSTO-1 knock down did not affect NLRP3 activity, or CRID3 mediated inhibition (Figure 20).

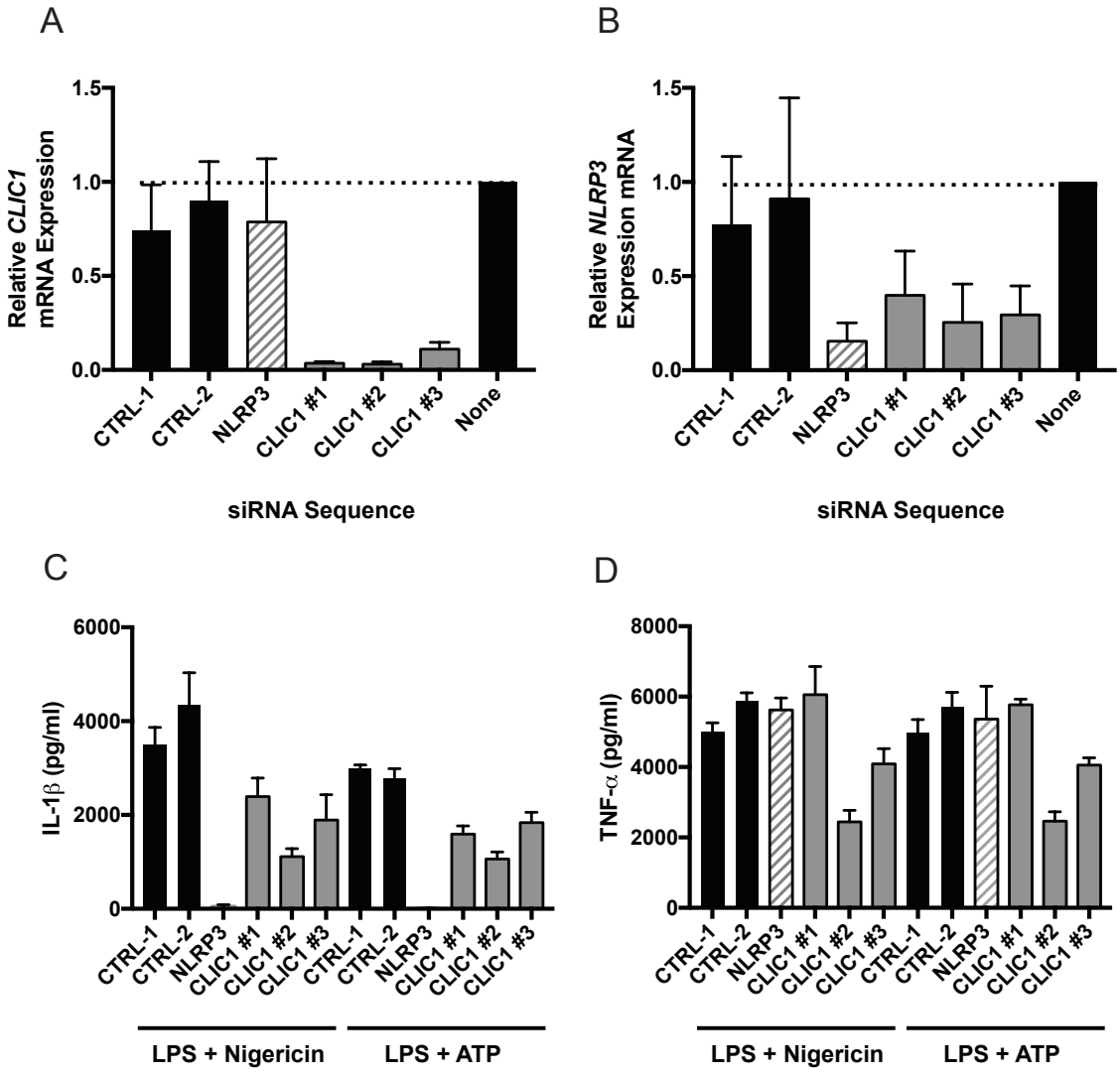

Figure 21: *CLIC1* mRNA knockdown does not Inhibit NLRP3 dependent IL-1β release. (**A-B**) Effect of *CLIC1* or *NLRP3* siRNA-mediated knockdown on (A) *CLIC1* mRNA, or (B) *NLRP3* mRNA determined by quantitative PCR and relative to CTRL-1 normalized to 1. Graphs of mean ± SEM (*n* = 3 experiments). (**C-D**) Effect of *CLIC1* or *NLRP3* siRNA-mediated knockdown on (C) IL-1β or (D) TNF-α in supernatants from immortalized mouse macrophage BALB/c cells stimulated with 200 ng/ml LPS for 2 h followed by 1.5 h treatment with 10 μM nigericin or 2 mM ATP. Graphs of mean ± SEM (*n* = 3 experiments).

CLIC1 siRNA knock down had a partial inhibition of priming, as shown in TNFα release. There was also a partial decrease in IL-1β release from NLRP3 activation with two of the siRNA sequences used. All CLIC1 siRNA sequences reduced CLIC1 mRNA levels well, but also partially inhibited NLRP3 mRNA levels (Figure 21).

To determine if the partial reduction in IL-1β release was due to lower levels of NLRP3 mRNA increase from priming, 19.5 cells, which constitutively express NLRP3 and do not require priming, were used for siRNA transfection. In these cells, nigericin induced specking was almost completely abolished by NLRP3 specific siRNA knock down, while CLIC1 specific siRNA knock down had no affect on nigericin induced specking (Figure 22). This suggests that CLIC1 may have an affect on NLRP3 levels during priming, but CLIC1 is not required for NLRP3 activity and is not likely to be the target of CRID3 inhibition.

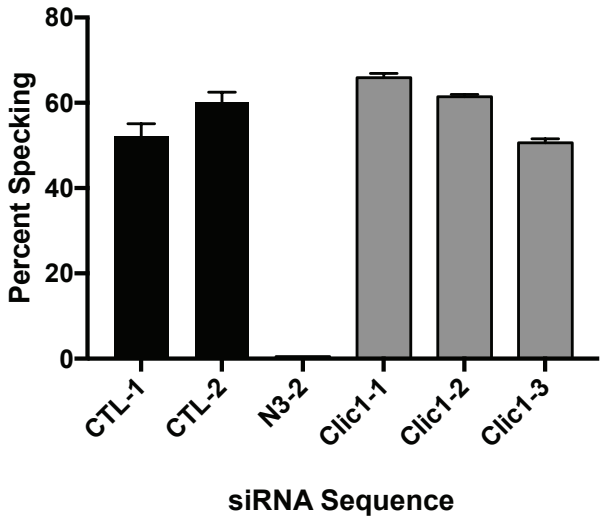

Figure 22: *CLIC1* mRNA knockdown does not Inhibit NLRP3 inflammasome-dependent ASC Speck formation

Immortalized mouse macrophage 19.5 reporter cells after *CLIC1* or *NLRP3* siRNA-mediated knockdown, were plated in triplicate and stimulated for 1.5 h treatment with 10 μM nigericin. Cells were fixed and the nuclei were stained using DRAQ5, then cells were imaged by confocal microscopy. Graphs of mean ± SEM (*n* = 2 experiments).

4.3.5 Investigation of 7-dehydrogedunin

7-dehydrogedunin (7DG), an inhibitor of Protein Kinase R (PKR), was discovered to be an inhibitor of LT activation of the NLRP1B inflammasome. Using the 19.5 reporter cell line, I was able to confirm that 7DG inhibited LT induced specking. 7DG also inhibited NLRP3 mediated ASC specking after activation with either nigericin or Leu-Leu-OMe (Figure 23). 7DG was also tested against AIM2 mediated ASC specking in the 19.5 reporter cell line and was found to be a poor inhibitor when compared to NLRP3 (Figure 24 A). Due to the difference in inhibition, 7DG was tested on the NOD2 based chimeric reporters. 7DG was able to dose dependently inhibit the NLRP3 PYD-NOD2 construct, and not inhibit the AIM2 PYD-NOD2 construct (Figure 24 B). 7DG is known to be a cysteine reactive compound, but was able to inhibit both the NLRP3 PYD-NOD2 and the complete NLRP3 PYD cysteine to alanine NOD2 construct (Figure 24 C). This suggests that PKR is a possible target for the inhibitors blocking the interaction of the NLRP3 PYD and ASC.

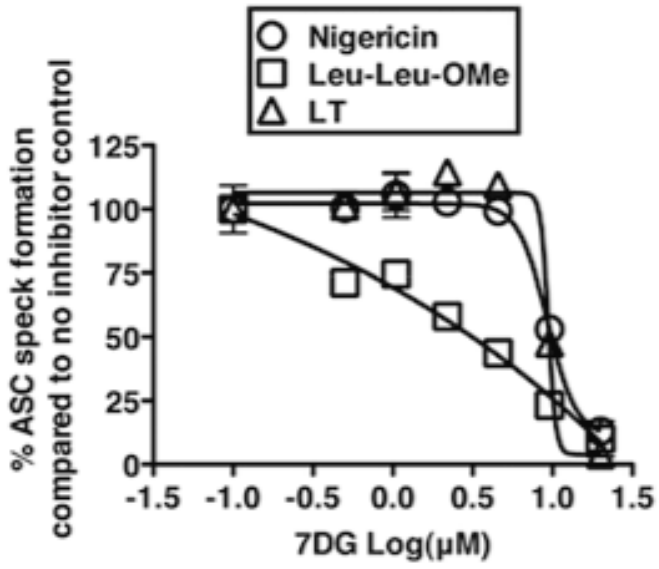

Figure 23 : 7-dehydrodegunin inhibits both NLRP1B and NLRP3 mediated ASC Specking. Immortalized mouse macrophage 19.5 reporter cells were incubated with inhibitor and specific stimuli, fixed and visualized to determine the percentage of cells that contain ASC specks relative to control (no inhibitor treatment). Data are representative of at least three independent experiments, each done in triplicate. Data are shown as mean ± s.d.
Figure published in Hett et al. 2013.

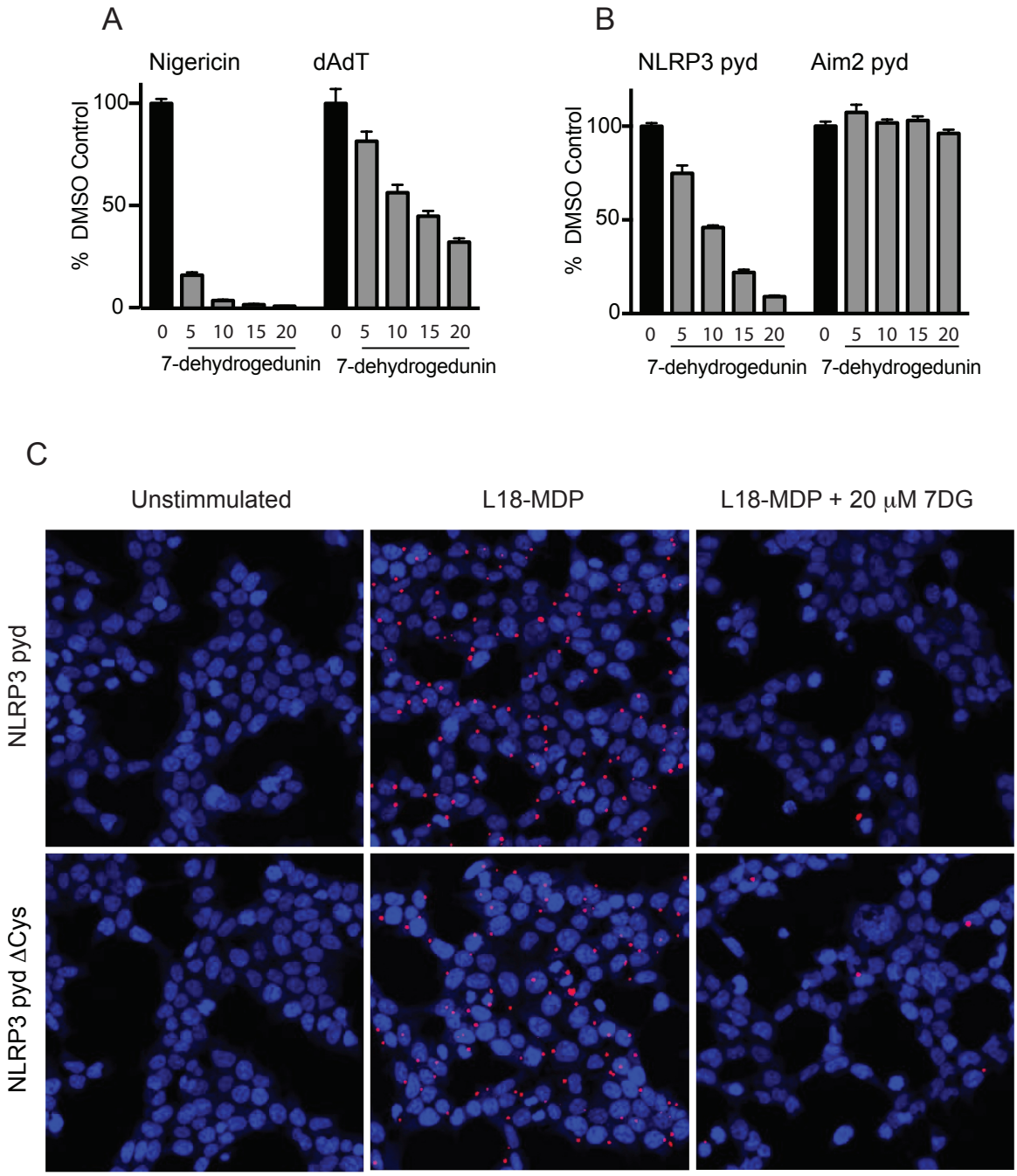

Figure 24 : 7-dehydrogedunin inhibits the NLRP3 pyrin domain, but does not target cysteines (A-C) Effect of 7-dehydrogedunin on ASC specking. (A) Immortalized mouse macrophage 19.5 reporter cells, were incubated with a titration of 7-dehydrogedunin for 1 h. They were then stimulated with 10μM nigericin for 1.5 h or 200 ng poly(dA-dT) for 2 h. (B) HEK-293T cells expressing ASC-TagBFP and either NOD2-NLRP3pyd or NOD2-AIM2pyd were incubated with a titration of 7-dehydrodegunin 1 h. They were then stimulated with 10 nM L18-MDP for 2 h. (C) HEK-293T cells expressing ASC-TagBFP and either NOD2-NLRP3pyd or NPD2-NLRP3pyd (C8A + C38A + C108A + C130A) were incubated in complete media or 25 μM pifithrin-μ for 1 h and were then stimulated with 10 nM L18-MDP for 2 h. Cells were fixed and the nuclei were stained with DRAQ5. Cells were imaged by confocal microscopy.

Discussion

4.4 Identifying novel small molecule inhibitors of NLRP3

In order to identify novel small molecular inhibitors of NLRP3, two compound libraries were screened for the ability to specifically block NLRP3 mediated inflammasome formation. NLRP3 activation was monitored by using a reporter cell line that expresses NLRP3 and fluorescently tagged ASC. When this cell line is treated with activators of the Inflammasome, it responds by assembling ASC into a large single speck. This fluorescent ASC speck can then be assayed by confocal microscopy of a fixed monolayer of cells. By comparing the number of ASC specks, verses the number of nuclei fluorescently stained with DRAQ5, the percent of activated cells within the field was determined. The compound libraries were assayed for the ability to inhibit the formation of ASC by two known NLRP3 activators with different modes of activity: Nigericin, which is a bacterial toxin that forms potassium ionophores in cell membranes, and Leu-Leu-OMe which is processed by cathepsin C in the lysosome, leading to lysosomal destabilization and releasing lysosomal contents into the cytosol. In order to confirm NLRP3 specific inhibition, the compound libraries were also assayed against two additional inflammasome receptors: Lethal Toxin activation of NLRP1B, and poly(dA-dT) activation of AIM2.
Six compounds from these libraries were confirmed as NLRP3 specific inhibitors. Two of these, BAY-11-7082 and Parthenolide, had been previously identified as NLRP3 inhibitors. Four of these compounds, CH55, ebselen, NSC632830, and pifithrin-μ, were novel NLRP3 inhibitors.

4.5 Mechanisms of NLRP3 inhibitors

Two steps are required for the NLRP3 inflammasome to be activated. In the first step, a priming stimulus activates the transcription factor NF-κB. The activation of NF-κB increases the expression of NLRP3 to a level high enough for function, and also initiates several forms of posttranslational modification of NLRP3 to modulate function. The requirement for this priming step complicates differentiating between inhibitors that directly target NLRP3 from inhibitors that indirectly affect NLRP3 by inhibiting priming. It becomes even more complicated when inhibitors have multiple targets of action. Examples of this are the NLRP3 inhibitors BAY 11-7082 and parthenolide. Both of these inhibitors inhibit the NF-κB activation required for priming, and both have been shown to directly target NLRP3 by inhibiting its ATPase activity. The reporter cell line expressing NLRP3 and fluorescently tagged ASC

avoids this problem by constitutively expressing enough NLRP3 so that priming is not required for function.

The mechanism of activation of NLRP3 is not clearly understood. NLRP3 is activated by several distinct mechanisms, including ATP activation of the P2X7 receptor, bacterial pore forming toxins, and destabilization of the lysosomal membrane. There are several factors resulting from these mechanisms that have been proposed to be important for NLRP3 activation, such a reactive oxygen species (ROS), Mitochondrial dysfunction, Potassium efflux from the cell, and the release of cathepsin proteases from the lysosome into the cytosol.

The lack of understanding of what is required for NLRP3 function makes it difficult to identify the target of NLRP3 inhibitors. It is known that for all activators of NLRP3 that the ATPase activity in the NACHT domain is required for the oligomerization of activated NLRP3, leading to its interaction with ASC and initiating the formation of the inflammasome. The ATPase activity of NLRP3 can be assayed, and almost all of the inhibitors that have been proposed to directly affect NLRP3 do so by inhibiting the ATPase activity.

The PYD of NLRP3 directly interacts with the PYD of ASC to form an inflammasome. The PYD of NLRP3 has been shown to be regulated by phosphorylation by Andrea Stutz, another member of the Latz lab[72]. Serine 8 is normally phosphorylated, and needs to be dephosphorylated to efficiently interact with ASC. Since the PYD domain of NLRP3 must interact with ASC for function, and small modifications of the PYD have been shown to affect this interaction, I created a reporter system that could be used to identify inhibitors that target this domain.

4.6 Chimeric receptors dependent on the NLRP3 PYD

In order to isolate the function of the PYD of NLRP3 from the NACHT and LRR domains, three chimeric receptor systems were tested. In each of these systems, activity was monitored by the ability of chimeric receptors to interact with ASC through the NLRP3 PYD and initiate an ASC speck upon activation. The PYD of NLRP3 was compared to the PYD of AIM2 as a specificity control, in all systems.

In the first system, the PYD was attached to the dimerization domain of the iDimerize system. When expressed in HEK cells with fluorescent ASC, the PYD could be forced to dimerize by the addition of the cell permeable homodimerizer. This system is the least complex, depending only upon the dimerizer domain and the PYD, but it is also the most artificial and thus least likely to work. Functional clonal lines expressing NLRP3 or AIM2 PYD were isolated, and upon the addition of the dimerizer, ASC specks were formed. While I was

able to isolate these functional clones, the PYD alone is highly active, and no further functional clones of PYD variants could be isolated.
In the second system, AIM2 was compared with chimeric AIM2 with the NLRP3 PYD replacing the native AIM2 PYD. AIM2 is an inflammasome receptor that only contains a DNA binding domain and a PYD, with no ATPase activity to be targeted by inhibitors. Functional clones were isolated for both receptors, which induced fluorescent ASC specking upon the transfection of dsDNA into the cell. Both the commonly used activator poly(dA-dT) and plasmid DNA caused receptor specific ASC speck formation, with plasmid DNA being a more potent activator. During the course of testing AIM2 activation in mouse immortalized macrophages, I discovered that a brief centrifugation of the cells after the DNA transfection mixture was added both increased the amount of activation and decreased the 4-hour time required. This allowed me to standardize the incubation time of all activators used to 2 hours in the HEK lines used to test inhibitors.
In the third system, NOD2 was used as the parental receptor. NOD2 has a structure similar to NLRP3, with a NACHT domain and an LRR domain. Where NLRP3 has a PYD that interacts with ASC upon activation, leading to the formation of an inflammasome, NOD2 has 2 CARD domains that interact with RIP2 upon activation, leading to the activation of NF-κB. A chimeric receptor that replaced the CARD domains of NOD2 with the CARD domain of NLRC4 had been previously published [62]. This chimeric receptor interacted with ASC after the addition of MDP, a NOD2 activator. I created similar chimeric receptors, replacing the CARD domains of NOD2 with the PYD of either NLRP3 or AIM2. Cell lines were made in HEK cells expressing ASC-TagBFP and either of these receptors. Both chimeric receptors were able to induce ASC specking after stimulation with L18-MDP, a more cell permeable version of MDP.
While the AIM2-NLRP3 PYD chimeric receptor is functional, its percent induced ASC specking is low, and constitutive background specking is high, when compared to the NOD2 based receptors. Having the best dynamic range, the chimeric NOD2 system was chosen to test the efficacy of inhibitors on modified versions of the NLRP3 PYD.

4.7 Inhibitors of the NLRP3 PYD

Eight NLRP3 inhibitors, four novel inhibitor identified in a reporter cell line screening of two small compound libraries and four published NLRP3 inhibitors, were assayed for the ability to inhibit the NLRP3 PYD from interacting with ASC to form a speck. Four of these compounds: 5Z-7-Oxozeanol, arglabin, parthenolide, and pifithrin-μ were shown to be specific NLRP3 PYD inhibitors. Three of these inhibitors: 5Z-7-Oxozeanol, arglabin, and parthenolide are known to covalently target cysteine residues. There are four cysteines in the NLRP3 PYD

used in the chimeric receptors, and interestingly it had been published that the crystal structure of the NLRP3 PYD contains a disulfide bond between cysteine 8 and cysteine 108. It was speculated in that paper that this bond could be important for NLRP3 regulation by ROS, but no supporting data was presented [64]. A version of the NLRP3 PYD-NOD2 chimera was made in which the four cysteines in the NLRP3 PYD were substituted with alanine. When this receptor was expressed in HEK cells with ASC-TagBFP, it was still capable of initiating ASC specks after activation with L18-MDP. This demonstrated that the four cysteines, and the disulfide bond between cysteines 8 and 108 are not required for function. When the four NLRP3 PYD specific inhibitors were assayed, only pifithrin-μ lost its inhibitory effect. This result was unexpected since pifithrin-μ is the one inhibitor that is not known to be cysteine reactive.

It is not at all clear what the target of the other NLRP3 PYD inhibitors is. Reactive cysteine compounds bind to many cysteines across the proteome. An example of an inhibitor with multiple targets is Parthenolide. Parthenolide inhibits NLRP3 by blocking the NF-kB activation required for priming. It also blocks the ATPase activity of the NACHT domain. I have show that Parthenolide also blocks the NLRP3 PYD from interacting with ASC. This does not appear to be a direct interaction with cysteines in the PYD, and suggests there could be another protein specifically required for NLRP3 interactions with ASC that contains an important cysteine residue.

4.8 Pifithrin-μ targets Cysteine 8 in the NLRP3 PYD

Three NLRP3 PYD-NOD2 variants were tested, each containing two cysteine to alanine substitutions: C8A, C38A, which are in the pyrin domain; C108A, C130A, which are in a small region outside the pyrin domain included in these chimeric constructs; and C8A, C108A, the reported disulfide bond.

Pifithrin-μ showed a similar loss of inhibition on both the C8A, C38A and the C8A, C108A constructs, but inhibited normally the C108A, C130A construct. This suggested that Cys-8 is the target, and not the disulfide bond. Reporter cell lines were made expressing NLRP3 PYD-NOD2 chimeric receptors where the four cysteines in the NLRP3 PYD were substituted to alanine individually. When pifithrin-μ was tested on these reporter lines, only the C8A containing line was unable to be inhibited normally. The four independent chimeric constructs that contain C8A are poorly inhibited by pifithrin-μ, and the four independent chimeric constructs, containing the cysteine at position 8 are inhibited normally. This demonstrates that C8 is the target of pifithrin-μ.

It is not clear how C8 is a target of pifithrin-μ. Pifithrin-μ is not known to be a covalent cysteine inhibitor. It is possible that it interacts non-covalently with C8, sterically inhibiting pyrin-pyrin interactions in a manner similar to the phosphorylation of nearby serine 5. It is also possible that it could interfere with the binding of the phosphatase required to dephosphorylate S5.

4.9 NLRP3 inhibitor CRID3

Based on the discovery that glyburide, a type 2 diabetes drug, was able to block the release of IL-1β, Pfizer screened libraries of related diarylsulfonylurea compounds for the ability to block the release of IL-1β in response to ATP activation. Active compounds from these screens were designated as cytokine release inhibitory drugs (CRIDS). Using epoxide-bearing, C14-labeled CRIDs, it was shown that GSTO1 and CLIC1 were the main binding targets for these compounds[66]. The lead drug, CRID3 was tested in a small clinical trial, but unfortunately, problems with potency and high dose liver toxicity has prevented CRID3 from being tested in additional trials for clinical use.

CRID3 has still continued to be of interest to researchers, and has been studied further. CRID3 has shown to be an NLRP3 specific inhibitor, and has been shown to be effective in several mouse models of NLRP3 mediated diseases. Several drug companies have NLRP3 inhibitor programs based on CRID3, and a company, Inflazome, was founded by Luke O'Neil to create better inhibitors based on CRID3.

In collaboration with Luke O'Neill to examine CRID3 as a potential therapeutic I used the 19.5 reporter cell line to show that CRID3 inhibits NLRP3 activation by nigericin or Leu-Leu-OMe, but does not reduce NLRP1B activation by lethal toxin, demonstrating its specificity as a NLRP3 inhibitor [67].

In collaboration with Pfizer to explore the efficacy and pharmacology of CRID3, I used the 19.5 reporter cell line to demonstrate that the presence of 10% serum reduces the potency of CRID3 by approximately 90% compared to serum free conditions. This helps to explain the unexpected low potency found in the clinical trial. I also investigated GSTO1 as the potential target of CRID3. I showed that IL-1β release by ATP activation of BALB/c iMacs was not significantly reduced by used siRNA knockdown of GSTO1 [73].

I have expanded this investigation and also show that siRNA knockdown of CLIC1, the second suggested target of CRID binding, has no significant effect on IL-1β release by BALB/c iMacs activated with nigericin or ATP. This result was confirmed by using siRNA knockdown of CLIC1 in the 19.5 reporter cell line and showing no reduction of nigericin induced ASC specking.

Since my investigations of CRID3, it has been shown that CRID3 is yet another inhibitor that targets the ATPase activity of NLRP3's NACHT domain[51,74]. This recent finding explains why CRID3 showed no ability to inhibit my NLRP3 PYD reporters.

4.10 NLRP3 inhibitor 7-dehydrogedunin

In a screen of small compounds, 7-dehydrogedunin (7DG) was identified as an inhibitor of LT induced cell death. 7DG is an inhibitor of Protein Kinase R (PKR), and the role of PKR in inflammasome activity was further explored.

After binding to dsDNA, PKR autophosphorylates, leading to the activation of several antiviral pathways. PKR has also been shown to be important for function in several inflammasomes, including NLRP3 [75] [76]. I participated in examining the ability of 7DG to inhibit NLRP3 as well as NLRP1B. In collaboration with Erik Hett, I was able to confirm that, in the 19.5 reporter line, 7DG inhibits ASC speck formation by LT activation of NLRP1B. 7DG was also able to inhibit NLRP3 activation by nigericin or Leu-Leu-OMe in the same system [77].

Further examination of 7DG in the 19.5 reporter cell line showed that AIM2 mediated ASC specking was poorly inhibited when compared to NLRP3. When tested on the chimeric NOD2 HEK ASC-TagBFP cell lines 7DG inhibits the NLRP3 PYD and not the AIM2 PYD construct. 7DG is also a cysteine reactive compound, and like the other NLRP3 PYD cysteine reactive inhibitors it was able to inhibit the construct in which the four cysteines in the NLRP3 PYD were converted to alanine. The possible role PKR plays in the PYD-PYD interactions between NLRP3 and ASC needs to be further examined.

4.11 Conclusion

NLRP3 is a pattern recognition receptor that responds to a variety of environmental or pathogen stresses. Its activity has been shown to be important for several important chronic diseases involving sterile inflammation, such as atherosclerosis, diabetes, and Alzheimer's disease. The development of NLRP3 inhibitory drugs has a huge clinical potential, and is being actively pursued by many drug development companies. The ligand, or mechanism of activation of NLRP3, is not fully understood and this greatly inhibits the design of targeted inhibitors. Currently, the ATPase activity of NLRP3 is the only known target of the majority of inhibitors, including CRID3, the best studied specific inhibitor of NLRP3 which cannot be used clinically due to liver toxicity.

The work presented here introduces a new system of chimeric receptors which is shown to be useful to screen the pyrin domain (PYD) as a potential target for NLRP3 inhibitors. Four inhibitors of NLRP3 were shown to specifically inhibit the PYD of NLRP3 from initiating the formation of an inflammasome through ASC. One of these four inhibitors, pifithrin-μ, was demonstrated to target cysteine 8 in the NLRP3 PYD.

6 List of Abbreviations

A	alanine
AIM2	absent in melanoma 2
ASC	apoptosis-associated speck-like protein containing a CARD
ATP	adenosine 5'-triphosphate
BCA	bichoninic acid
BFP	blue fluorescent protein
bp	basepair
BSA	bovine serum albumen
C	carbon
CAPS	cryopyrin-associated periodic syndrome
CARD	caspase activation and recruitment domain
cDNA	complementary DNA
CLIC1	chloride intracellular channel protein 1
CTB	Cell Titer Blue
DAMP	danger-associated molecular pattern
DMEM	Dulbecco's modified Eagle medium
DMSO	dimethylsulfoxide
DNA	deoxyribonucleic acid
DTT	dithiothreitol
dNTP	deoxynucleoside 5'-triphosphate
EDTA	ethylenediaminetetraacetic acid
ELISA	enzyme linked immunosorbent assay
FBS	fetal bovine serum
GSDMD	gasdermin D
GSTO1	glutathione S-transferase omega 1
h	hour(s)
HPRT	hypoxanthine-guanine phosphoribosyltransferase
iMAC	immortalized macrophage
gag	group specific antigen
GFP	green fluorescent protein
HEK	human embryonic kidney cells
IL-1b	Interleukin-1 beta
kb	kilobase
L18-MDP	MDP with a C18 fatty acid chain
LF	lethal factor
LPS	lipopolysaccharide
LRR	leucine-rich repeat
MDP	muramyl dipeptide
min	minute(s)
MyD88	myeloid differentiation primary-response protein 88
NLR	NOD-like receptor
NACHT	NAIP, CIITA, HET-E and TP1
NLRC	NLR family CARD containing
NLRP	NLR family PYD containing
PA	protective antigen

PCR	polymerase chain reaction
NOD	nucleotide oligomerization dfomain
PAMP	pathogen associated molecular pattern
PKR	double-stranded RNA-dependent protein kinase
PRR	pattern recognition receptor
PYD	pyrin domain
RNA	ribonucleic acid
s	second(s)
siRNA	small inerfering RNA
TAE	tris-acetate-EDTA
TLR	Toll-like receptor
TNF	tumor necrosis factor
TRIS	tris(hydroxymethyl) aminomethane
UV	ultraviolet
VSV-G	vesticular stomatitus virus protein G
wt	wildtype
xg	times gravitational acceleration

7 List of Figures

8 References

1. Janeway, C. A., Jr. & Medzhitov, R. I NNATEI MMUNER ECOGNITION. *Annu. Rev. Immunol.* **20,** 197–216 (2002).
2. TOLERANCE, DANGER, AND THE EXTENDED FAMILy*. 1–55 (2002).
3. Boehm, T. & Swann, J. B. Origin and Evolution of Adaptive Immunity. *Annu. Rev. Anim. Biosci.* **2,** 259–283 (2014).
4. yjbm00627-0094a. 1–1 (2008).
5. CRISPR/Cas, the Immune System of Bacteria and Archaea. 1–5 (2010).
6. CRISPR elements in Yersinia pestis acquire new repeats by preferential uptake of bacteriophage DNA, and provide additional tools for evolutionary studies. *Microbiology* **151,** 653–663 (2005).
7. Clustered regularly interspaced short palindrome repeats (CRISPRs) have spacers of extrachromosomal origin. *Microbiology* **151,** 2551–2561 (2005).
8. Mojica, F. J. M., D ez-Villase or, C. S., Garc a-Mart nez, J. S. & Soria, E. Intervening Sequences of Regularly Spaced Prokaryotic Repeats Derive from Foreign Genetic Elements. *J Mol Evol* **60,** 174–182 (2005).
9. Hale, C. R. *et al.* RNA-Guided RNA Cleavage by a CRISPR RNA-Cas Protein Complex. *Cell* **139,** 945–956 (2009).
10. Control of adaptive immunity by the innate immune system. 1–11 (2015). doi:10.1038/ni.3123REVIEW
11. The Dorsoventral Regulatory Gene Cassette. 1–11 (1996).
12. Defective LPS Signaling in C3H/HeJ and C57BL/10ScCr Mice: Mutations in Tlr4 Gene. 1–5 (1998).
13. TLRs and innate immunity. 1–10 (2009). doi:10.1182/blood-2008
14. Miyake, K. Innate immune sensing of pathogens and danger signals by cell surface Toll-like receptors. *Seminars in Immunology* **19,** 3–10 (2007).
15. Choi, S. Similar structures but different roles … an updated perspective on TLR structures. 1–13 (2011). doi:10.3389/fphys.2011.00041/abstract
16. O'Neill, L. A. J. & Bowie, A. G. The family of five: TIR-domain-containing adaptors in Toll-like receptor signalling. *Nat Rev Immunol* **7,** 353–364 (2007).
17. Nie, L., Cai, S.-Y., Shao, J.-Z. & Chen, J. Toll-Like Receptors, Associated Biological Roles, and Signaling Networks in Non-Mammals. *Front. Immunol.* **9,** E21–19 (2018).
18. Dinarello, C. A. Immunological and Inflammatory Functions of the Interleukin-1 Family. *Annu. Rev. Immunol.* **27,** 519–550 (2009).
19. Fink, S. L. & Cookson, B. T. Caspase-1-dependent pore formation during pyroptosis leads to osmotic lysis of infected host macrophages. *Cellular Microbiology* **8,** 1812–1825 (2006).

20. The Inflammasome: A Molecular Platform Triggering Activation of Inflammatory Caspases and Processing of proIL. 1–10 (2002).
21. Levinsohn, J. L. *et al.* Anthrax Lethal Factor Cleavage of Nlrp1 Is Required for Activation of the Inflammasome. *PLoS Pathog* **8,** e1002638–7 (2012).
22. Van Opdenbosch, N. *et al.* Activation of the NLRP1b inflammasome independently of ASC-mediated caspase-1 autoproteolysis and speck formation. *Nature Communications* 1–14 (2019). doi:10.1038/ncomms4209
23. Jin, T. *et al.* Structures of the HIN Domain:DNA Complexes Reveal Ligand Binding and Activation Mechanisms of the AIM2 Inflammasome and IFI16 Receptor. *Immunity* **36,** 561–571 (2012).
24. Morrone, S. R. *et al.* Assembly-driven activation of the AIM2 foreign-dsDNA sensor provides a polymerization template for downstream ASC. *Nature Communications* **6,** 48–13 (2015).
25. Hornung, V. *et al.* AIM2 recognizes cytosolic dsDNA and forms a caspase-1-activating inflammasome with ASC. *Nature* **458,** 514–518 (2009).
26. Fernandes-Alnemri, T., Yu, J.-W., Datta, P., Wu, J. & Alnemri, E. S. AIM2 activates the inflammasome and cell death in response to cytoplasmic DNA. *Nature* **458,** 509–513 (2009).
27. Lu, A. *et al.* Unified Polymerization Mechanism for the Assembly of ASC-Dependent Inflammasomes. *Cell* **156,** 1193–1206 (2014).
28. Bauernfeind, F. G. *et al.* Cutting edge: NF-kappaB activating pattern recognition and cytokine receptors license NLRP3 inflammasome activation by regulating NLRP3 expression. *J. Immunol.* **183,** 787–791 (2009).
29. Shim, D.-W. & Lee, K.-H. Posttranslational Regulation of the NLR Family Pyrin Domain-Containing 3 Inflammasome. *Front. Immunol.* **9,** 241–7 (2018).
30. Elliott, E. I. & Sutterwala, F. S. Initiation and perpetuation of NLRP3 inflammasome activation and assembly. *Immunol. Rev.* **265,** 35–52 (2015).
31. Muñoz-Planillo, R. *et al.* K+ Efflux Is the Common Trigger of NLRP3 Inflammasome Activation by Bacterial Toxins and Particulate Matter. *Immunity* **38,** 1142–1153 (2013).
32. Shimada, K. *et al.* Oxidized Mitochondrial DNA Activates the NLRP3 Inflammasome during Apoptosis. *Immunity* **36,** 401–414 (2012).
33. Multiple Cathepsins Promote Pro. 1–18 (2015). doi:10.4049/jimmunol.1500509/-/DCSupplemental
34. Mariathasan, S. *et al.* Cryopyrin activates the inflammasome in response to toxins and ATP. *Nature* **440,** 228–232 (2006).
35. Ramos, H. J. *et al.* IL-1β Signaling Promotes CNS-Intrinsic Immune Control of West Nile Virus Infection. *PLoS Pathog* **8,** e1003039–16 (2012).

36. Allen, I. C. *et al.* The NLRP3 Inflammasome Mediates In Vivo Innate Immunity to Influenza A Virus through Recognition of Viral RNA. *Immunity* **30,** 556–565 (2009).
37. Wang, X. *et al.* NLRP3 Inflammasome Participates in Host Response to Neospora caninum Infection. *Front. Immunol.* **9,** 177–14 (2018).
38. Gorfu, G. *et al.* Dual role for inflammasome sensors NLRP1 and NLRP3 in murine resistance to Toxoplasma gondii. *mBio* **5,** 137–12 (2014).
39. Hoffman, H. M., Mueller, J. L., Broide, D. H., Wanderer, A. A. & Kolodner, R. D. Mutation of a new gene encoding a putative pyrin-like protein causes familial cold autoinflammatory syndrome and Muckle–Wells syndrome. *Nat Genet* **29,** 301–305 (2001).
40. Finetti, M., Omenetti, A., Federici, S., Caorsi, R. & Gattorno, M. Chronic Infantile Neurological Cutaneous and Articular (CINCA) syndrome: a review. *Orphanet Journal of Rare Diseases* 1–11 (2016). doi:10.1186/s13023-016-0542-8
41. Martinon, F., Pétrilli, V., Mayor, A., Tardivel, A. & Tschopp, J. Gout-associated uric acid crystals activate the NALP3 inflammasome. *Nature* **440,** 237–241 (2006).
42. Wen, H. *et al.* Fatty acid–induced NLRP3-ASC inflammasome activation interferes with insulin signaling. *Nat. Immunol.* **12,** 408–415 (2011).
43. Masters, S. L. *et al.* Activation of the NLRP3 inflammasome by islet amyloid polypeptide provides a mechanism for enhanced IL-1β in type 2 diabetes. *Nat. Immunol.* **11,** 897–904 (2010).
44. Duewell, P. *et al.* NLRP3 inflammasomes are required for atherogenesis and activated by cholesterol crystals. *Nature* 1–7 (2010). doi:10.1038/nature08938
45. Couturier, J. *et al.* Activation of phagocytic activity in astrocytes by reduced expression of the inflammasome component ASC and its implication in a mouse model of Alzheimer disease. *J Neuroinflammation* 1–13 (2016). doi:10.1186/s12974-016-0477-y
46. Heneka, M. T. *et al.* NLRP3 is activated in Alzheimer's disease and contributes to pathology in APP/PS1 mice. *Nature* **493,** 674–678 (2012).
47. Review NLRP3 In ammasome and the IL-1 Pathway in Atherosclerosis. 1–19 (2018). doi:10.1161/CIRCRESAHA.118.311362.)
48. Zahid, A., Li, B., Kombe, A. J. K., Jin, T. & Tao, J. Pharmacological Inhibitors of the NLRP3 Inflammasome. *Front. Immunol.* **10,** 1367–10 (2019).
49. Coll, R. C. *et al.* MCC950 directly targets the NLRP3 ATP- hydrolysis motif for inflammasome inhibition. *Nat. Chem. Biol.* 1–8 (2019). doi:10.1038/s41589-019-0277-7
50. Tapia-Abellan, A. *et al.* MCC950 closes the active conformation of NLRP3 to an inactive state. *Nat. Chem. Biol.* 1–14 (2019). doi:10.1038/s41589-019-0278-6

51. Vande Walle, L. *et al.* MCC950/CRID3 potently targets the NACHT domain of wild-type NLRP3 but not disease-associated mutants for inflammasome inhibition. *Plos Biol* **17,** e3000354–24 (2019).
52. Primiano, M. J. *et al.* Efficacy and Pharmacology of the NLRP3 Inflammasome Inhibitor CP-456,773 (CRID3) in Murine Models of Dermal and Pulmonary Inflammation. *J. Immunol.* **197,** 2421–2433 (2016).
53. Gordon, R. *et al.* Inflammasome inhibition prevents α-synuclein pathology and dopaminergic neurodegeneration in mice. *Sci. Transl. Med.* **10,** eaah4066–26 (2018).
54. Dempsey, C. *et al.* Inhibiting the NLRP3 inflammasome with MCC950 promotes non-phlogistic clearance of amyloid-Î² and cognitive function in APP/PS1 mice. *Brain Behavior and Immunity* **61,** 306–316 (2017).
55. Stutz, A., Horvath, G. L., Monks, B. G. & Latz, E. in *Methods and Protocols* (eds. De Nardo, C. & Latz, E.) **vol 1040,** (2013).
56. Juliana, C. *et al.* Anti-inflammatory compounds parthenolide and Bay 11-7082 are direct inhibitors of the inflammasome. *J. Biol. Chem.* **285,** 9792–9802 (2010).
57. Albrecht, M., Domingues, F. S., Schreiber, S. & Lengauer, T. Structural localization of disease-associated sequence variations in the NACHT and LRR domains of PYPAF1 and NOD2. *FEBS Lett.* **554,** 520–528 (2003).
58. Negroni, A., Pierdomenico, M., Cucchiara, S. & Stronati, L. NOD2 and inflammation: current insights. *JIR* **Volume 11,** 49–60 (2018).
59. Maharana, J. *et al.* Identification of MDP (muramyl dipeptide)-binding key domains in NOD2 (nucleotide-binding and oligomerization domain-2) receptor of Labeo rohita. *Fish Physiol Biochem* **39,** 1007–1023 (2012).
60. Grimes, C. L., Ariyananda, L. D. Z., Melnyk, J. E. & O'Shea, E. K. The Innate Immune Protein Nod2 Binds Directly to MDP, a Bacterial Cell Wall Fragment. *J. Am. Chem. Soc.* **134,** 13535–13537 (2012).
61. Mo, J. *et al.* Pathogen sensing by nucleotide-binding oligomerization domain-containing protein 2 (NOD2) is mediated by direct binding to muramyl dipeptide and ATP. *J. Biol. Chem.* **287,** 23057–23067 (2012).
62. Hasegawa, M. *et al.* ASC-mediated NF-kappaB activation leading to interleukin-8 production requires caspase-8 and is inhibited by CLARP. *Journal of Biological Chemistry* **280,** 15122–15130 (2005).
63. Hasegawa, M. *et al.* Mechanism of ASC-mediated apoptosis: Bid-dependent apoptosis in type II cells. *Oncogene* **26,** 1748–1756 (2006).
64. Crystal Structure of NALP3 Protein Pyrin Domain (PYD) and Its Implications in Inflammasome Assembly. 1–10 (2011).

65. Identification and Characterization of a Novel Class of Interleukin-1 Post-Translational Processing Inhibitors. 1–11 (2001).
66. Laliberte, R. E. Glutathione s-transferase omega 1-1 is a target of cytokine release inhibitory drugs and may be responsible for their effect on interleukin-1beta posttranslational processing. *J. Biol. Chem.* **278,** 16567–16578 (2003).
67. Coll, R. C. *et al.* A small-molecule inhibitor of the NLRP3 inflammasome for the treatment of inflammatory diseases. *Nat. Med.* 1–26 (2015). doi:10.1038/nm.3806
68. Van Gorp, H. *et al.* Familial Mediterranean fever mutations lift the obligatory requirement for microtubules in Pyrin inflammasome activation. *Proceedings of the National Academy of Sciences* **113,** 14384–14389 (2016).
69. PhD, C. R. *et al.* Sputum transcriptomics reveal upregulation of IL-1 receptor family members in patients with severe asthma. *Journal of Allergy and Clinical Immunology* **141,** 560–570 (2018).
70. Chen, S. *et al.* Blockade of the NLRP3/Caspase-1 Axis Ameliorates Airway Neutrophilic Inflammation in a Toluene Diisocyanate-Induced Murine Asthma Model. *Toxicological Sciences* **66,** 1047–14 (2019).
71. Xu, X. *et al.* Selective NLRP3 inflammasome inhibitor reduces neuroinflammation and improves long-term neurological outcomes in a murine model of traumatic brain injury. *Neurobiology of Disease* **117,** 15–27 (2018).
72. Stutz, A. *et al.* NLRP3 inflammasome assembly is regulated by phosphorylation of the pyrin domain. *J. Exp. Med.* **214,** 1725–1736 (2017).
73. Primiano, M. J. *et al.* Efficacy and Pharmacology of the NLRP3 Inflammasome Inhibitor CP-456,773 (CRID3) in Murine Models of Dermal and Pulmonary Inflammation. *J. Immunol.* **197,** 2421–2433 (2016).
74. Coll, R. C. *et al.* MCC950 directly targets the NLRP3 ATP-hydrolysis motif for inflammasome inhibition. *Nat. Chem. Biol.* **15,** 556–559 (2019).
75. Stunden, H. J. & Latz, E. PKR stirs up inflammasomes. *Cell Res.* **23,** 168–170 (2012).
76. Lu, B. *et al.* Novel role of PKR in inflammasome activation and HMGB1 release. *Nature* **488,** 670–674 (2012).
77. Hett, E. C. *et al.* Chemical genetics reveals a kinase-independent role for protein kinase R in pyroptosis. *Nat. Chem. Biol.* **9,** 398–405 (2013).

9 Acknowledgement

First, I would like to thank my Supervisor, Prof. Eicke Latz for giving me the opportunity to join his lab in Bonn and pursue my PhD studies under his guidance. Eicke's knowledge of, and enthusiasm for, the field of innate immunology has been a great motivation to me during my studies, and made it a great experience. Thank you for your kindness and patience during this time.
I would like to thank Prof. Michael Hoch for agreeing to be my second examiner, and I would like to thank Prof. Michael Pankratz for replacing Prof. Hoch after he could no longer continue, due to his increased duties upon becoming a rector.
I would like to thank the other members of my examination board for their time and participation.
I would like to thank Dr. Douglas Golenbock for enabling me to pursue this PhD, and for his support and immense patience throughout the entire process.
I would also like to thank Dr. Philip Denner for developing and performing the confocal based screens, without which this study would not have been possible.
I would especially like to thank Rainer Stahl, who has aided me scientifically by designing and creating many of the plasmid constructs used in this study. Rainer has also helped me deal with many problems related to my lack of German proficiency, and has helped me get through the intricacies of Germany bureaucracy. I don't know how I could have successfully completed my time in Germany without all his help. I also miss the many interesting discussions we have had over cloning strategies and scientific projects during my time in the lab.
Thank you to Andrea Stutz for helping me get started, and for all the work that became the initial basis for my project.
Thank you to Gabor Horvath for all the help with fluorescent constructs, interesting discussions, and for being a great office mate; Tomasz Prochnicki for all the help, science discussions, and late night company; Mario Lauterbach for helping me get settled in Germany; and all the other members of the Latz lab for their help, useful discussions, and for creating a pleasant and productive lab environment.
Thank you to Dr. Evelyn Kurt Jones for her guidance in software use and figure design needed for this thesis.
Finally, I would like to thank my mother for her support, and for her enthusiasm for me to complete my PhD studies.

10 Appendix

Protein Sequences

hAIM2 Full-length

MESKYKEILLLTGLDNITDEELDRFKFFLSDEFNIATGKLHTANRIQVATLMIQNAGAVSAVMK
TIRIFQKLNYMLLAKRLQEEKEKVDKQYKSVTKPKPLSQAEMSPAASAAIRNDVAKQRAAPK
VSPHVKPEQKQMVAQQESIREGFQKRCLPVMVLKAKKPFTFETQEGKQEMFHATVATEKE
FFFVKVFNTLLKDKFIPKRIIIIARYYRHSGFLEVNSASRVLDAESDQKVNVPLNIIRKAGETPKI
NTLQTQPLGTIVNGLFVVQKVTEKKKNILFDLSDNTGKMEVLGVRNEDTMKCKEGDKVRLTF
FTLSKNGEKLQLTSGVHSTIKVIKAKKKT

hNLRP3 Full-length

MKMASTRCKLARYLEDLEDVDLKKFKMHLEDYPPQKGCIPLPRGQTEKADHVDLATLMIDF
NGEEKAWAMAVWIFAAINRRDLYEKAKRDEPKWGSDNARVSNPTVICQEDSIEEEWMGLL
EYLSRISICKMKKDYRKKYRKYVRSRFQCIEDRNARLGESVSLNKRYTRLRLIKEHRSQQER
EQELLAIGKTKTCESPVSPIKMELLFDPDDEHSEPVHTVVFQGAAGIGKTILARKMMLDWAS
GTLYQDRFDYLFYIHCREVSLVTQRSLGDLIMSCCPDPNPPIHKIVRKPSRILFLMDGFDELQ
GAFDEHIGPLCTDWQKAERGDILLSSLIRKKLLPEASLLITTRPVALEKLQHLLDHPRHVEILG
FSEAKRKEYFFKYFSDEAQARAAFSLIQENEVLFTMCFIPLVCWIVCTGLKQQMESGKSLAQ
TSKTTTAVYVFFLSSLLQPRGGSQEHGLCAHLWGLCSLAADGIWNQKILFEESDLRNHGLQ
KADVSAFLRMNLFQKEVDCEKFYSFIHMTFQEFFAAMYYLLEEEKEGRTNVPGSRLKLPSR
DVTVLLENYGKFEKGYLIFVVRFLFGLVNQERTSYLEKKLSCKISQQIRLELLKWIEVKAKAKK
LQIQPSQLELFYCLYEMQEEDFVQRAMDYFPKIEINLSTRMDHMVSSFCIENCHRVESLSLG
FLHNMPKEEEEEEKEGRHLDMVQCVLPSSSHAACSHGLVNSHLTSSFCRGLFSVLSTSQSL
TELDLSDNSLGDPGMRVLCETLQHPGCNIRRLWLGRCGLSHECCFDISLVLSSNQKLVELD
LSDNALGDFGIRLLCVGLKHLLCNLKKLWLVSCCLTSACCQDLASVLSTSHSLTRLYVGENA
LGDSGVAILCEKAKNPQCNLQKLGLVNSGLTSVCCSALSSVLSTNQNLTHLYLRGNTLGDK
GIKLLCEGLLHPDCKLQVLELDNCNLTSHCCWDLSTLLTSSQSLRKLSLGNNDLGDLGVMM
FCEVLKQQSCLLQNLGLSEMYFNYETKSALETLQEEKPELTVVFEPSW

hNOD2 Full-Length

MGEEGGSASHDEEERASVLLGHSPGCEMCSQEAFQAQRSQLVELLVSGSLEGFESVLDW
LLSWEVLSWEDYEGFHLLGQPLSHLARRLLDTVWNKGTWACQKLIAAAQEAQADSQSPKL
HGCWDPHSLHPARDLQSHRPAIVRRLHSHVENMLDLAWERGFVSQYECDEIRLPIFTPSQR
ARRLLDLATVKANGLAAFLLQHVQELPVPLALPLEAATCKKYMAKLRTTVSAQSRFLSTYDG
AETLCLEDIYTENVLEVWADVGMAGPPQKSPATLGLEELFSTPGHLNDDADTVLVVGEAGS
GKSTLLQRLHLLWAAGQDFQEFLFVFPFSCRQLQCMAKPLSVRTLLFEHCCWPDVGQEDIF
QLLLDHPDRVLLTFDGFDEFKFRFTDRERHCSPTDPTSVQTLLFNLLQGNLLKNARKVVTSR
PAAVSAFLRKYIRTEFNLKGFSEQGIELYLRKRHHEPGVADRLIRLLQETSALHGLCHLPVFS
WMVSKCHQELLLQEGGSPKTTTDMYLLILQHFLLHATPPDSASQGLGPSLLRGRLPTLLHLG
RLALWGLGMCCYVFSAQQLQAAQVSPDDISLGFLVRAKGVVPGSTAPLEFLHITFQCFFAAF
YLALSADVPPALLRHLFNCGRPGNSPMARLLPTMCIQASEGKDSSVAALLQKAEPHNLQITA
AFLAGLLSREHWGLLAECQTSEKALLRRQACARWCLARSLRKHFHSIPPAAPGEAKSVHAM
PGFIWLIRSLYEMQEERLARKAARGLNVGHLKLTFCSVGPTECAALAFVLQHLRRPVALQLD
YNSVGDIGVEQLLPCLGVCKALYLRDNNISDRGICKLIECALHCEQLQKLALFNNKLTDGCAH
SMAKLLACRQNFLALRLGNNYITAAGAQVLAEGLRGNTSLQFLGFWGNRVGDEGAQALAE
ALGDHQSLRWLSLVGNNIGSVGAQALALMLAKNVMLEELCLEENHLQDEGVCSLAEGLKKN
SSLKILKLSNNCITYLGAEALLQALERNDTILEVWLRG NTFSLEEVDKLGCRDTRLLL

hNLRP3 PYD-hAIM2 Chimera

**MKMASTRCKLARYLEDLEDVDLKKFKMHLEDYPPQKGCIPLPRGQTEKADHVDLATLMID
FNGEEKAWAMAVWIFAAINRRDLYEKAKRDEPKWGSDNARVSNPTVICQEDSIEEEWMG
LLEYLSRISICKMKKD**PEQKQMVAQQESIREGFQKRCLPVMVLKAKKPFTFETQEGKQEMF
HATVATEKEFFFVKVFNTLLKDKFIPKRIIIIARYYRHSGFLEVNSASRVLDAESDQKVNVPLNII
RKAGETPKINTLQTQPLGTIVNGLFVVQKVTEKKKNILFDLSDNTGKMEVLGVRNEDTMKCK
EGDKVRLTFFTLSKNGEKLQLTSGVHSTIKVIKAKKKT

hAIM2 PYD-hNOD2 Chimera

**ESKYKEILLLTGLDNITDEELDRFKFFLSDEFNIATGKLHTANRIQVATLMIQNAGAVSAVM
KTIRIFQKLNYMLLAKRLQEEKEKVDKQYKSVTKPKPLSQAEMSPAASAAIRNDVAKQRA
APKVSPHVK**KYMAKLRTTVSAQSRFLSTYDGAETLCLEDIYTENVLEVWADVGMAGPPQKS
PATLGLEELFSTPGHLNDDADTVLVVGEAGSGKSTLLQRLHLLWAAGQDFQEFLFVFPFSC
RQLQCMAKPLSVRTLLFEHCCWPDVGQEDIFQLLLDHPDRVLLTFDGFDEFKFRFTDRERH
CSPTDPTSVQTLLFNLLQGNLLKNARKVVTSRPAAVSAFLRKYIRTEFNLKGFSEQGIELYLR
KRHHEPGVADRLIRLLQETSALHGLCHLPVFSWMVSKCHQELLLQEGGSPKTTTDMYLLILQ
HFLLHATPPDSASQGLGPSLLRGRLPTLLHLGRLALWGLGMCCYVFSAQQLQAAQVSPDDI
SLGFLVRAKGVVPGSTAPLEFLHITFQCFFAAFYLALSADVPPALLRHLFNCGRPGNSPMAR
LLPTMCIQASEGKDSSVAALLQKAEPHNLQITAAFLAGLLSREHWGLLAECQTSEKALLRRQ
ACARWCLARSLRKHFHSIPPAAPGEAKSVHAMPGFIWLIRSLYEMQEERLARKAARGLNVG
HLKLTFCSVGPTECAALAFVLQHLRRPVALQLDYNSVGDIGVEQLLPCLGVCKALYLRDNNI
SDRGICKLIECALHCEQLQKLALFNNKLTDGCAHSMAKLLACRQNFLALRLGNNYITAAGAQ
VLAEGLRGNTSLQFLGFWGNRVGDEGAQALAEALGDHQSLRWLSLVGNNIGSVGAQALAL
MLAKNVMLEELCLEENHLQDEGVCSLAEGLKKNSSLKILKLSNNCITYLGAEALLQALERNDT
ILEVWLRGNTFSLEEVDKLGCRDTRLLL

hNLRP3 PYD-hNOD2 Chimera

**KMASTRCKLARYLEDLEDVDLKKFKMHLEDYPPQKGCIPLPRGQTEKADHVDLATLMIDF
NGEEKAWAMAVWIFAAINRRDLYEKAKRDEPKWGSDNARVSNPTVICQEDSIEEEWMGL
LEYLSRISICK**KYMAKLRTTVSAQSRFLSTYDGAETLCLEDIYTENVLEVWADVGMAGPPQK
SPATLGLEELFSTPGHLNDDADTVLVVGEAGSGKSTLLQRLHLLWAAGQDFQEFLFVFPFS
CRQLQCMAKPLSVRTLLFEHCCWPDVGQEDIFQLLLDHPDRVLLTFDGFDEFKFRFTDRER
HCSPTDPTSVQTLLFNLLQGNLLKNARKVVTSRPAAVSAFLRKYIRTEFNLKGFSEQGIELYL
RKRHHEPGVADRLIRLLQETSALHGLCHLPVFSWMVSKCHQELLLQEGGSPKTTTDMYLLIL
QHFLLHATPPDSASQGLGPSLLRGRLPTLLHLGRLALWGLGMCCYVFSAQQLQAAQVSPD
DISLGFLVRAKGVVPGSTAPLEFLHITFQCFFAAFYLALSADVPPALLRHLFNCGRPGNSPMA
RLLPTMCIQASEGKDSSVAALLQKAEPHNLQITAAFLAGLLSREHWGLLAECQTSEKALLRR
QACARWCLARSLRKHFHSIPPAAPGEAKSVHAMPGFIWLIRSLYEMQEERLARKAARGLNV
GHLKLTFCSVGPTECAALAFVLQHLRRPVALQLDYNSVGDIGVEQLLPCLGVCKALYLRDNN
ISDRGICKLIECALHCEQLQKLALFNNKLTDGCAHSMAKLLACRQNFLALRLGNNYITAAGAQ
VLAEGLRGNTSLQFLGFWGNRVGDEGAQALAEALGDHQSLRWLSLVGNNIGSVGAQALAL
MLAKNVMLEELCLEENHLQDEGVCSLAEGLKKNSSLKILKLSNNCITYLGAEALLQALERNDT
ILEVWLRGNTFSLEEVDKLGCRDTRLLL

Cysteines in NLRP3 PYD

MKMASTR**C**KLARYLEDLEDVDLKKFKMHLEDYPPQKG**C**IPLPRGQTEKADHVDLATLMIDF
NGEEKAWAMAVWIFAAINRRDLYEKAKRDEPKWGSDNARVSNPTVI**C**QEDSIEEEWMGLL
EYLSRISI**C**K

11 List of Publications

1. Hunninghake, G. W., **B. G. Monks**, L. J. Geist, M. M. Monick, M. A. Monroy, M. F. Stinski, A. C. Webb, J. M. Dayer, P. E. Auron, and M. J. Fenton. 1992. The functional importance of a cap site-proximal region of the human prointerleukin 1 beta gene is defined by viral protein trans-activation. ***Mol Cell Biol*** *12: 3439*.
2. Buras, J. A., **B. G. Monks**, and M. J. Fenton. 1994. The NF-beta A-binding element, not an overlapping NF-IL-6-binding element, is required for maximal IL-1 beta gene expression. ***J Immunol*** *152: 4444*.
3. **Monks, B. G**., B. A. Martell, J. A. Buras, and M. J. Fenton. 1994. An upstream protein interacts with a distinct protein that binds to the cap site of the human interleukin 1 beta gene. ***Mol Immunol*** *31: 139*.
4. Wurfel, M. M., **B. G. Monks**, R. R. Ingalls, R. L. Dedrick, R. Delude, D. Zhou, N. Lamping, R. R. Schumann, R. Thieringer, M. J. Fenton, S. D. Wright, and D. Golenbock. 1997. Targeted deletion of the lipopolysaccharide (LPS)-binding protein gene leads to profound suppression of LPS responses ex vivo, whereas in vivo responses remain intact. ***J Exp Med*** *186: 2051.*
5. Pollack, M., C. A. Ohl, D. T. Golenbock, F. Di Padova, L. M. Wahl, N. L. Koles, G. Guelde, and **B. G. Monks**. 1997. Dual effects of LPS antibodies on cellular uptake of LPS and LPS- induced proinflammatory functions. ***J Immunol*** *159: 3519.*
6. Ingalls, R. R., **B. G. Monks**, R. Savedra, Jr., W. J. Christ, R. L. Delude, A. E. Medvedev, T. Espevik, and D. T. Golenbock. 1998. CD11/CD18 and CD14 share a common lipid A signaling pathway. ***J Immunol*** *161: 5413.*
7. Ingalls, R. R., **B. G. Monks**, and D. T. Golenbock. 1999. Membrane expression of soluble endotoxin-binding proteins permits LPS signaling in Chinese hamster ovary fibroblasts independently of CD14. ***J Biol Chem*** *274: 13993-8.*
8. Heine, H., C. J. Kirschning , E. Lien , **B. G. Monks**, M. Rothe, and D. T. Golenbock. 1999. Cells that carry A null allele for toll-like receptor 2 are capable of responding to endotoxin. ***J Immunol*** *162: 6971-5*.
9. Heine H; Delude RL; **Monks BG**; Espevik T; Golenbock DT. 1999. Bacterial lipopolysaccharide induces expression of the stress response genes hop and H411. ***J Biol Chem*** *274: 21049-55.*
10. Lien E; Means TK; Heine H; Yoshimura A; Kusumoto S; Fukase K; Fenton MJ; Oikawa M; Qureshi N; **Monks B**; Finberg RW; Ingalls RR; Golenbock DT. 2000.Toll-like receptor 4 imparts ligand-specific recognition of bacterial lipopolysaccharide. ***J Clin Invest*** *105: 497-504.*

11. Moore KJ, Andersson LP, Ingalls RR, **Monks BG**, Li R, Arnaout MA, Golenbock DT, Freeman MW. 2001. Divergent response to LPS and bacteria in CD14-deficient murine macrophages. ***J Immunol*** *165: 4272-4280.*
12. Ram, S., M. Cullinane, A. M. Blom, S. Gulati, D. P. McQuillen, **B. G. Monks**, C. O'Connell, R. Boden, C. Elkins, M. K. Pangburn, B. Dahlback, and P .A. Rice. 2001. Binding of C4b-binding Protein to Porin: A Molecular Mechanism of Serum Resistance of *Neisseria gonorrhoeae.* ***J Exp Med*** *193: 281-295.*
13. Ram, S., M. Cullinane, A. M. Blom, S. Gulati, D. P. McQuillen, R. Boden, **B. G. Monks**, C. O'Connell, C. Elkins, M. K. Pangburn, B. Dahlback, and P .A. Rice. 2001. C4bp binding to porin mediates stable serum resistance of *Neisseria gonorrhoeae.* ***International Pharmacology 1*** *(2001): 423-432.*
14. Schromm AB, Lien E, Henneke P, Chow JC, Yoshimura A, Heine H, Latz E, **Monks BG**, Schwartz DA, Miyake K, Golenbock DT. 2001. Molecular Genetic Analysis of an Endotoxin Nonresponder Mutant Cell Line. A point mutation in a conserved region of md-2 abolishes endotoxin-induced signaling. ***J Exp Med*** *194: 79-88.*
15. Flo TH, Ryan L, Latz E, Takeuchi O, **Monks BG**, Lien E, Halaas O, Akira S, Skjak-Braek G, Golenbock DT, Espevik T. 2002. Involvement of toll-like receptor (TLR) 2 and TLR4 in cell activation by mannuronic acid polymers. ***J Biol Chem*** *2002 Sept 20;277(38):35489-95.*
16. Latz E, Visintin A, Lien E, Fitzgerald K, **Monks BG**, Kurt-Jones E, Golenbock DT, Espevik T. 2002. LPS rapidly traffics to and from the Golgi apparatus with the TLR4/MD-2/CD14 complex in a process that is distinct from the initiation of signal transduction. ***J Biol Chem*** *2002 Dec 6;277(49):47834-43.*
17. Visintin A, Latz E, **Monks BG**, Espevik T, Golenbock DT. 2003. Lysines 128 and 132 enable LPS binding to MD-2, leading to Toll-like receptor 4 aggregation and signal transduction. ***J Biol Chem****. 2003 Nov 28;278(48):48313-20.*
18. Fitzgerald KA, Rowe DC, Barnes BJ, Caffrey DR, Visintin A, Latz E, **Monks B**, Pitha PM, Golenbock DT. 2003. LPS-TLR4 signaling to IRF-3/7 and NF-kappaB involves the toll adapters TRAM and TRIF. ***J Exp Med*** *2003 Oct 6;198(7):1043-55.*
19. Espevik T, Latz E, Lien E, **Monks B**, Golenbock DT. 2003. Cell distributions and functions of Toll-like receptor 4 studied by fluorescent gene constructs. ***Scand J Infect Dis*** *2003;35(9):660-4.*
20. Latz E, Schoenemeyer A, Visintin A, Fitzgerald KA, **Monks BG**, Knetter CF, Lien E, Nilsen NJ, Espevik T, Golenbock DT. 2004. TLR9 signals after translocating from the ER to CpG DNA in the lysosome. ***Nat Immunol*** *2004 Feb;5(2):190-8*.
21. Rothenfusser S, Goutagny N, DiPerna G, Gong M, **Monks BG**, Schoenemeyer A, Yamamoto M, Akira S, Fitzgerald KA. 2005. The RNA helicase Lgp2 inhibits TLR-

independent sensing of viral replication by retinoic acid-inducible gene-I. ***J Immunol***. *2005 Oct 15;175(8):5260-8.*

22. Visintin A, Halmen KA, Latz E, **Monks BG**, Golenbock DT. 2005 Pharmacological inhibition of endotoxin responses is achieved by targeting the TLR4 coreceptor, MD-2. ***J Immunol***. *Nov 15;175(10):6465-72.*
23. Rowe DC, McGettrick AF, Latz E, **Monks BG**, Gay NJ, Yamamoto M, Akira S, O'Neill LA, Fitzgerald KA, Golenbock DT. 2006. The myristoylation of TRIF-related adaptor molecule is essential for Toll-like receptor 4 signal transduction. ***Proc Natl Acad Sci U S A***. *2006 Apr 18;103(16):6299-304.*
24. Visintin A, Iliev DB, **Monks BG**, Halmen KA, Golenbock DT. 2006. MD-2. ***Immunobiology***. *2006;211(6-8):437-47.*
25. Visintin A, Halmen KA, Khan N, **Monks BG**, Golenbock DT, Lien E. 2006 MD-2 expression is not required for cell surface targeting of Toll-like receptor 4 (TLR4). ***J Leukoc Biol***. *2006 Dec;80(6):1584-92.*
26. Parroche P, Lauw FN, Goutagny N, Latz E, **Monks BG**, Visintin A, Halmen KA, Lamphier M, Olivier M, Bartholomeu DC, Gazzinelli RT, Golenbock DT. 2007. Malaria hemozoin is immunologically inert but radically enhances innate responses by presenting malaria DNA to Toll-like receptor 9. ***Proc Natl Acad Sci U S A***. *2007 Feb 6;104(6):1919-24.*
27. Latz E, Verma A, Visintin A, Gong M, Sirois CM, Klein DC, **Monks BG**, McKnight CJ, Lamphier MS, Duprex WP, Espevik T, Golenbock DT. 2007. Ligand-induced conformational changes allosterically activate Toll-like receptor 9. ***Nat Immunol***. *2007 Jul;8(7):772-9.*
28. Ngampasutadol J, Ram S, Gulati S, Agarwal S, Li C, Visintin A, **Monks B**, Madico G, Rice PA. 2008. Human Factor H Interacts Selectively with Neisseria gonorrhoeae and Results in Species-Specific Complement Evasion. ***J Immunol.*** *2008 Mar 1;180(5):3426-35.*
29. Halle A, Hornung V, Petzold GC, Stewart CR, **Monks BG**, Reinheckel T, Fitzgerald KA, Latz E, Moore KJ, Golenbock D. 2008. The NALP3 inflammasome is involved in the innate immune response to amyloid-beta. ***Nat Immunol.*** *2008 Aug;9(8):857-65.*
30. Nagpal K, Plantinga TS, Wong J, **Monks BG**, Gay NJ, Netea MG, Fitzgerald KA, Golenbock DT. 2009. A TIR domain variant of MYD88 adapter-like (MAL)/TIRAP results in loss of MYD88 binding and reduced TLR2/TLR4 signaling. ***J Biol Chem***. *2009 Sep 18;284(38):25742-8.*
31. Bauernfeind FG, Horvath G, Stutz A, Alnemri ES, MacDonald K, Speert D, Fernandes-Alnemri T, Wu J, **Monks BG**, Fitzgerald KA, Hornung V, Latz E. 2009. Cutting edge: NF-kappaB activating pattern recognition and cytokine receptors license NLRP3 inflammasome activation by regulating NLRP3 expression. ***J Immunol*****.** 2009 Jul

15;183(2):787-91.

32. Goutagny N, Jiang Z, Tian J, Parroche P, Schickli J, **Monks BG**, Ulbrandt N, Ji H, Kiener PA, Coyle AJ, Fitzgerald KA. 2009. Cell Type-Specific Recognition of Human Metapneumoviruses (HMPVs) by Retinoic Acid-Inducible Gene I (RIG-I) and TLR7 and Viral Interference of RIG-I Ligand Recognition by HMPV-B1 Phosphoprotein. ***J Immunol***. *2010 Feb 1;184(3):1168-79.*
33. Rathinam VA, Jiang Z, Waggoner SN, Sharma S, Cole LE, Waggoner L, Vanaja SK, **Monks BG**, Ganesan S, Latz E, Hornung V, Vogel SN, Szomolanyi-Tsuda E, Fitzgerald KA. The AIM2 inflammasome is essential for host defense against cytosolic bacteria and DNA viruses. ***Nat Immunol*.** 2010 May;11(5):395-402.
34. Meng J, Drolet JR, **Monks BG**, Golenbock DT. MD-2 residues tyrosine 42, arginine 69, aspartic acid 122, and leucine 125 provide species specificity for lipid IVA. ***J Biol Chem***. *2010 Sep 3;285(36):27935-43.*
35. Nagpal K, Plantinga TS, Sirois CM, **Monks BG**, Latz E, Netea MG, Golenbock DT. Natural Loss-of-function Mutation of Myeloid Differentiation Protein 88 Disrupts Its Ability to Form Myddosomes. ***J Biol Chem.*** *2011 Apr 1;286(13):11875-82.*
36. Shaughnessy J, Ram S, Bhattacharjee A, Pedrosa J, Tran C, Horvath G, **Monks B**, Visintin A, Jokiranta TS, Rice PA. Molecular Characterization of the Interaction between Sialylated Neisseria gonorrhoeae and Factor H. ***J Biol Chem***. 2011 Jun 24;286(25):22235-42.
37. Bartok E, Bauernfeind F, Khaminets MG, Jakobs C, **Monks B**, Fitzgerald KA, Latz E, Hornung V. iGLuc: a luciferase-based inflammasome and protease activity reporter. ***Nat Methods***. 2013 Feb;10(2):147-54
38. Conlon J, Burdette DL, Sharma S, Bhat N, Thompson M, Jiang Z, Rathinam VA, **Monks B**, Jin T, Xiao TS, Vogel SN, Vance RE, Fitzgerald KA. Mouse, but not human STING, binds and signals in response to the vascular disrupting agent 5,6-dimethylxanthenone-4-acetic acid. ***J Immunol*.** 2013 May 15;190(10):5216-25.
39. Hett EC, Slater LH, Mark KG, Kawate T, **Monks BG**, Stutz A, Latz E, Hung DT. Chemical genetics reveals a kinase-independent role for protein kinase R in pyroptosis. ***Nat Chem Biol.*** *2013 Jun;9(6):398-405*. Erratum in: Nat Chem Biol. 2013 Jul;9(7):466.
40. Stutz A, Horvath GL, **Monks BG**, Latz E. ASC speck formation as a readout for inflammasome activation. ***Methods Mol Biol.*** *2013;1040:91-101.*
41. Carpenter S, Aiello D, Atianand MK, Ricci EP, Gandhi P, Hall LL, Byron M, **Monks B**, Henry-Bezy M, Lawrence JB, O'Neill LA, Moore MJ, Caffrey DR, Fitzgerald KA. A long noncoding RNA mediates both activation and repression of immune response genes. ***Science.*** *2013 Aug 16;341(6147):789-92*
42. Gupta R, Ghosh S, **Monks B**, Deoliveira R, Tzeng T, Kalantari P, Nandy A,

Bhattacharjee B, Chan J, Ferreira F, Rathinam V, Sharma S, Lien E, Silverman N, Fitzgerald K, Firon A, Trieu-Cuot P, Henneke P, Golenbock D. RNA and β-hemolysin of Group B streptococcus induce IL-1β by activating NLRP3 inflammasomes in mouse macrophages. ***J Biol Chem***. *2014 Apr 1.*

43. Franklin BS, Bossaller L, De Nardo D, Ratter JM, Stutz A, Engels G, Brenker C, Nordhoff M, Mirandola SR, Al-Amoudi A, Mangan MS, Zimmer S, **Monks BG**, Fricke M, Schmidt RE, Espevik T, Jones B, Jarnicki AG, Hansbro PM, Busto P, Marshak-Rothstein A, Hornemann S, Aguzzi A, Kastenmüller W, Latz E. The adaptor ASC has extracellular and 'prionoid' activities that propagate inflammation. ***Nat Immunol.*** *2014 Aug;15(8):727-37*
44. Coll RC, Robertson AA, Chae JJ, Higgins SC, Muñoz-Planillo R, Inserra MC, Vetter I, Dungan LS, **Monks BG**, Stutz A, Croker DE, Butler MS, Haneklaus M, Sutton CE, Núñez G, Latz E, Kastner DL, Mills KH, Masters SL, Schroder K, Cooper MA, O'Neill LA. A small-molecule inhibitor of the NLRP3 inflammasome for the treatment of inflammatory diseases. ***Nat Med.*** *2015 Feb 16*
45. Shaughnessy J, Gulati S, Agarwal S, Unemo M, Ohnishi M, Su XH, Monks BG, Visintin A, Madico G, Lewis LA, Golenbock DT, Reed GW, Rice PA, Ram S. A Novel Factor H-Fc Chimeric Immunotherapeutic Molecule against Neisseria gonorrhoeae. ***J Immunol***. *2016 Feb 15;196(4):1732-40.*
46. Tzeng TC, Schattgen S, **Monks B**, Wang D, Cerny A, Latz E, Fitzgerald K, Golenbock DT. A Fluorescent Reporter Mouse for Inflammasome Assembly Demonstrates an Important Role for Cell-Bound and Free ASC Specks during In Vivo Infection. ***Cell Rep.*** *2016 Jul 12;16(2):571-82*
47. Primiano MJ, Lefker BA, Bowman MR, Bree AG, Hubeau C, Bonin PD, Mangan M, Dower K, **Monks BG**, Cushing L, Wang S, Guzova J, Jiao A, Lin LL, Latz E, Hepworth D, Hall JP Efficacy and Pharmacology of the NLRP3 Inflammasome Inhibitor CP-456,773 (CRID3) in Murine Models of Dermal and Pulmonary Inflammation. ***J Immunol***. *2016 Sep 15;197(6):2421-33.*

Eidesstattliche Erklärung

An Eides statt versichere ich, dass die vorgelegte Arbeit – abgesehen von den ausdrücklich bezeichneten Hilfsmitteln – persönlich, selbständig und ohne Benutzung anderer als der angegebenen Hilfsmittel angefertigt wurde, die aus anderen Quellen direkt oder indirekt übernommenen Daten und Konzepte unter Angabe der Quelle kenntlich gemacht sind, die vorgelegte Arbeit oder ähnliche Arbeiten nicht bereits anderweitig als Dissertation eingereicht worden ist bzw. sind, kein früherer Promotionsversuch unternommen worden ist, für die inhaltlich materielle Erstellung der vorgelegten Arbeit keine fremde Hilfe, insbesondere keine entgeltliche Hilfe von Vermittlungs- bzw. Beratungsdiensten (Promotionsberater oder andere Personen) in Anspruch genommen wurde sowie keinerlei Dritte vom Doktoranden unmittelbar oder mittelbar geldwerte Leistungen für Tätigkeiten erhalten haben, die im Zusammenhang mit dem Inhalt der vorgelegten Arbeit stehen.

Die vorgelegte Dissertation wurde an den nachfolgend aufgeführten Stellen auszugsweise veröffentlicht:

Chemical genetics reveals a kinase-independent role for protein kinase R in pyroptosis.
Hett EC, Slater LH, Mark KG, Kawate T, Monks BG, Stutz A, Latz E, Hung DT. *Nat Chem Biol. 2013 Jun;9(6):398-405*. Erratum in: Nat Chem Biol. 2013 Jul;9(7):466.

A small-molecule inhibitor of the NLRP3 inflammasome for the treatment of inflammatory diseases.
Coll RC, Robertson AA, Chae JJ, Higgins SC, Muñoz-Planillo R, Inserra MC, Vetter I, Dungan LS, Monks BG, Stutz A, Croker DE, Butler MS, Haneklaus M, Sutton CE, Núñez G, Latz E, Kastner DL, Mills KH, Masters SL, Schroder K, Cooper MA, O'Neill LA.*Nat Med. 2015 Feb 16*

Efficacy and Pharmacology of the NLRP3 Inflammasome Inhibitor CP-456,773 (CRID3) in Murine Models of Dermal and Pulmonary Inflammation.
Primiano MJ, Lefker BA, Bowman MR, Bree AG, Hubeau C, Bonin PD, Mangan M, Dower K, Monks BG, Cushing L, Wang S, Guzova J, Jiao A, Lin LL, Latz E, Hepworth D, Hall JP *J Immunol. 2016 Sep 15;197(6):2421-33*